INFORMATION TO USERS

This dissertation was produced from a microfilm copy of the original document. While the most advanced technological means to photograph and reproduce this document have been used, the quality is heavily dependent upon the quality of the original submitted.

The following explanation of techniques is provided to help you understand markings or patterns which may appear on this reproduction.

1. The sign or "target" for pages apparently lacking from the document photographed is "Missing Page(s)". If it was possible to obtain the missing page(s) or section, they are spliced into the film along with adjacent pages. This may have necessitated cutting thru an image and duplicating adjacent pages to insure you complete continuity.

2. When an image on the film is obliterated with a large round black mark, it is an indication that the photographer suspected that the copy may have moved during exposure and thus cause a blurred image. You will find a good image of the page in the adjacent frame.

3. When a map, drawing or chart, etc., was part of the material being photographed the photographer followed a definite method in "sectioning" the material. It is customary to begin photoing at the upper left hand corner of a large sheet and to continue photoing from left to right in equal sections with a small overlap. If necessary, sectioning is continued again — beginning below the first row and continuing on until complete.

4. The majority of users indicate that the textual content is of greatest value, however, a somewhat higher quality reproduction could be made from "photographs" if essential to the understanding of the dissertation. Silver prints of "photographs" may be ordered at additional charge by writing the Order Department, giving the catalog number, title, author and specific pages you wish reproduced.

University Microfilms

300 North Zeeb Road
Ann Arbor, Michigan 48106

A Xerox Education Company

DISSERTATION

WATER INFILTRATION UNDER CENTER-PIVOTS

Submitted by

John W. Addink

In partial fulfillment of the requirements

for the Degree of Doctor of Philosophy

Colorado State University

Fort Collins, Colorado

August, 1972

COLORADO STATE UNIVERSITY

August, 1972

WE HEREBY RECOMMEND THAT THE DISSERTATION PREPARED UNDER OUR SUPERVISION BY JOHN W. ADDINK ENTITLED WATER INFILTRATION UNDER CENTER-PIVOTS BE ACCEPTED AS FULFILLING IN PART REQUIREMENTS FOR THE DEGREE OF DOCTOR OF PHILOSOPHY.

Committee on Graduate Work

E. Gordon Kruse

Dale F. Heermann

Robert E. Danielson

Donald L. Miles

Raymond V. Skogerboe
Adviser

Gordon M. Harper
Head of Department

ABSTRACT OF DISSERTATION

WATER INFILTRATION UNDER CENTER-PIVOTS

Center-pivot sprinkler systems have become popular in recent years because of their labor saving advantage over other systems and because of their ability to economically irrigate rolling terrain and light soils. A center-pivot system consists of a water pipeline suspended in the air by means of cables or trusses and self-propelled towers. The system revolves very slowly in a circle while distributing water to the soil by means of sprinklers connected above the pipeline.

Center-pivots apply water at a high rate thereby causing runoff. This study examined the potential reduction in runoff by changing the normal symmetrical application rate pattern to a front-humped non-symmetrical application rate pattern.

Laboratory experiments and a model were utilized in the study. The laboratory equipment consisted of a spray bar capable of applying varying rates to eight soil plots and a drying apparatus capable of drying the soil plots between tests. The model consisted of a numerical solution to a moisture flow equation which combined Darcy's law and the continuity equation.

Two 2-step patterns and one constant application rate pattern were used in laboratory tests to study the relationships between time

and infiltration rate, between depth of intake and infiltration rate, and to help develop the numerical model.

Three simulated center-pivot application rate patterns were used in laboratory tests to help determine the most desirable type of center-pivot application rate pattern as well as to verify the numerical model. The model's predicted infiltration curves fit reasonably the laboratory infiltration data. The conclusion drawn, for the differences that existed between the model and laboratory data, was that the model erred in not including soil shrinking and swelling in calculating its hydraulic conductivity values.

The numerical model was extended to predict conditions beyond the conditions of the laboratory infiltration tests. Possible effects of including shrinking and swelling in the extension of model tests are suggested.

A modified potential intake rate theory used to study runoff under center-pivots was tested. The advantages and disadvantages of applying this theory are delineated.

Some design considerations for selecting center-pivot application rate patterns are presented with a design graph being presented for one set of physical conditions.

The main conclusions drawn from the study are that a numerical moisture-flow model can be a helpful research tool and that

non-symmetrical application rate patterns have potential for reducing runoff ten percent or more under center-pivot sprinkler systems.

John W. Addink
Agricultural Engineering Department
Colorado State University
Fort Collins, Colorado 80521
August, 1972

ACKNOWLEDGMENTS

The author wishes to give special thanks to his advisor, Mr. Gaylord V. Skogerboe, and project leader, Mr. Donald L. Miles, for their advice, encouragement, and inspiration which made this work possible. The help and advice of the other members of the Graduate Committee, Dr. Dale F. Hermann, Dr. Gordon Kruse and Dr. Robert Danielson is gratefully acknowledged.

The help of Dr. Roger E. Smith, Agricultural Research Service, Tuscon, Arizona, for the use of his program is also sincerely appreciated.

Thanks are also due to other members of the Agricultural Engineering Department for their suggestions. A special thanks is due to Mr. Sam Busch for help in constructing the equipment and in running the drying blowers.

This investigation was supported by funds provided by the United States Department of Interior as authorized under the Water Resources Research Act of 1964, Public Law 88-379 and Colorado Agricultural Experiment Station.

TABLE OF CONTENTS

LIST OF TABLES

LIST OF FIGURES

LIST OF SYMBOLS

Symbol	Description	Dimension
A	A symmetrical application rate pattern with a 60-minute time length	-
A'	Packing factor	-
A_t	Area of tube	L^2
a_i	Off-diagonal element in matrix J	-
B	A non-symmetrical front-humped application rate pattern with a 52-minute time length	-
B'	Particle shape factor	-
B_m	A modified non-symmetrical, front-humped application rate pattern with a 60-minute time length	-
b_i	Diagonal element in matrix J	-
C	A non-symmetrical front-humped application rate pattern with a 40-minute time length	-
C_m	A modified symmetrical front-humped application rate pattern with a 60-minute time length	-
c_i	Off-diagonal element in matrix J	-
D	A symmetrical application rate pattern with a 40-minute time length	-
D'	Distance from the soil surface to the wetted front	L
D_a	Actual water depth applied over time 0 to t	L

Symbol	Description	Dimension
D_p	Potential depth of infiltration at time t, obtained by integrating the flooded infiltration rate, I', over time 0 to t	-
d_m	Geometric mean of rated size of adjacent sieves	L
E	A symmetrical application rate pattern with a 90-minute time length	-
E'	Constant specified by soil type and surface and cropping conditions	-
e	Base of Naperin logarithms	-
F	Constant which Philip called soil sorptivity	$LT^{-\frac{1}{2}}$
F_p	Storage potential of the soil above the impeding strata; equals total porosity minus antecedent water	L
G	Constant specified by soil type and surface and cropping conditions	-
H	Hydraulic head	L
h	Ponded water depth on the soil surface	L
I	Rate of infiltration	LT^{-1}
I'	Infiltration rate at t = 0	LT^{-1}
I_m	Modified potential infiltration rate	LT^{-1}
I_o	Infiltration rate at unit time	LT^{-1}
ID	Intake depth	L
i	Subscript, refers to node number for finite difference grid in length dimension	-
J	Nonlinear operator matrix	-

Symbol	Description	Dimension
j	Superscript, refers to node number for finite difference grid in time dimension	-
K	Saturated hydraulic conductivity	LT^{-1}
K_m	Modified saturated hydraulic conductivity	LT^{-1}
k	Intrinsic permeability, or permeability, a function of the geometry of the media for porous media that are stable in the presence of the fluid occupying them	L^2
k_f	Constant	-
k_r	Relative permeability or relative conductivity	-
k_s	Pore shape factor	-
L	Length of tube	L
M_j	Total number of time steps	-
N	Number of grid points used to divide the soil column for a finite difference approximation	-
n	Exponent, refers to slope of ponded infiltration curve	-
nl	Soil layer at saturated and unsaturated nodes	-
n2	First soil layer in front of wetting front	-
$P_{v+\frac{1}{2}}$	Percentage of sand held between adjacent sieves v and v + 1	-
P_b	Air entry pressure, or bubbling pressure	$ML^{-1}T^{-2}$
P_c	Capillary pressure	$ML^{-1}T^{-2}$
Q	Flow velocity	LT^{-1}
Q_p	Input to node from outside	LT^{-1}

Symbol	Description	Dimension
q_t	Total flow through a tube	L^3T^{-1}
R	Application rate	LT^{-1}
RHS, rhs	Abbreviation of right hand side of Equation 4.8	-
r	Exponent in Equation 5.1	-
r_t	Tube radius	L
S	Saturation	-
S_o	Subscript which refers to Soltrol fluid	-
SL	Represents $\partial S/\partial \psi$	L^{-1}
STOR	Abbreviation for part of Equation 4.3	LT^{-1}
s	Specific surface of porous media	L^{-1}
T	Tortuosity of flow path	-
t	Time	T
t_k	Time of ponding (Kincaid)	T
t_s	Time of ponding (El Shafei)	T
$\bar{u}$	Average velocity in tube	LT^{-1}
V_b	Bulk volume, volume per unit area	L
w	Subscript refers to water	-
Y	A parameter related to soil hydraulic properties	LT^{-1}
Z, z	Depth, measured downward from the surface	L

Symbol	Description	Dimension
γ	Unit weight	$ML^{-2}T^{-2}$
ϵ	Error value	-
θ_d	Water content at depth d	-
μ	Dynamic viscosity	$ML^{-1}T^{-1}$
ρ	Density of soil	ML^{-3}
ϕ	Porosity	-
ψ	Soil water pressure potential	L

CHAPTER I

INTRODUCTION

Background

Irrigation is very important in the United States, particularly in the western states. According to the 1959 Agricultural Census, 25 percent of the total value of all crop production was obtained from irrigated cropland which represented only 10 percent of the total crop area (37). As more land is diverted from agricultural to urban and industrial use and the demand for food increases, additional land is being irrigated, with sprinkler irrigation being used on much of this newly irrigated land.

Self-propelled, continuously-moving sprinkler laterals have become quite popular, with the most popular type being the center-pivot. There are two main reasons for the popularity of these systems. First, farmers are finding it increasingly difficult to attract the quality of help they need. Their answer to this problem is usually a higher level of mechanization or automation. A center-pivot sprinkler is one of the lowest-cost automatic irrigation systems. Secondly, parts of large aquifers, such as the Ogallala formation in eastern Colorado, lie beneath rolling terrain of sandy soils. Groundwater supplies from such

formations are used to feed center-pivot sprinkler irrigation systems which can irrigate these soils economically with light, frequent irrigations.

Most center-pivot sprinkler laterals consist of a water pipe supported 8 to 12 feet above the ground by towers spaced 90 to 125 feet apart. Sprinklers are mounted on the upper side of the pipeline. The towers are self-propelled by electric or hydraulic power and are self-aligning with one another. One end of the pipeline is fixed at the center or pivot with the water entering the pipeline at that point. The pipeline and towers rotate around the pivot, thereby irrigating a circular area which represents approximately 80 percent of a square field. There are many variations of pipe size, tower spacing, sprinkler spacing, drive mechanism, and pipe support.

Other continuously-moving sprinkler laterals do not travel in a circle, but in a straight line. This study is applicable to all continuously-moving sprinkler laterals.

Problem

Because of the high price per unit of lateral length of a self-propelled system, the average area irrigated per foot of length is made as large as possible. The consequence is a high application rate. The problems caused by high application rates are greater for a

circular-moving system because the outer one-half of the lateral irrigates approximately three times as much area as the inner one-half.

Peak application rates by self-propelled systems exceed the infiltration rate of many soils. The excess water runs from the higher to the lower spots in the field or runs off the field. The resulting uneven irrigation, wasted water and leached fertilizer cause decreased crop yields. Erosion can occur causing soil loss, thereby resulting in the transport of sediment particles and adsorbed pollutants to nearby streams and rivers.

Purpose of Research

Various sprinkler application rate patterns are being used on self-propelled systems. Two patterns are shown in Figure 1.1. Pattern "a" is typical of most patterns in use and consists of a symmetrical semi-elliptical pattern. Pattern "b" is a proposed pattern which attempts to reduce runoff and consists of a non-symmetrical front-humped pattern.

A typical ponded infiltration curve would not be the same as the sprinkler infiltration curve (Figure 1.2). Under surface irrigation, the initial application rate almost immediately exceeds the initial infiltration rate. Under sprinkler irrigation, the initial application rate is less than the initial potential infiltration rate, but the application

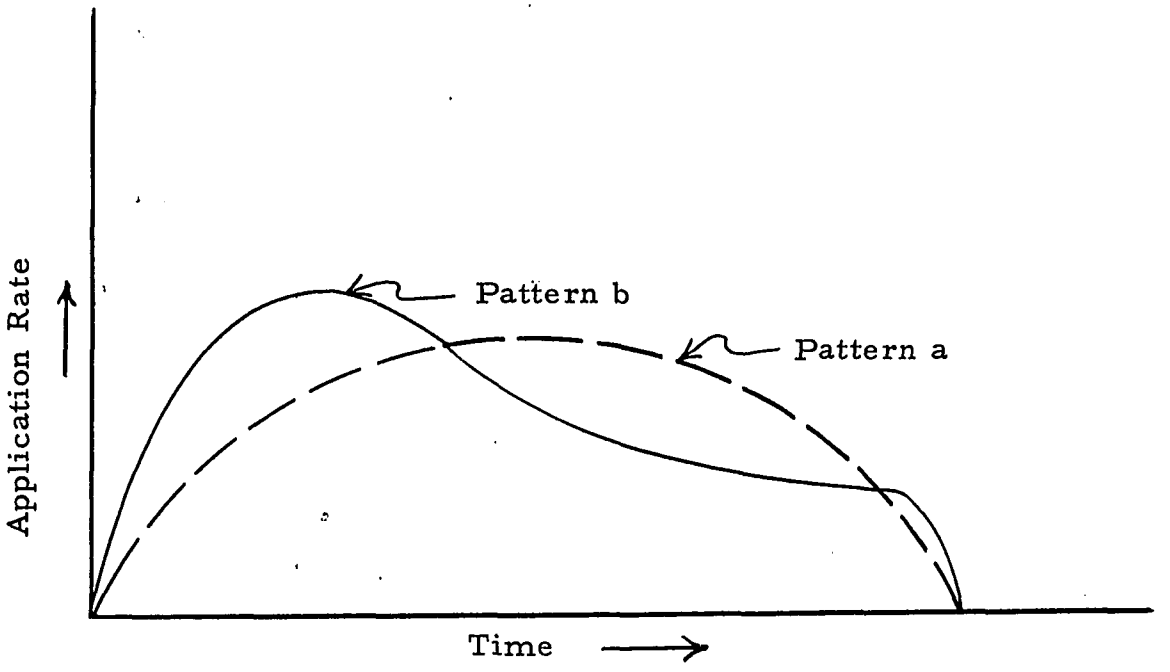

Figure 1.1 Center-pivot application rate patterns

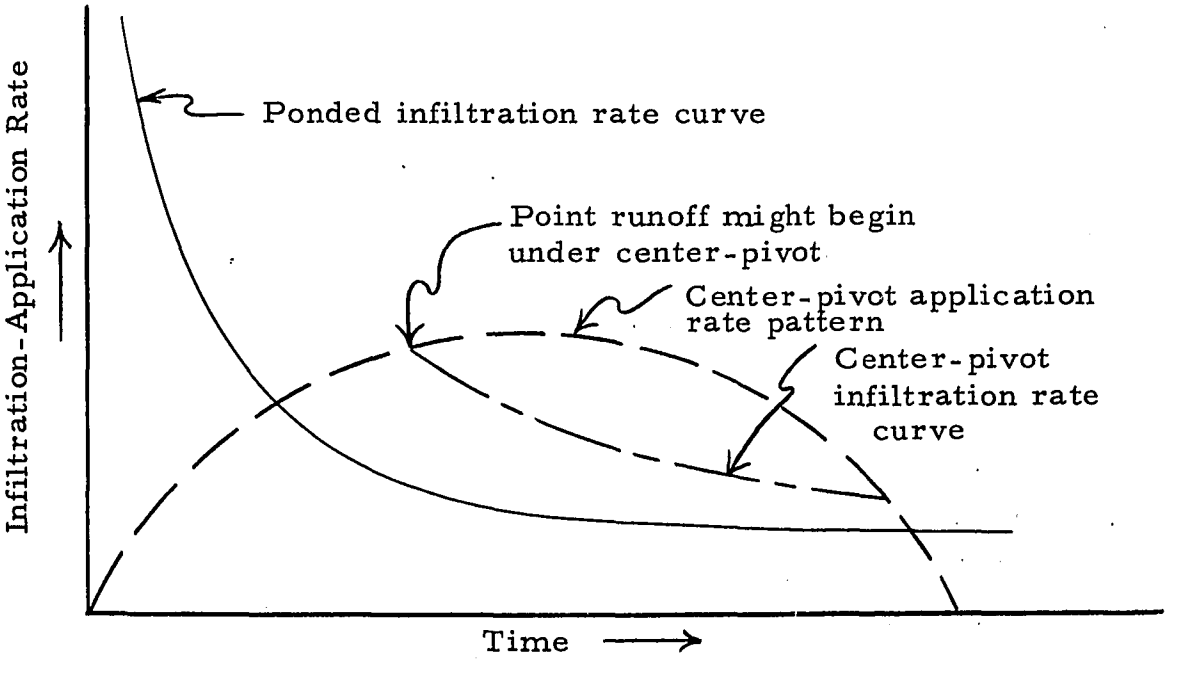

Figure 1.2 Ponded infiltration rate curve and infiltration rate curve for a center-pivot pattern

rate increases until it may exceed the infiltration rate of the soil, thereby resulting in surface runoff (Figure 1.2).

The purpose of this study is to evaluate the effect of the application rate pattern on runoff under moving sprinkler laterals and to develop a prediction technique for evaluating infiltration and runoff under several application rate patterns.

Scope of Research

Laboratory experiments were conducted to simulate two different series of sprinkler application rate patterns. The first series consisted of one constant and two 2-step application rate patterns. The second series consisted of three simulated center-pivot application rate patterns. Two or three tests, using six plots per test, were run of each pattern. For each test, runoff was measured with time which allowed computation of infiltration rate.

Two soils - sandy clay loam and loam - were used in the experiments. Soil parameters measured included initial moisture content, density, and moisture-tension-relative permeability relationships.

A numerical model incorporating measured soil parameters was utilized to obtain one-dimensional, vertical infiltration solutions. With the numerical model, it was possible to change one variable at a time, thereby allowing an evaluation of the effect of each variable upon

infiltration and runoff. With actual experiments using soil, it is not always possible to change one variable without influencing others.

In order to verify the model, the initial conditions and application rate patterns of the laboratory experiments were used in the numerical model. After verifying the model, the parameters were varied to extend the model to conditions beyond the laboratory infiltration experiments.

Chapter II

LITERATURE REVIEW

Considerable literature has been written on water infiltration under rainfall, surface irrigation, and sprinkler irrigation. The effects of many variables on infiltration have been studied. Equations have been proposed which attempt to simplify the study of infiltration. Numerical models to study infiltration and water movement in the soil have become popular in the last ten years. Each of these areas will be examined in this literature review.

Infiltration Variables

Water infiltration into soil is a complex process. Small changes in physical and chemical actions cause large changes in infiltration rates. The first section of the literature review will examine some of the infiltration variables as studied by other researchers.

Soil Physical Properties

Soil can be considered to consist of three phases: the solid, solution, and gas phases. The solid phase consists of the soil particles. The solution and gas phase occupy the space between the soil

particles. This space is called pore space and consists of irregularly-shaped interconnected capillaries or small tubes.

During vertical infiltration, water enters the soil at the surface and flows through the pore space because of two main forces acting on the water; namely, gravity and capillarity.

The ratio of the volume of pore space to the bulk volume of the soil is called porosity. Primary porosity is the pore space between individual soil grains, while secondary porosity is between aggregates of soil grains. A soil having a relatively high value of secondary porosity is called a structured soil.

Total porosity and pore space distribution have a significant effect on the hydraulic behavior of a soil. Porosity and pore size are affected by mean particle size and distribution, the degree of structuring, and the shape of the particles. Some of the empirical and semi-theoretical equations which related permeability or conductivity to some of these physical properties of soils will now be presented.

The Fair-Hatch equation (18), which is listed below, gives the permeability of a sand as a function of porosity, packing, particle shape, and particle size.

$$k = \frac{1}{A' \left[\frac{(1-\phi)^2}{\phi^3} \left(\frac{B'}{100} \sum_{v=0}^{N} \frac{P_{v+\frac{1}{2}}}{d_{m_{v+\frac{1}{2}}}} \right)^2 \right]} \qquad (2.1)$$

in which

k = intrinsic permeability, a function of the geometry of the media for porous media that are stable in the presence of the fluid occupying them.

A' = a packing factor

ϕ = porosity

B' = a shape factor

$P_{v+\frac{1}{2}}$ = percentage of sand held between adjacent sieves v and v+1

N = number of sieves used

d_m = geometric mean of rated size of adjacent sieves v and v+1.

According to Equation 2.1, increasing the porosity from 0.4 to 0.5 will triple the permeability, and increasing the average particle diameter by 20 percent increases the permeability 44 percent.

The Carmen-Kozeny equation (6) is somewhat similar to the Fair-Hatch equation.

$$k = \frac{\phi^3}{s^2 k_s T} \qquad (2.2)$$

in which

k and ϕ = defined in Equation 2.1

s = specific surface of porous medium

k_s = a pore shape factor

T = tortuosity of the flow path.

Both the Fair-Hatch and Carmen-Kozeny equations (Equations 2.1 and 2.2) are more accurate in determining the intrinsic permeability of sand than of other soils. These equations do give an indication of the importance of certain factors, particularly porosity, for describing infiltration into soils.

Moisture Content

Moisture weakens the bonds between soil particles and lubricates the soil particles. An increase in moisture content causes an increase in settlement for most loosely packed soils (27). Since moisture tension forces depend on moisture content, Keller (27) theorized that the total strength of aggregates of some moistened soils is almost wholly dependent on moisture tension forces.

Day and Holmgren (11) used micro-photography to study compression in soils. They found that aggregates lose strength and deform particularly in the area of contact between aggregates. As shown in Equations 2.1 and 2.2, a small percentage decrease in porosity causes a much larger percentage decrease in permeability. Therefore, deformation of aggregates caused by moisture can decrease permeability considerably.

Surface puddling results in considerable disruption of the surface soil aggregates (3). On a disturbed soil, the bulk density increases during wetting, particularly at the surface, thereby reducing the infiltration rate.

The degree of saturation has a very significant effect on the infiltration rate of a soil. An increase in saturation decreases the capillary pressure, thereby decreasing the potential gradient of the capillary force which reduces the moisture movement. An increase in saturation increases the relative permeability, thereby partially offsetting the decrease in gradient; however, normally the gradient decreases faster than the relative permeability increases.

An increase in saturation also provides less available water storage which causes the wetting front to advance faster. As the wetting front advances faster, the gradient of the capillary pressure at the surface decreases faster, which reduces the infiltration rate. Other effects of moisture content will be discussed under swelling and shrinking.

Water Drop Energy

Surface puddling caused by a saturated condition is only one factor causing a crust to be formed at the soil surface. Another factor which may be much more important is the water drop energy as the energy is dissipated in the surface layer of the soil. Many researchers have studied the decrease in infiltration rate caused by increased drop energy.

Bityukov (3) applied water on a loam soil at the rate of 0.5 mm per minute using various drop sizes. He examined the relationship

between percent of disruption of aggregates and diameter of drops. The percentage disruption of aggregates was checked by observation of individual soil particles before and after irrigation. A 1.0 mm drop size caused a 5.4 percent disruption of aggregates, a 2.3 mm drop size caused a 11.2 percent disruption of aggregates, and a 5.2 mm drop size caused a 14.0 percent disruption in aggregates.

Levine (32) studied the effect of sprinkler drop size on infiltration into six soils (Figure 2.1). Approximately 5 to 60 percent decrease in infiltration rate was observed by Levine as the apparent drop diameter increased from a range of 0-5 mm to a range of 15-25 mm.

Levine did not measure actual drop size but measured the wetted diameter a drop caused when falling on a paper towel. The wetted diameter was termed apparent drop size. Frost and Schwalen (21) actually measured drop sizes using a sprinkler with the same nozzle sizes Levine used. Correlating Levine's and Frost and Schwalen's data gives the following approximate relationships: 2.5 mm apparent drop diameter = 0.4 mm actual drop diameter, 10 mm apparent drop diameter = 1.2 mm actual drop diameter and 20 mm apparent drop diameter = 3.0 mm actual drop diameter.

Many center pivots have much larger sprinklers than Levine used. Larger drops would result from the larger sprinkler causing greater decreases in soil infiltration rates.

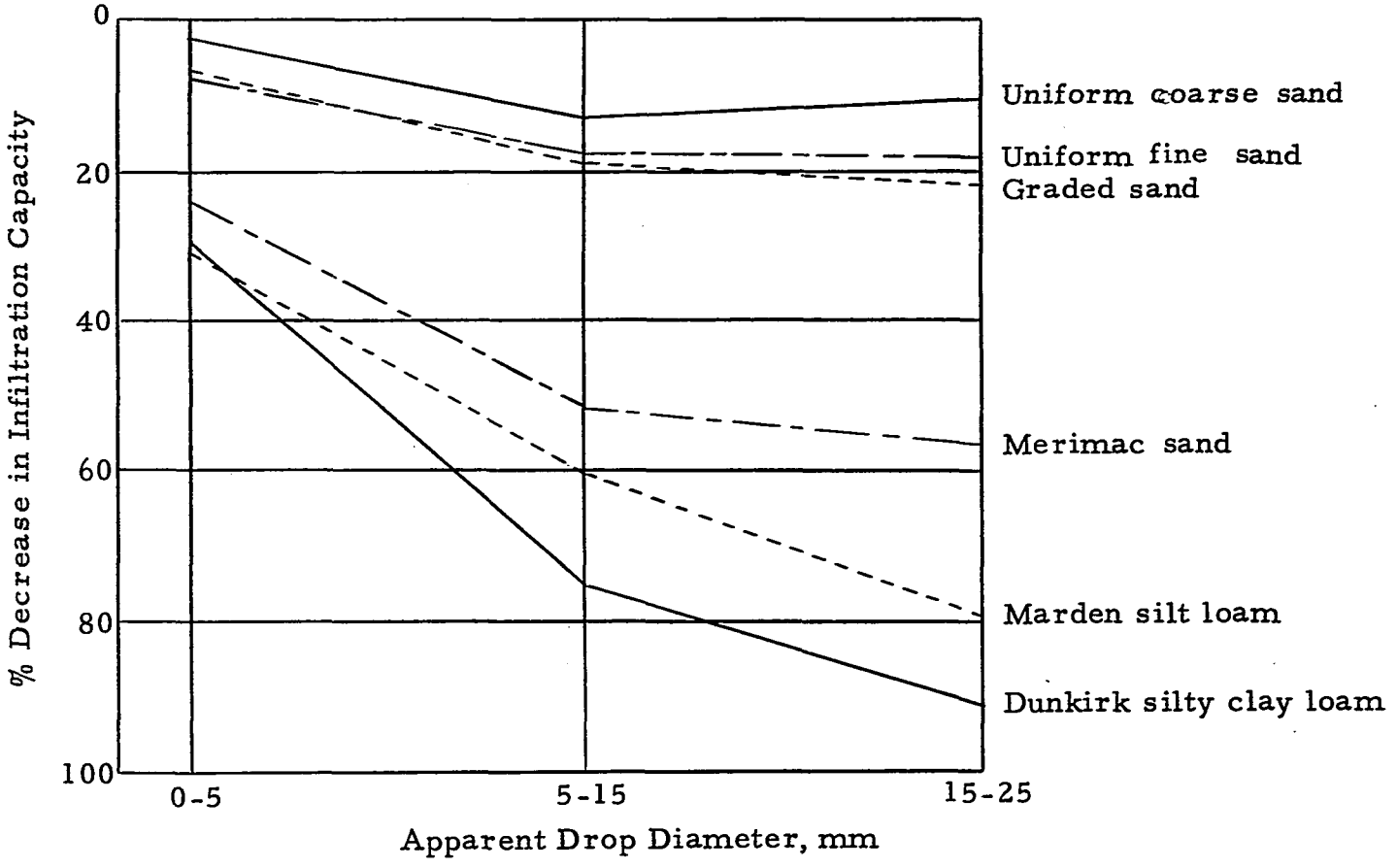

Figure 2.1 Effect of impact of various size drops on infiltration (32)

Ellison and Slater (17) studied the relationship between drop velocity and infiltration on four soils composed primarily of silt and fine sand. As the drop velocity increased from 0 to 20 feet per second, the infiltration rate at the end of one hour decreased from a range of 2.0 to 6.7 inches per hour to nearly zero. The infiltration rates at five minutes were greatly reduced as the drop velocity increased. The average rainfall intensity on these tests was very high, being approximately seven inches per hour.

Laws (31) compared infiltration into soil using different drop sizes. The infiltration rate decreased approximately 70 percent as the drop size increased from 1.0 to 2.2 mm.

Infiltration tests were undertaken by Bisal (2) using drop heights of 6.55 m and 0.46 m. The infiltration rate of a loam soil under the 6.55 m drop height was approximately one-half the rate under the 0.46 m drop height. The infiltration rate of a clay soil under the 6.55 m drop height was approximately 1/6 the rate under the 0.46 m drop height. The velocity at impact produced by the rainfall simulator at 6.55 m would be approximately three times the velocity for the 0.46 m drop height.

Surface Protection

Many tests have been conducted using rainfall simulators to compare infiltration of a bare soil with infiltration of the same soil

having a burlap, straw, or fiberglass protection. The protective cover is suspended a few inches above the soil surface. Duley (14) performed infiltration tests on a sandy loam soil and initially protected the surface with straw. The infiltration rate with the straw cover was 1.2 inches per hour. When the straw was removed, the infiltration rate was reduced almost immediately to 0.3 inches per hour. The crust was then removed and burlap placed over the soil. The infiltration rate with the burlap cover was 1.5 inches per hour. When the burlap was removed, the infiltration rate dropped rapidly to 0.25 inches per hour.

Two silt loams, a silty clay loam, and a clay loam with the surface protected by straw or other materials maintained a high infiltration rate for a considerable period of time (14). Once the protective cover was removed, the intake rate was quickly and severely reduced.

Swartzendruber, et al., (48) compared infiltration into several soils with and without fiberglass protection. Total infiltration amounts for a silt loam and a loam soil were three to four times higher into the fiberglass-protected surface as compared with the unprotected surface. Sprinkling tests on a sandy loam soil showed little difference in intake rate with and without a fiberglass cover.

Laboratory measurements of rain and no-rain permeability on fifty-seven different wet soils are given by Mannering (33). The

rain treatment consisted of applying simulated rainfall to soil samples from above. The no-rain treatment consisted of saturating soil samples from below. The mean ratio of permeabilities of rain over no-rain was 0.41. In only two of the fifty-seven soils was the permeability after thirty minutes higher for the rain treatment than for the no-rain treatment. These two soils were a silt loam and a fine, sandy loam. A gravelly, sandy loam and a sandy loam had thirty-minute rain/no-rain permeability ratios between 0.75 and 1.0. Three loams, one silty clay, one silty-clay loam, and one clay loam had thirty-minute rain/no-rain permeability ratios less than 0.29. The other forty-seven soils had rain/no-rain permeability ratios between 0.30 and 0.75. Surprisingly, one sand with only 4 percent silt and 2 percent clay content had a permeability ratio of rain over no-rain of 0.25; however, the permeability was quite high even after the rain treatment.

Mannering also compared infiltration in the field between seven protected and unprotected soils. Two one-hour 7.0 cm applications were made twenty-four hours apart. A sand showed no difference in intake rate between protected and unprotected applications the first day. During the second day, the unprotected/protected intake rate ratio was 0.70. On two sandy loams the unprotected/protected intake rate ratio was approximately 0.5 during the first day. The second day the ratio was approximately 0.3. With three silty loams the

ratio was between 0.2 and 0.5. A silty clay had an 0.7 ratio during the first day and a 1.0 ratio during the second day. All of these comparisons are final intake rate ratios.

Peale and Beale (39) compared infiltration into a sandy clay loam between straw incorporated into the soil and straw spread on the soil surface. Infiltration rates for the incorporated straw was twice the rate of the untreated bare soil, but only 1/10 the rate of the soil whose surface was protected from raindrop action by placing straw on the soil surface.

A protected surface can also result from a 20 mm water layer developing on the soil surface (38). Palmer's (38) tests showed that the drop impact stress increased as the water layer depth increased from 0 to approximately 5 mm. The water layer had to be deeper than 20 mm before the stress became less than the stress at the zero water depth.

McIntyre (35) divided impact of raindrops at the soil surface into four successive processes. These processes are: (1) a rapid wetting at the surface causing low cohesion and high splash rates; (2) formation of a crust on the surface, a decrease in splash and accumulation of water; (3) removal of the crust by water turbulence and an increase in permeability; and (4) percolation of sufficient water to cause dissipation of drop energy on the soil once more, and an increase in splash rate.

Application Rate

As the application rate increases, the drop energy per unit area also increases (assuming drop size does not change). Mantell and Goldberg (34) conducted a study to examine the effect of water application rate on the structure of a clay soil with high aggregate stability. Application amounts of 5.6 mm with a drop size of 2.59 mm and with a two meter height of fall were used. After water application, the air permeability of the wet crust was determined. Increasing the application rate from 1.7 to 3.4 mm per hour decreased air permeability 50 percent. Increasing the application rate from 3.4 to 20.7 mm per hour decreased the air permeability 50 percent further.

Moldenhauer and Long (36) used a rainfall simulator to apply water at rates from 3.4 to 7.0 cm per hour on a fine sand, a loam, a silt, a silty clay loam, and a silty clay. Total infiltration in 90 minutes was the same regardless of intensity rate except on the fine sand. On the fine sand, total infiltration increased from 5 to 7 cm as the intensity was increased from 3.4 to 7.0 cm per hour. Runoff on all soils with an intensity of 6.78 cm per hour began in one-half the time that runoff began with a 3.43 cm per hour intensity.

Infiltration decreased 50 percent on a silt loam soil used by Sor and Bertrand (45) when the simulated rainfall intensity was increased from 1.6 to 2.8 inches per hour. On a sandy loam soil, the

infiltration only decreased 20 percent as the intensity was increased from 1.6 to 2.8 inches per hour.

Crust Breakup

Tillage operations will break up a crust, thereby producing a disturbed soil with an increased infiltration rate. Sixty-five percent of the applied water occurred as runoff on an uncultivated crusted silt loam soil, but only 1.7 percent runoff occurred on the same soil with a broken surface on tests performed by Borst and Woodburn (4). Borst and Woodburn applied artificial rainfall at an intensity of 2.2 inches per hour for one hour. A straw mulch of two tons per acre was applied on the surface.

Swelling and Shrinking

As a soil shrinks, the pores increase in size and cracks begin to form. When moisture is added, the soil swells, closing the cracks and reducing the pore size.

The size of the pores has a very significant effect on the infiltration capacity of a soil. Corey (9) discusses Poiseulle's equation which shows the effect that the radius of a tube has on the fluid velocity in the tube.

$$\overline{u} = -\frac{r_t^2 \, \Delta H}{8\mu \, L} \qquad (2.3)$$

in which

$\bar{u}$ = average velocity in the tube

r_t = tube radius

μ = dynamic viscosity

H = hydraulic head

L = length of tube

The total flow through a tube is given below and shows that the flow is proportional to the fourth power of the tube radius.

$$q_t = A_t \bar{u} = -\frac{\pi r_t^4 \Delta H}{4\mu L} \qquad (2.4)$$

in which

q_t = total flow through a tube

A_t = cross sectional area of tube.

Reasons for Swelling

Schmehl[1] states that the interlayer bond is related to the amount of swelling. If the interlayer bond is relatively strong, polar molecules such as water cannot enter the basal plane and the clay or other mineral is essentially non-expanding. If the bond is weaker, the clay will swell in a polar solvent. Swelling is inversely proportional to bonding energy, and bonding energy is directly proportional to the amount of clay surface.

---

[1]Class Notes, Soil Chemistry, Ag 560, Colorado State University, Spring, 1971.

The first few layers of water molecules absorbed on the clay surface may be considered part of the clay surface and will affect some properties of the clay. The bonding energy holding the water molecules to the clay surface become progressively weaker with each successive water layer.

Each layer's surface has an electrical double layer resulting from ionic concentration in the free water. Both layers contain ions of the same charge causing the double layer on one clay surface to repulse or push away the double layer on the other clay surface. The adjacent clay surfaces are repulsed, causing soil swelling.

The amount of swell varies considerably with clay type (Table 2. 1) (50). Free swelling is defined as the increase in volume of the substrata upon the addition of a certain volume of water. The decreasing order of swell is montmorillonite > illite > halloysite > kaolinite.

Table 2. 1 Free swelling data for various clay minerals (in percent) (50)

Ca--montmorillonite	45-145
Na--montmorillonite	1,400-1,600
Na--hectorite	1,600-2,000
Illite	15-60
Kaolinite	5-60

The nature of the ion adsorbed on the surface affects swelling as shown in comparing the Ca and Na montmorillonite. Baver and Winterkorn (1) found that, for Wyoming bentonite, swelling decreased in the following order: sodium > lithium > potassium > calcium > magnesium > hydrogen.

The magnitude of swelling also varies with variation in particle size distribution, electrolyte content of the solution phase, void size, and distribution of void sizes.

Time Dependence of Swelling

When water infiltrates into a soil, the least resistance to flow occurs in the larger inter-granular spaces. More resistance, or slower flow, occurs in the inter-crystal spaces and smaller inter-granular spaces. The slowest flow occurs into the interlayer regions which must expand to accept water molecules. The interlayer region is the area where most of the swelling occurs. Baver and Winterkorn (1) reported on rate of water intake with various colloids and ions adsorbed on the clay surface. As shown in Figure 2.2, time has considerable effect on swelling. The rate of water intake also varies considerably with what ion is adsorbed on the surface. The rate of water intake was the slowest percentage-wise with the colloids of highest ultimate swells: e.g., Li and Na Putnam colloids. Many researchers--e.g., Winterkorn and Baver (53), Tressler and Williamson (49), Dubose (13), --show soils continue to swell for hours or days.

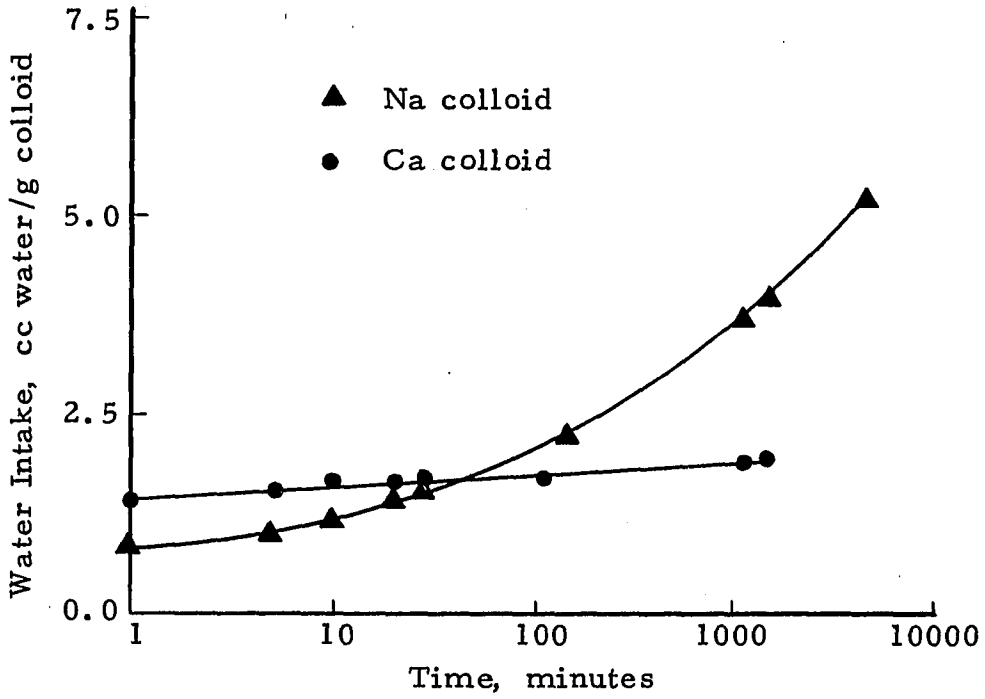

Figure 2.2 Cumulative water intake by Putnam colloid saturated with different cations (1)

Infiltrating Fluid

The most common infiltrating fluid--water--usually contains impurities. The capillary potential is directly proportional to the surface tension, which is reduced by impurities.

Hydraulic conductivity is indirectly proportional to the solution viscosity as shown in Equation 2.3. The fluid viscosity is changed by adding impurities and by the interaction of the water with the soil. Water near the soil particles has an increase in viscosity because of an electrical potential between the water and the soil. This potential can have an important effect on hydraulic conductivity in very fine-textured soils.

Infiltration Equations

Measuring the variables affecting infiltration is difficult. The effect some variables have on infiltration is impossible to define at present. Some empirical and semi-theoretical equations have been proposed to simplify the study of infiltration. Some of these equations will now be reviewed.

Green-Ampt (22) proposed an infiltration law:

$$I = K(h + D' - P_{b/\gamma})/D' \qquad (2.5)$$

in which

I = rate of infiltration

h = ponded water depth on the surface

P_b = air entry pressure or bubbling pressure

γ = specific weight of water

D' = distance from the soil surface to the wetted front

K = saturated hydraulic conductivity of the soil.

The advancing water front is assumed to be a precisely-defined surface. This front separates saturated soil behind it, of uniform hydraulic conductivity K, from unsaturated and as yet uninfluenced soil beyond it.

Kostiakov (30) developed an empirical equation stating

$$I = I_o t^n \qquad (2.6)$$

in which

I = infiltration rate at time t

I_o = infiltration rate at unit time

t = time elapsed from start of infiltration

n = constant, $-1 < n < 0$

In this equation, I goes to zero as t become infinite, which is not true under vertical infiltration.

Horton (26) proposed an intuitive equation

$$I = I_c + (I_o - I_c)\, e^{-k_f t} \qquad (2.7)$$

in which

I_c = final or steady state infiltration rate

t, I, I_o = defined for Equation 2.6

I' = infiltration rate at $t = 0$

e = base of Naperian logarithms

k_f = constant.

Horton assumed that the process involved in the reduction of I as rain continued is of a similar nature to exhaustion processes. Included were the processes of rainpacking, in-washing, breaking down of the crumb-structure of the soil, the swelling of colloids and in cases where they occur, the closing of cracks. Horton attributed most changes in I to occur at or close to the surface, except for pure sands and clayey soils with deep and numerous cracks.

For soils with a restricting strata, Holton (24) proposed an infiltration equation

$$I = E' F_p^G + I_c \qquad (2.8)$$

in which

I and I_c = defined in previous equations

F_p = storage potential of the soil above an impeding strata; equals total porosity minus antecedent water expressed in units of L

E' and G = constants specified by soil type and surface and cropping conditions.

Equation 2.8 allows for the effect of initial soil moisture content. The equation also allows the infiltration rate to become a constant value. The problem is determining the control depth to be used in computing the storage potential, F_p. Holton, et al., (25) further divided F_p into gravitational water and plant-available water capacity.

Philip (41) derived an equation from an analysis of the partial differential form of the moisture flow equation applied to water movement in vertical columns.

$$I = 0.5 F t^{-0.5} + Y \qquad (2.9)$$

in which

F = constant which Philip called soil sorptivity

Y = a parameter related to soil hydraulic properties

I and t = previously defined.

The infiltration equations described above have several limitations. Most parameters cannot be determined from physical properties of the soil. Infiltration from a ponded surface is the only upper boundary condition considered. For sprinkler irrigation or rainfall, a ponded condition is usually not the initial upper boundary condition.

Infiltration Studies Involving Non-Ponded Conditions

This section contains published analytical and numerical solutions to infiltration problems which do not necessarily involve ponded conditions at the surface.

Analytical Solutions

El-Shafei (16) hypothesized that "the time at which surface ponding occurs, t_s, is the time at which the cumulative rain (sprinkler) infiltration is equal to the cumulative flooded (ponded) infiltration." The surface ponding time, t_s, is the time runoff begins under rainfall or sprinkling.

In equation form:

$$Rt_s = \int_0^{t_s} I_o t^n \, dt \qquad (2.10)$$

in which

R = application rate

n = a constant

I_o = flooded infiltration rate at unit time.

Integrating the right side of Equation 2.10 results in:

$$Rt_s = I_o \frac{t_s^{1+n}}{1+n} \qquad (2.11)$$

Solving for time of surface ponding, t_s, under sprinkler irrigation results in:

$$t_s = \left[\frac{I_o}{(1+n)\,R} \right]^{\frac{-1}{n}} \qquad (2.12)$$

El-Shafei does not predict what form the infiltration rate curve takes after runoff begins. All of the tests he presents have either a flooded surface condition or a constant application rate.

Kincaid, et al., (28) studied runoff under center pivot sprinkler systems. Their proposed modified potential infiltration rate, I_m, before runoff began was

$$I_m = I D_p / D_a, \tag{2.13}$$

in which

I = flooded infiltration rate at time t

D_p = potential depth of infiltration at time t, obtained by integrating the flooded infiltration rate, I, over time 0 to t

D_a = actual water depth applied over time 0 to t.

Using a constant application rate, R,

$$I_m = R \text{ at } t = t_k, \tag{2.14}$$

in which

t_k = surface ponding time for Kincaid, et al. (28).

The depth applied, D_a, at time of runoff, t_k, is

$$D_a = R t_k. \tag{2.15}$$

The potential infiltrated depth, D_p, at time t_s is

$$D_p = \int_0^{t_k} I \, dt, \tag{2.16}$$

and

$$I = I_o t_k^n \text{ at } t = t_k . \tag{2.17}$$

Substituting for I in Equation 2.16

$$D_p = \frac{I_o t_k^{1+n}}{1+n} . \tag{2.18}$$

Substituting values from Equations 2.14, 2.15, 2.27 and 2.18 into Equation 2.13 results in

$$R = (I_o t_k^n) \frac{\left(\frac{I_o t_k^{1+n}}{1+n}\right)}{R t_k} . \tag{2.19}$$

Solving for surface ponding time, t_k

$$t_k = \left[\frac{I_o}{R\sqrt{1+n}} \right]^{-\frac{1}{n}} . \tag{2.20}$$

The ratio for surface ponding times of Kincaid, et al., (26) (Equation 2.20), to El-Shafei (16) (Equation 2.12), using a constant application rate, is

$$\frac{t_k}{t_s} = \sqrt{1+n}^{-\frac{1}{n}} . \tag{2.21}$$

For $n = -0.5$, $\frac{t_k}{t_s} = 0.5$.

Kincaid, et al., (28) defines the infiltration rate after runoff begins as

$$I = I_o (t - \Delta t)^n \tag{2.22}$$

in which

$$\Delta t = t_k - t_o$$

and defining t_o by the equation

$$I (\text{at } t = t_o) = I_m (\text{at } t = t_k). \tag{2.23}$$

Numerical Solutions

Another approach to the solution of vertical infiltration problems is numerical solution of moisture flow equations. Some of the equations which are presently available will be described below.

Darcy (10) formulated a law for saturated flow in soil

$$Q = - K \frac{\Delta H}{\Delta Z} \tag{2.24}$$

in which

Q = flow velocity

Z = vertical dimension measured positive downward from the soil surface

K = saturated conductivity

H = hydraulic head.

Childs and Collis-George (7) (8) verified Darcy's law under unsaturated flow conditions. Darcy's law for unsaturated flow is

$$Q = - K k_r \frac{\Delta H}{\Delta Z} \tag{2.25}$$

in which

k_r = relative permeability or relative conductivity, or ratio of unsaturated conductivity value to saturated conductivity.

The continuity equation for one dimension is

$$\frac{\partial Q}{\partial Z} = - \frac{\partial(\phi S)}{\partial t} \tag{2.26}$$

in which

ϕ = porosity

S = volumetric saturation, $\frac{\text{volume of water}}{\text{volume of pores}}$

t = time.

Combining Equations 2.25 and 2.26 results in

$$\frac{\partial}{\partial Z} (K k_r \frac{\partial H}{\partial Z}) = \frac{\partial(\phi S)}{\partial t} . \tag{2.27}$$

Substituting $- Z + \psi$ for H produces

$$\frac{\partial(\phi S)}{\partial t} = K \frac{\partial}{\partial Z} (k_r \frac{\partial \psi}{\partial Z}) - K \frac{\partial k_r}{\partial Z} \tag{2.28}$$

in which ψ is the capillary potential.

This equation (Equation 2.28) is sometimes called the Richards equation after L. A. Richards (43). To solve this equation at any point in the soil requires a knowledge of the relationships among ψ, S, and k_r for the particular soil. Boundary conditions are required,

such as a sprinkler application rate at the surface and a water table at the bottom surface. The initial conditions required usually consist of specifying ψ or S throughout the soil at t = 0.

A solution of Equation 2.28 will provide water content and pressure head curves at a particular time. Thus, the flow of water in the soil can be followed or described.

No analytical solution exists for Equation 2.28. However, many numerical solutions have been published. The techniques continue to become more sophisticated to solve more complex problems.

Klute (29) and Philip (40) numerically solved Equation 2.28 for horizontal and vertical flow from a constant surface saturation. For horizontal flow, the last term $K \frac{\partial k_r}{\partial Z}$ in Equation 2.24 does not appear and Z is a horizontal distance, which considerably simplifies the solution. A constant surface saturation is also a simplified and restricted solution. However, these earlier investigations are very important because they represent the beginning of the numerical solutions for moisture flow problems.

Hanks and Bowers (23) allowed for a two-layered system of soils. Solutions were obtained for vertical upward and vertical downward infiltrations and for horizontal infiltration into two soils. Uniform initial moisture contents were used.

Edwards and Larson (15) modified Hanks and Bowers solution, taking into consideration the surface seal produced under rainfall.

Good agreement was obtained between estimated and field-measured infiltration for a silt loam protected from raindrop impact when water content, capillary pressure, conductivity relations, measured on undisturbed cores, were used as computer input. When the surface was unprotected from raindrop impact, infiltration was overestimated unless the surface seal was taken into consideration. As the surface seal develops, the suction through the seal is shown to increase.

These first solutions of Klute (29), Philip (40), and Hanks and Bowers (23) allow for a constant inlet boundary condition, which is applicable only to a flooded condition. Whisler and Klute (52), Rubin (44), and Freeze (20) presented infiltration solutions for either rainfall or ponding at the upper boundary. Whisler and Klute studied the phenomenon of hysteresis in columns with non-uniform initial moisture contents. Rubin used a uniform initial moisture content.

Smith and Woolhiser (47) allowed for rainfall and ponded conditions and included overland flow resulting from runoff. Good agreement was obtained between measured and predicted hydrographs for a 40-foot laboratory flume and for an experimental watershed.

Use of Equation 2.28 to study moisture flow in soil has increased in recent years for several reasons. Rapid solutions of the equation are obtained using high-speed computers. With a computer model, it is possible to change only one variable at a time to determine its effect upon the solution. With actual experiments using

soil, it is not always possible to change one variable without influencing others.

CHAPTER III

EXPERIMENTAL DESIGN

The purpose of this study is to evaluate the effect of application rate patterns on surface runoff under moving sprinkler laterals and to develop a technique (model) for predicting infiltration and runoff under several application rate patterns.

Field or laboratory experiments and models can be utilized to study and predict infiltration or runoff. A model is usually easy to work with after it is developed; however, if a model is used by itself many infiltration variables may be inadvertently omitted. Variables are easier to control in the laboratory than in the field. Therefore, laboratory experiments were chosen to study infiltration and runoff under several types of sprinkler irrigation application rate patterns. The results of the laboratory experiments could then be used in verifying a numerical model which described infiltration and runoff under a variety of application rate patterns.

Patterns

Two different sets of application rate patterns were used in the laboratory experiments and model simulation (Figure 3.1). The first set consisted of one constant and two 2-step application rate

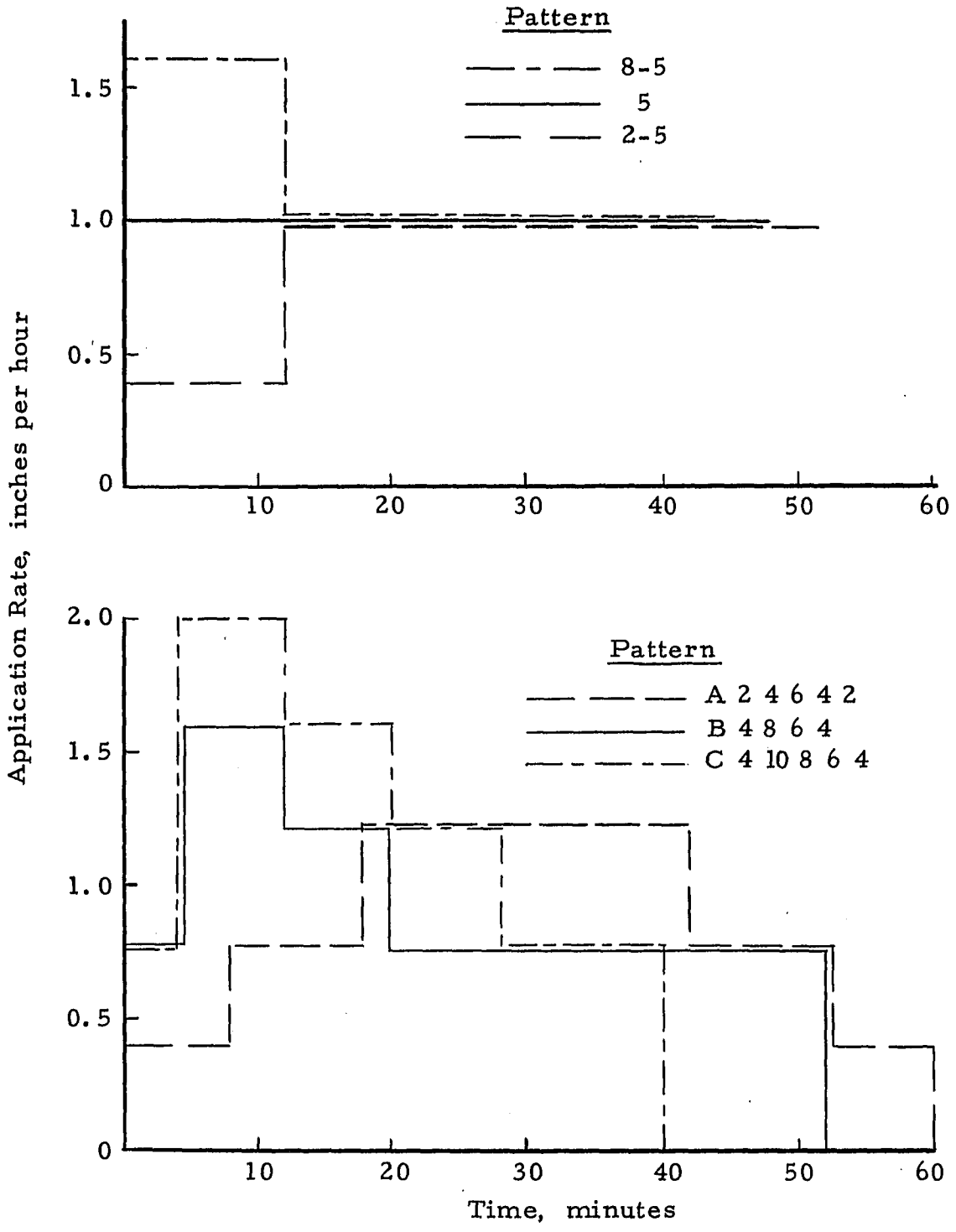

Figure 3.1 Application rate patterns used in the laboratory experiments and model simulation

patterns, while the second set consisted of three simulated center-pivot application rate patterns.

The first set of patterns was used to determine relationships between infiltration rate with time and to determine relationships between infiltration rate and depth of intake. The first set of patterns are also essential for verifying the model. The second set of patterns was used to study the effect of the application rate pattern on runoff and to compare laboratory results with the model predictions.

Laboratory Experiments

In the laboratory experiments, water was applied to the soil which was placed in eight soil compartments (plots). Water, which did not infiltrate into the soil, ran off the surface and was collected and measured. Between tests, heated air was forced through the soil to dry the soil (Figure 3.2).

Two types of soil were used to study a wider range of conditions than one soil would have permitted. One soil contained a high percentage of sand, and the other soil contained a high percentage of silt.

An undisturbed soil would have been desirable for the laboratory experiments, but there was no practical way of transferring undisturbed samples from the field to the laboratory. However, field conditions were approximated by not disturbing the soil between tests.

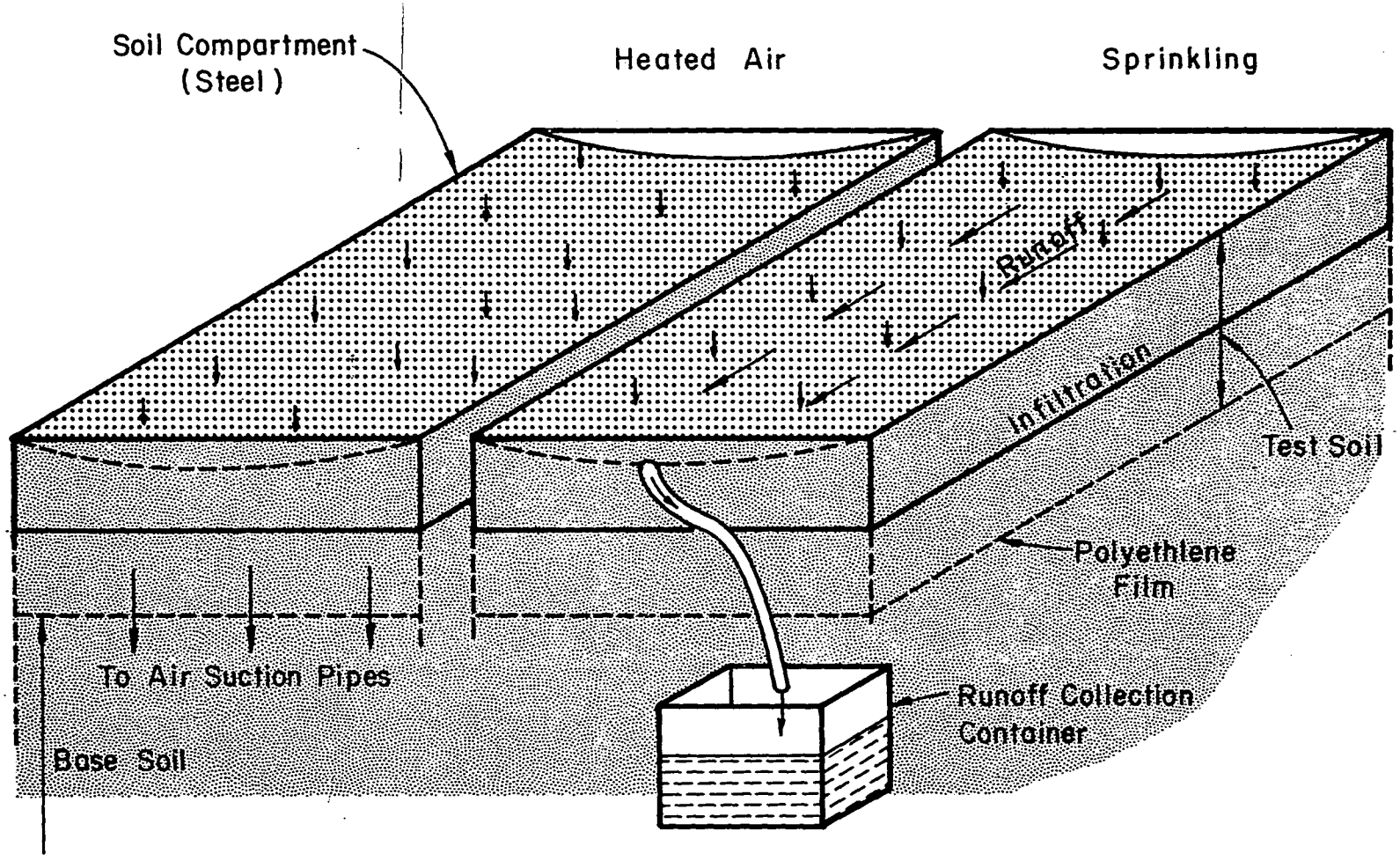

Figure 3.2 Sprinkling and drying of soil

Irrigation in the field is performed when the soil moisture content is below field capacity. Therefore, heated air was forced through the soil to dry the upper soil below field capacity. Drying the soil allowed shrinking to occur.

Drop size was not treated as a variable in this experiment because of the additional time which would have been required to perform an adequate study of drop size effect. Many problems would be encountered in changing drop size while changing application rate. Also, in the field, crops may protect the soil from the sprinkler drops reducing the drop size effect. A fine spray was used for the experiments to essentially eliminate the effects of drop size.

Large drops would have caused more crusting than was caused by the fine spray used; however, a crust did form as a result of puddling.

The initial moisture content was not changed much in the laboratory experiments because of the difficulty in varying the moisture content. The initial moisture content could have been changed more if the soil had been removed, dried, and replaced but this disturbed condition was not considered desirable in these tests.

Numerical Model

The physical process being modeled involved applying water to the surface of a porous media, water infiltration into the porous media, and water runoff at the surface when the application rate exceeded the infiltration rate (Figure 3.3). The porous media was soil and had to be described in the model in terms of porosity, initial moisture contents, saturated conductivities, and relationships between moisture content, capillary pressure, and relative permeability. Movement of water into and through the soil was described by Equation 2.28.

The numerical model was very versatile but had to be calibrated to reasonably fit the laboratory experiments. Because the model was versatile it could handle stratified soils, any initial moisture content, and nearly any boundary condition. However, the model did not allow for a change in conductivity caused by swelling.

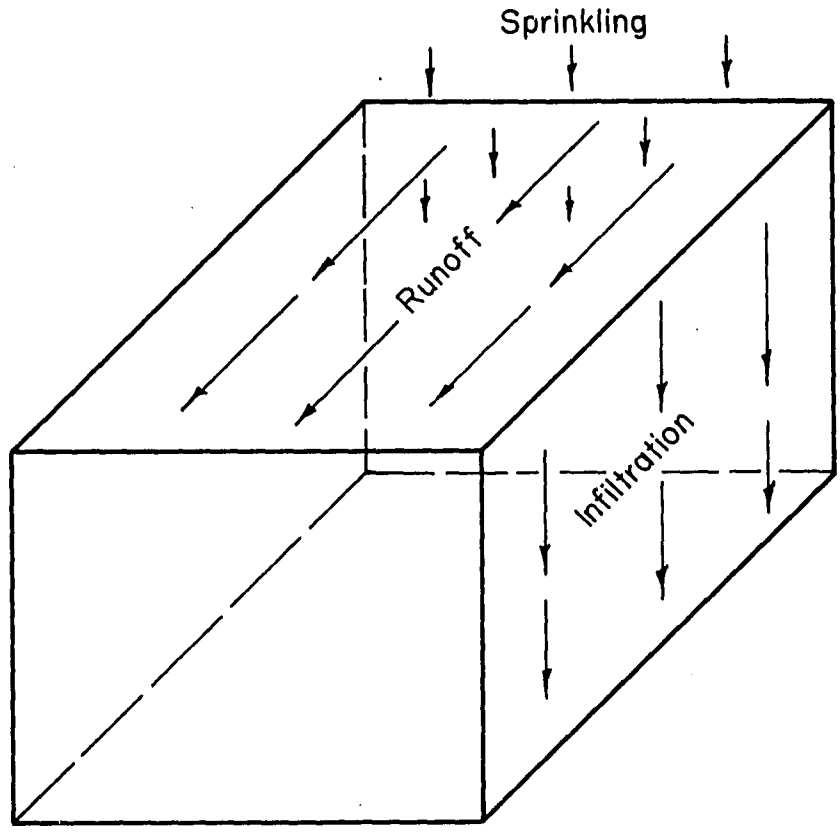

Figure 3.3 Model simulating sprinkling, infiltration, and runoff

Chapter IV

PROCEDURE

Laboratory Infiltration Experiments

Equipment

The main components of the equipment are the soil compartments separating the plots, soil drying equipment, traveling spray bar, runoff collection containers, and tensiometers (Figures 4.1 and 4.2).

Soil Separation

Soil was placed in eight compartments, each having surface dimensions of 12" x 23.5". Each compartment had sheet steel sides 5" deep with polyethylene film extending an additional 4" to the bottom of the test soil. These dividers defined the drainage area of each compartment and prevented lateral water movement between samples. The bottom of each compartment was open to permit contact with the base soil.

Soil Drying Equipment

Air pipes were placed in a clay loam soil in the base. The lower soil acted as a sump for the water to drain into from the test soil.

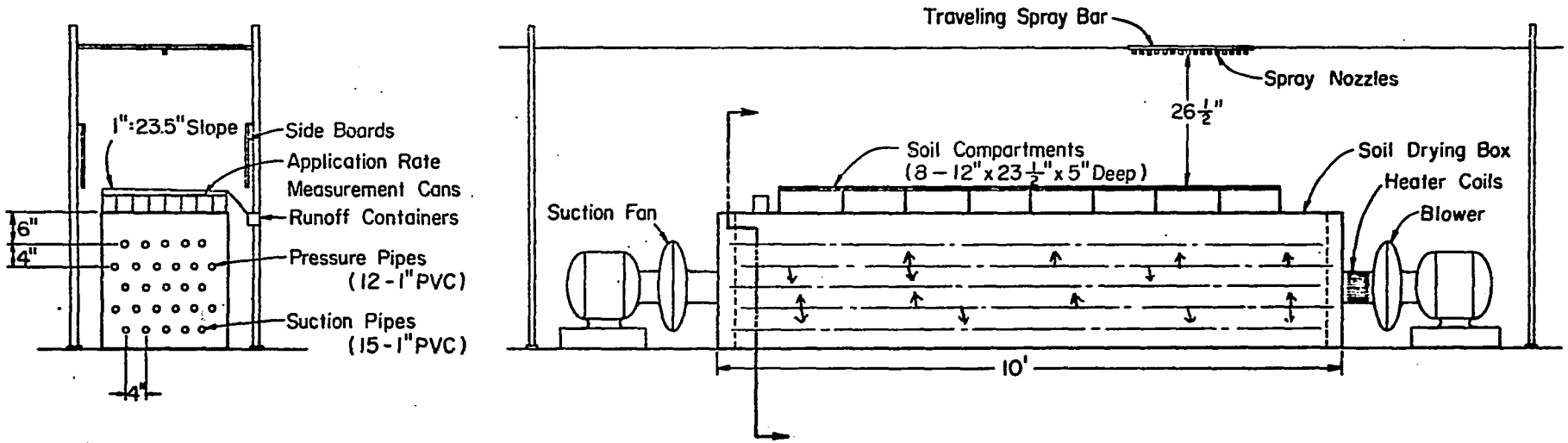

Figure 4.1 Apparatus used for laboratory sprinkler infiltration tests showing air flow between pressure and suction pipes in the soil mass

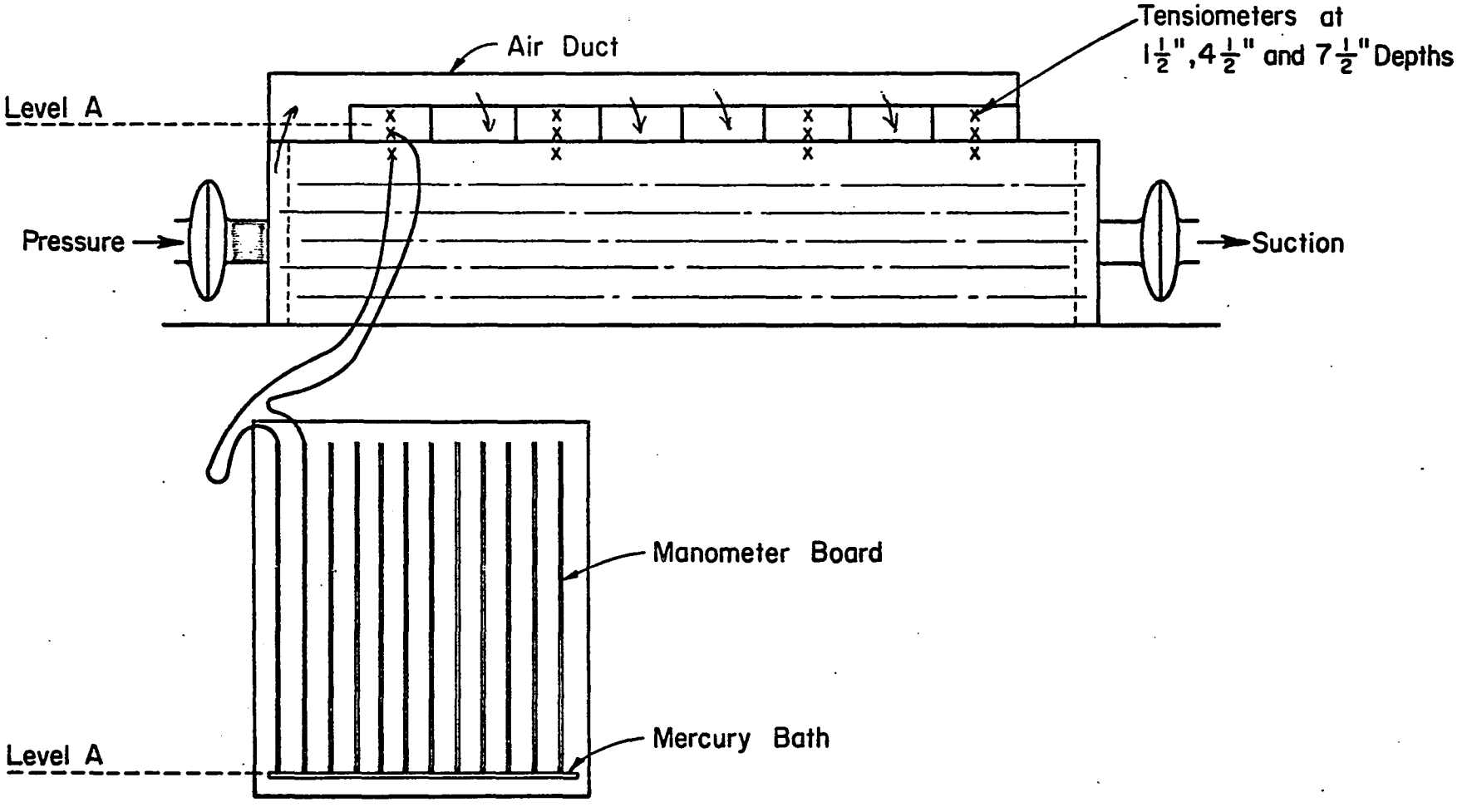

Figure 4.2 Schematic drawing showing location of tensiometers and air duct causing heated air to flow through the soil surface to suction pipes

While a test was being conducted, the wetting front did not extend into the lower soil.

Initially, tests were run and the soil was dried by passing heated air through the soil from the pressure pipes to the suction pipes (Figure 4. 1). However, it was difficult to bring the moisture level of the surface soil much below field capacity.

To obtain drier soil, an air duct was placed over the soil (Figure 4. 2). Most of the pressure pipes were plugged causing the majority of the air to pass through the surface of the soil down to the suction pipes.

Spray Bar

The sprinkler apparatus consisted of a traveling spray bar with valve controlled nozzles which allowed application rates of 0. 2 to 6. 4 inches per hour. Tests were conducted to obtain a nozzle with a uniform application perpendicular to the lines of travel. The nozzle chosen was an 8001E of Spraying Systems Company operated at 50 ± 3 psi. Each nozzle applied approximately 0. 2 inches per hour.

Water was supplied to the traveling spray bar from a tank pressurized with air which was controlled by a regulator.

The depth applied during a test was measured with eight measurement cans which were placed next to the soil compartment at the suction end. The cans were placed perpendicular to the line of travel of the spray bar and were used to determine uniformity of the pattern.

Runoff Collection

The soil surface in the soil compartments had a slope of 2.4 percent towards the runoff outlet and also had a small slope to the center of the compartment to prevent ponding. Runoff was collected in graduated containers. Volume of runoff was read and recorded at two or four minute intervals. The rate of runoff was calculated by dividing the runoff volume by the time interval. The intake rate was the difference between the application rate and the rate of runoff.

Tensiometers

Tensiometers connected to manometers were used to monitor the soil moisture tension (Figure 4.2). Twelve small tensiometers (three per compartment) were installed in soil compartments 1, 3, 6 and 8 as numbered from the suction end. These tensiometers were installed at the end opposite the outlet end (Figure 4.2).

Soils

The topsoil was sieved through a 2.362 mm sieve. Analyses of the two soils used in the experiments are shown in Table 4.1.

After the soil was first placed in the compartment, it was sprinkled a number of times for settlement purposes. The crust was removed and the soil compartments refilled after initial settlement and between each series of tests. Data from the first four runs of a series were not used because of the initial sharp decrease in

Table 4.1 Analyses of soil

Texture	Sand %	Silt %	Clay %	Organic Matter %	Conductivity (Salts) mmhos/cm
Sandy clay loam	59.8	19.0	21.2	1.0	1.9
Loam	34.6	46.0	19.2	1.3	1.0

infiltration rates before the soil stabilized. The continued small decrease in infiltration rates was attributed to formation of a crust and microbiological activity in the soil.

Test Procedure

The tensiometer readings were recorded before beginning a test. After filling the tank with tap water, the tank was pressurized and a selected number of spray nozzles on the traveling spray bar were operated. When the pressure reached 50 psi, the spray bar was started in motion, spraying back and forth across the soil compartments.

Every two or four minutes the runoff volumes in the runoff containers were read and recorded. The runoff volumes in the containers were read in the same sequence from left to right at the end of each time interval. Nozzles were turned on or off at specified times as required to produce the desired application rate pattern.

At the end of the test, tensiometer readings were recorded and the volume of water in each application rate measurement can was recorded.

After the air duct was replaced over the soil compartments, the pressure and suction blowers and the heating coils were turned on to dry the soil 15 hours for two nights - or 30 hours total - prior to the next test run.

Numerical Simulation Model

Equations and Assumptions

Smith (46) describes a combination infiltration and overland flow model. The infiltration component of the model, with modifications, is used in this study.

The soil-moisture movement is described by the following equation.

$$\frac{\partial(\phi S)}{\partial t} = K \frac{\partial}{\partial Z}\left(k_r \frac{\partial \psi}{\partial Z} - K \frac{\partial k_r}{\partial Z}\right) \qquad (2.28)$$

The following assumptions are implied by the use of this equation.

1. The gas phase moves under negligible pressure gradients.
2. Darcy's law, Equation 2.25, is valid for unsaturated water movement in soil.
3. Moisture tension, ψ, and relative permeability, k_r, are unique, non-hysteric functions of moisture saturation, S.
4. The soil is a stable non-changing media.

Assumption 1 is reasonable in laboratory studies if the air pressure at the base of a soil sample is atmospheric. Assumption 1 is

also reasonable under most field conditions. Deviations from assumption 2 are small and difficult to prove. Assumption 3 will produce only small errors if an imbibition curve is used and if assumption 4 is correct.

Assumption 4 could be considerably in error for soils containing montmorillonite clay, which are allowed to shrink and develop large cracks. However, the soil was assumed stable because this assumption would considerably simplify the model and because it was initially thought that this assumption would not cause noticeable errors.

Solution of the Equation

To solve Equation 2.28 on a digital computer, the equation is written in finite difference form. The solution of the equation proceeds in time and one dimension of distance. A complete description of the equation and its solution is given by Smith (46), while a general description will be given in this chapter.

An overall view of the solution is shown by the flow chart of the computer program (Figure 4.3). The superscripts j refer to time and the subscripts i refer to distances in the flow chart.

The first step in getting Equation 2.28 into final form for solution is to multiply Equation 2.28 by dz resulting in

$$\frac{\partial}{\partial t}(V_b \phi S) = K \frac{\partial}{\partial Z}\left(k_r \frac{\partial \psi}{\partial Z}\right) dz - K \frac{\partial k_r}{\partial z} dz \qquad (4.1)$$

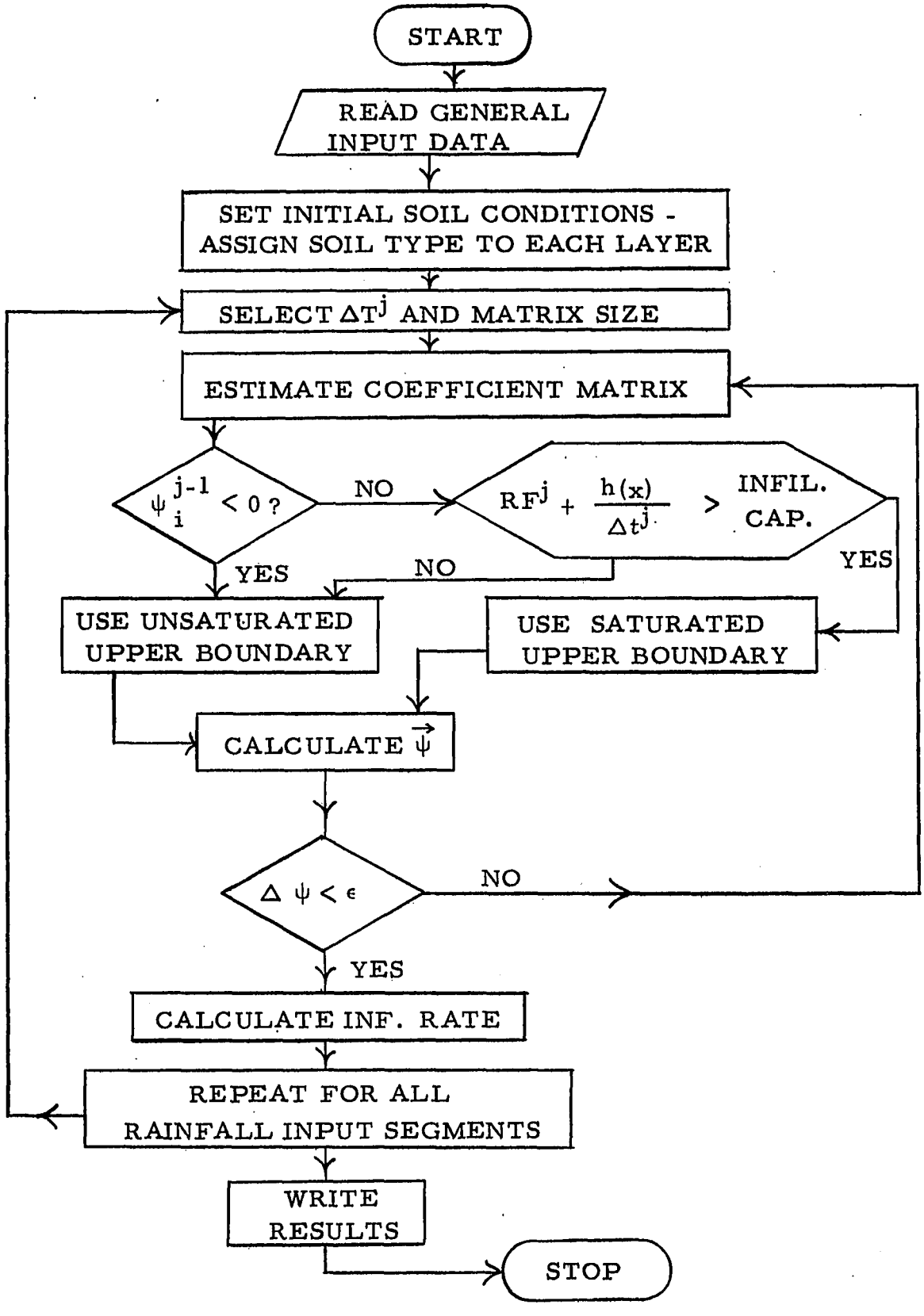

Figure 4.3 Flow chart of computer program

in which V_b is the incremental bulk volume or simply dz for this case of one-dimensional flow.

Swelling Soils

Smith (46) allows for a change in porosity, ϕ, of Equation 4.1. The basic relationship is taken from Philip (42), whereby void volume is expressed as a function of the moisture content. At lower saturation values, ϕ is considered constant in Smith's program. At higher saturation values, ϕ can increase with an increase in moisture content.

Allowing for a change in ϕ changes Equation 4.1 to

$$V_b \frac{\partial}{\partial S}(\phi S) \frac{\partial S}{\partial \psi} \frac{\partial \psi}{\partial t} = K \frac{\partial}{\partial Z}\left(k_r \frac{\partial \psi}{\partial Z}\right) dz - K \frac{\partial k_r}{\partial z} dz. \quad (4.2)$$

In this study, ϕ remains constant for a particular soil. The reasoning being that if swelling is to be accounted for, the most important area to consider would be the change in permeability due to change in pore size (e.g., Pouieulle's equation).

Finite Difference Formulations

A finite difference solution grid is shown in Figure 4.4. Equation 4.2 is written in a finite difference form based on time and distance averaged quantities, a form known as the Crank-Nicholsen finite difference form. Equation 4.2 becomes

$$[STOR] \frac{\Delta S}{\Delta \psi} \Delta \psi = \frac{K}{\Delta Z} \Delta \left[k_r \frac{\Delta \psi}{\Delta Z}\right] \Delta Z - K \frac{\Delta k_r}{\Delta Z} \Delta Z \quad (4.3)$$

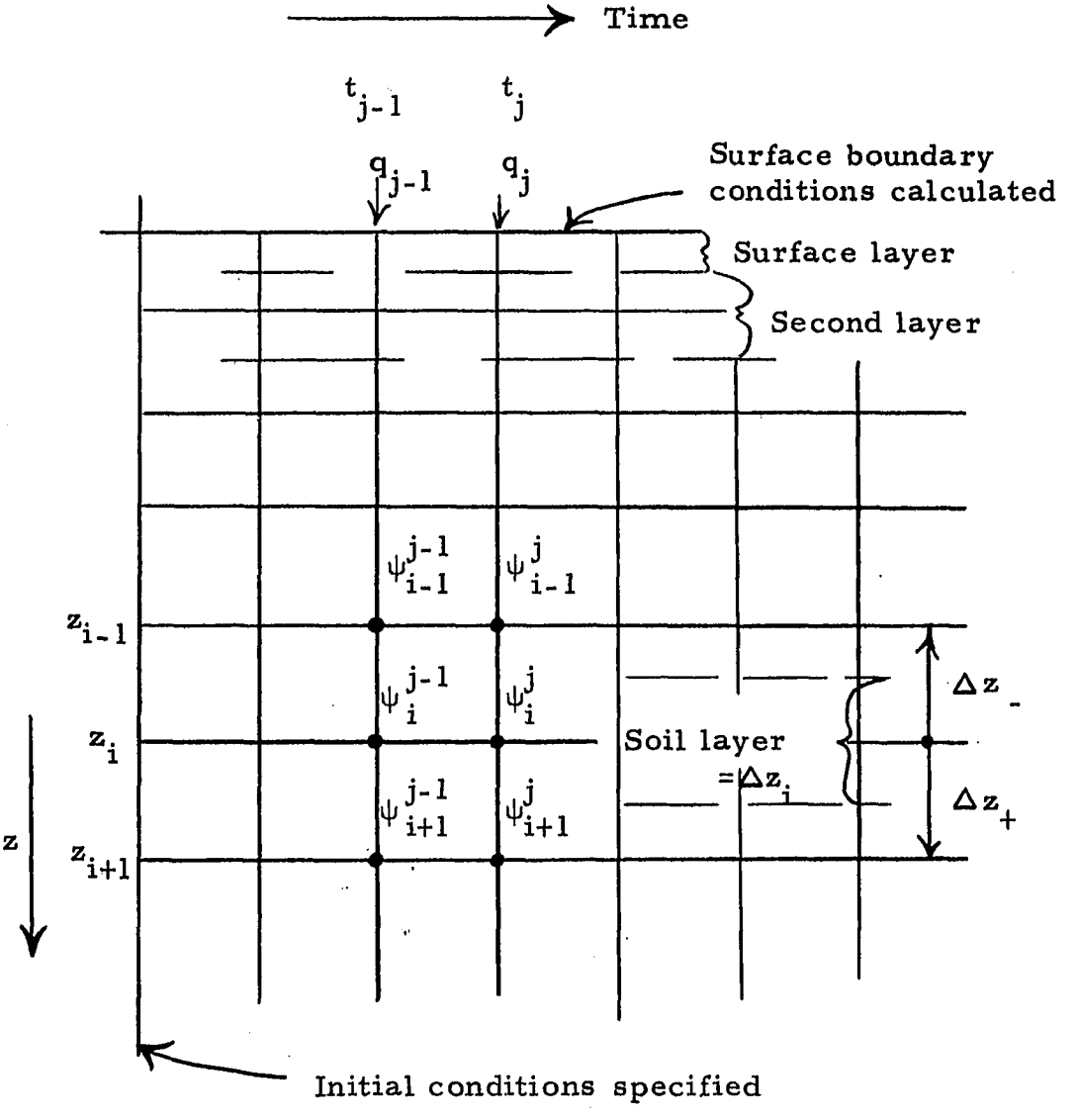

Figure 4.4 Finite difference solution grid and notation used in solution at Equation 2.28

in which $STOR = \left[\frac{V_b}{\Delta t} \quad \frac{\Delta\phi S}{\Delta S}\right]$.

Using the notation shown in Figure 4.4, let

$$\Delta\psi_+^{j-\frac{1}{2}} = \frac{1}{2}\left[\psi_{i+1}^{j} - \psi_i^{j} + \psi_{i+1}^{j-1} - \psi_i^{j-1}\right]$$

and

$$\Delta\psi_-^{j-\frac{1}{2}} = \frac{1}{2}\left[\psi_i^{j} - \psi_{i-1}^{j} + \psi_i^{j-1} - \psi_{i-1}^{j-1}\right]$$

in which

$i = 1, 2, 3, \cdots, N \qquad j = 1, 2, 3, \cdots, M_j$

N = total number of soil layers,

M_j = total number of time steps.

The relative permeabilities are defined at the node from which flow originates and are

$$k_{r_+}^{j-\frac{1}{2}} = \frac{1}{2}\left[k_{r_i}^{j} + k_{r_i}^{j-1}\right]$$

$$k_{r_-}^{j-\frac{1}{2}} = \frac{1}{2}\left[k_{r_{i-1}}^{j} + k_{r_{i-1}}^{j-1}\right] .$$

The distance step sizes are

$$\Delta\bar{Z}_+ = Z_{i+1} - Z_i$$

$$\Delta\bar{Z}_- = Z_i - Z_{i-1} .$$

Saturated conductivity between adjacent layers is taken as the harmonic mean:

$$K_+ = K_{i+\frac{1}{2}} = \frac{2\Delta\bar{Z}_+}{\frac{\Delta Z_{i+1}}{K_{i+1}} + \frac{\Delta Z_i}{K_i}}$$

$$K_- = K_{i-\frac{1}{2}} = \frac{2\Delta\bar{Z}_-}{\frac{\Delta Z_i}{K_i} + \frac{\Delta Z_{i-1}}{K_{i-1}}}$$

Using these definitions and reversing sides, Equation 4.3 may be expanded to:

$$K_{i+\frac{1}{2}}\, k_{r_+}^{j-\frac{1}{2}} \left[\frac{\psi_{i+1}^j - \psi_i^j + \psi_{i+1}^{j-1} - \psi_i^{j-1}}{2\Delta\bar{Z}_+}\right]$$

$$- K_{i-\frac{1}{2}}\, k_{r_-}^{j-\frac{1}{2}} \left[\frac{\psi_i^j - \psi_{i-1}^j + \psi_i^{j-1} - \psi_{i-1}^{j-1}}{2\Delta\bar{Z}_-}\right]$$

$$- K_{i+\frac{1}{2}}\, k_{r_+}^{j-\frac{1}{2}} + K_{i-\frac{1}{2}}\, k_{r_-}^{j-\frac{1}{2}} = \left[\mathrm{STOR}\right]_i^{j-\frac{1}{2}} \mathrm{SL}_i^{j-\frac{1}{2}} \; X$$

$$\left[\psi_i^j - \psi_i^{j-1}\right] - Q_{p_i} \qquad (4.4)$$

in which

Q_{p_i} = input to node i from the outside, used only at the surface for rainfall input up to ponding: $Q_{p_i} = 0$ for $i > 1$, and

$$SL_i^{j-\frac{1}{2}} = \left[\frac{\Delta S}{\Delta \psi}\right]_i^j \quad .$$

Separating the ψ terms of Equation 4.4:

$$\left[\frac{K_{i-\frac{1}{2}}\, k_{r_-}}{2\Delta\overline{Z}_-}\right] \psi_{i-1}^j - \left[\frac{K_{i+\frac{1}{2}}\, k_{r_+}}{2\Delta\overline{Z}_+} + \frac{K_{i-\frac{1}{2}}\, k_{r_-}}{2\Delta\overline{Z}_-} + [STOR]_i^{j-\frac{1}{2}} \times [SL]_i^{j-\frac{1}{2}}\right] \psi_i^j + \left[\frac{K_{i+\frac{1}{2}}\, k_{r_+}}{2\Delta\overline{Z}_+}\right] \psi_{i+1}^j = RHS_i^{j-\frac{1}{2}} \qquad (4.5)$$

in which

$$RHS_i^{j-\frac{1}{2}} = -[STOR]_i^{j-\frac{1}{2}} [SL]_i^{j-\frac{1}{2}} \psi_i^{j-\frac{1}{2}} - Q_{p_i}$$

$$- \frac{K_{i-\frac{1}{2}}\, k_{r_+}}{2\Delta\overline{Z}_+} \left[\psi_{i+1}^{j-1} - \psi_i^{j-1} - 2\Delta\overline{Z}_+\right]$$

$$+ \frac{K_{i-\frac{1}{2}}\, k_{r_-}}{2\Delta\overline{Z}_-} \left[\psi_i^{j-1} - \psi_{i-1}^{j-1} - 2\Delta\overline{Z}_-\right] \quad . \qquad (4.6)$$

A set of N linear equations in N variables of the form

$$a_i \psi_{i-1} + b_i \psi_i + c_i \psi_{i+1} = RHS_i \qquad (4.7)$$

is represented by Equation 4.5 or as a matrix equation

$$[J]\ \vec{\psi} = \overrightarrow{RHS} \quad . \qquad (4.8)$$

Equation 4.7 will be written in a N x N matrix $[J]$ and an N-dimensional vector $\overrightarrow{RHS}$ after applying the boundary conditions.

Upper Boundary Conditions

For the upper boundary i-1 does not exist and Equation 4.7 is

$$b_1 \psi_1 + c_1 \psi_2 = RHS_1 \quad .$$

At the soil surface, for the rainfall and ponded case, $K_{i-\frac{1}{2}}$ does not exist and Equations 4.5 and 4.6 become

$$\left[\frac{K_{1\frac{1}{2}}\, k_{r_+}}{2\Delta\overline{Z}_+}\right]\left[\psi_2^j - \psi_1^j\right] - \left[STOR\right]_1^{j-\frac{1}{2}} \left[SL\right]_1^{j-\frac{1}{2}} \psi_1^j$$

$$= - \left[STOR\right]_1^{j-\frac{1}{2}} \left[SL\right]_1^{j-\frac{1}{2}} \psi_1^{j-1} - Q_{p_1}$$

$$- \frac{K_{1\frac{1}{2}}\, k_{r_+}}{2\Delta\overline{Z}_+} \left[\psi_2^{j-1} - \psi_1^{j-1} - 2\Delta\overline{Z}_+\right] . \qquad (4.9)$$

For the ponded case, $\psi_1^j = h$ which is the depth of water on the surface. The known ψ_1^j terms are placed on the right hand side of Equation 4.7 and the first equation in the set for this case is for the second layer i = 2.

As saturation proceeds below the surface to some node nl (Figure 4.5) the ψ_i^j terms are calculated from knowing Z(nl) and h (depth of ponding) for all $i < nl$ and these ψ_i terms are moved to the right side of Equation 4.7. The ψ_n^j term is

$$\psi_n^j = Z(nl) \left[1 - \frac{Q}{K(nl)}\right] + h \qquad (4.10)$$

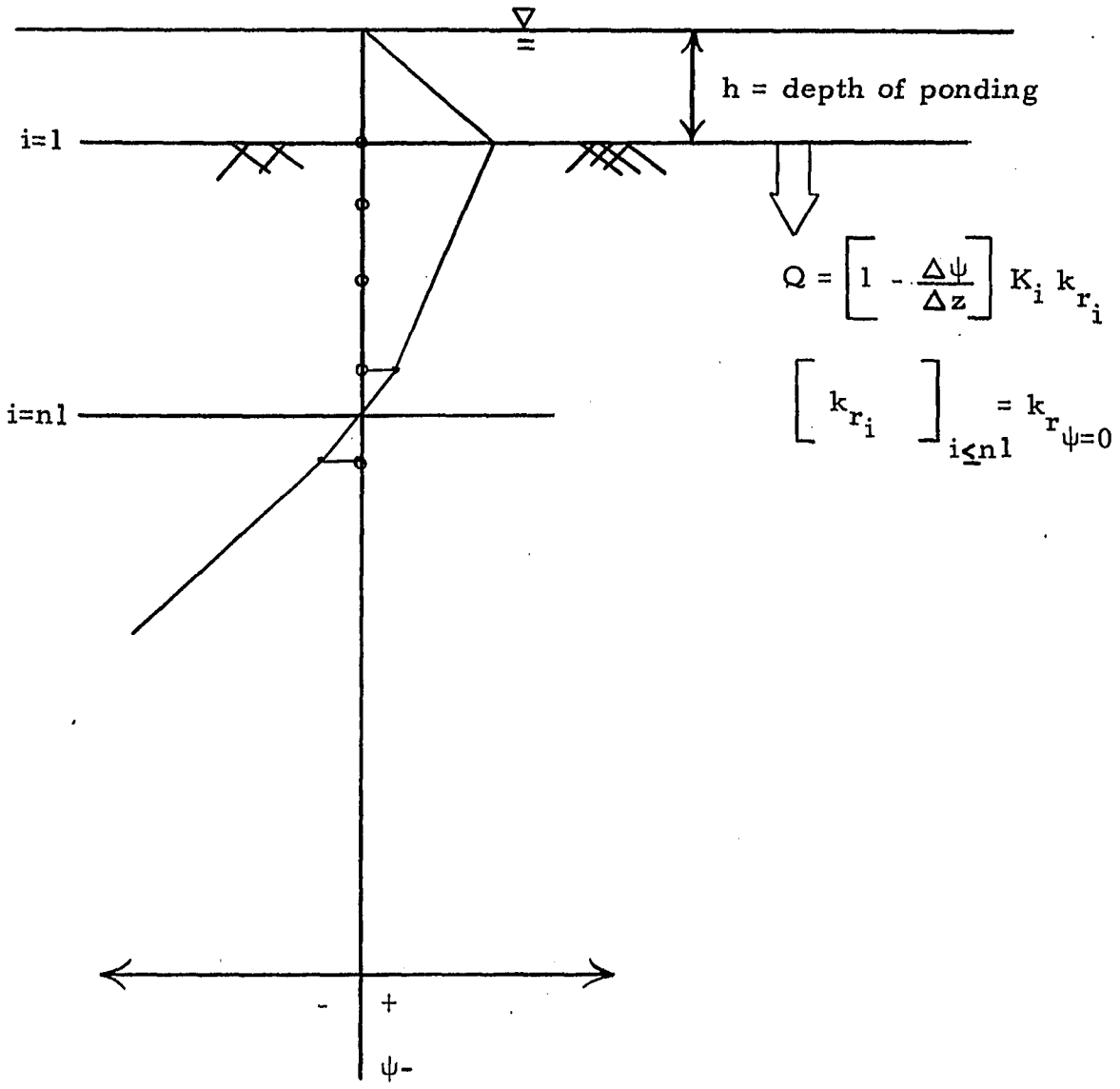

Figure 4.5 Pressure relations when water is ponded on the soil surface

which is Darcy's law in the form

$$Q = K(n)\left(1 + \frac{h - \psi_n^j}{Z(n)}\right)_i \quad . \tag{4.11}$$

Also, $\frac{\partial S}{\partial \psi} = 0$ for $i < n$.

Lower Boundary Conditions

The lower boundary condition is a sufficient soil depth (semi-infinite) so that no significant water movement occurs below the soil depth under study.

When soil water movement has progressed to a point $n2$ in a column, all terms in $n2 + 1$ are known from initial conditions and are set on the right side of Equation 4.7. Point $n2$ is chosen such that $i \leq n2$, $|\psi_i^{j-1} - \psi_i^0| \leq \epsilon$, where ϵ is a very small error value.

Matrix Solution

Using the upper and lower boundary conditions just described, Equation 4.8 is written as follows

$$\begin{bmatrix} b_1 & c_1 & & & & \\ a_2 & b_2 & c_2 & & & \\ & a_3 & b_3 & b_3 & & \\ & & & & & \\ & & & a_{n2-1} & b_{n2-1} & c_{n2-1} \\ & & & & a_{n2} & b_{n2} \end{bmatrix} \begin{bmatrix} \psi_1 \\ \psi_2 \\ \psi_3 \\ \\ \psi_{n2-1} \\ \psi_{n2} \end{bmatrix} = \begin{bmatrix} rhs_1 \\ rhs_2 \\ rhs_3 \\ \\ rhs_{n2-1} \\ rhs_{n2} \end{bmatrix} . \tag{4.12}$$

The column vector ψ can be solved by a recursion algorithm for Gauss elimination as given by Varga (51).

Solution of Equation for a Given Time Step

Soil Data Input

A table of soil hydraulic relations ψ vs. S vs. k_r values are experimentally obtained in the laboratory and used as input to the computer program. Intermediate points are found by linear interpolation. Any one of the three variables may be used to find corresponding values of the other two.

Equipment used (Figure 4.6) to obtain ψ vs. S vs. k_r relationships (for lower tensions) is located in the Porous Media Laboratory at Colorado State University. A pressure plate was used to obtain ψ vs. S relationships at higher tensions. A log k vs. log ψ relationship discussed by Brooks and Corey (5) is used to calculate ψ vs. k_r relationships at higher tensions.

The main items of equipment required (Figure 4.6) are the soil sample, fluid inlet, fluid discharge, flow measurement container, attenuation instrument and two manometers. The fluids used were Soltrol and water.

The head or moisture tension can be varied by changing q_{in} or the outlet elevation, which also changes k_r and S when $S < 1.0$. Steady state relationships of S vs. k_r were found. For steady state flow, $q_{in} = q_{out}$. H_1 should be approximately equal to H_2 to

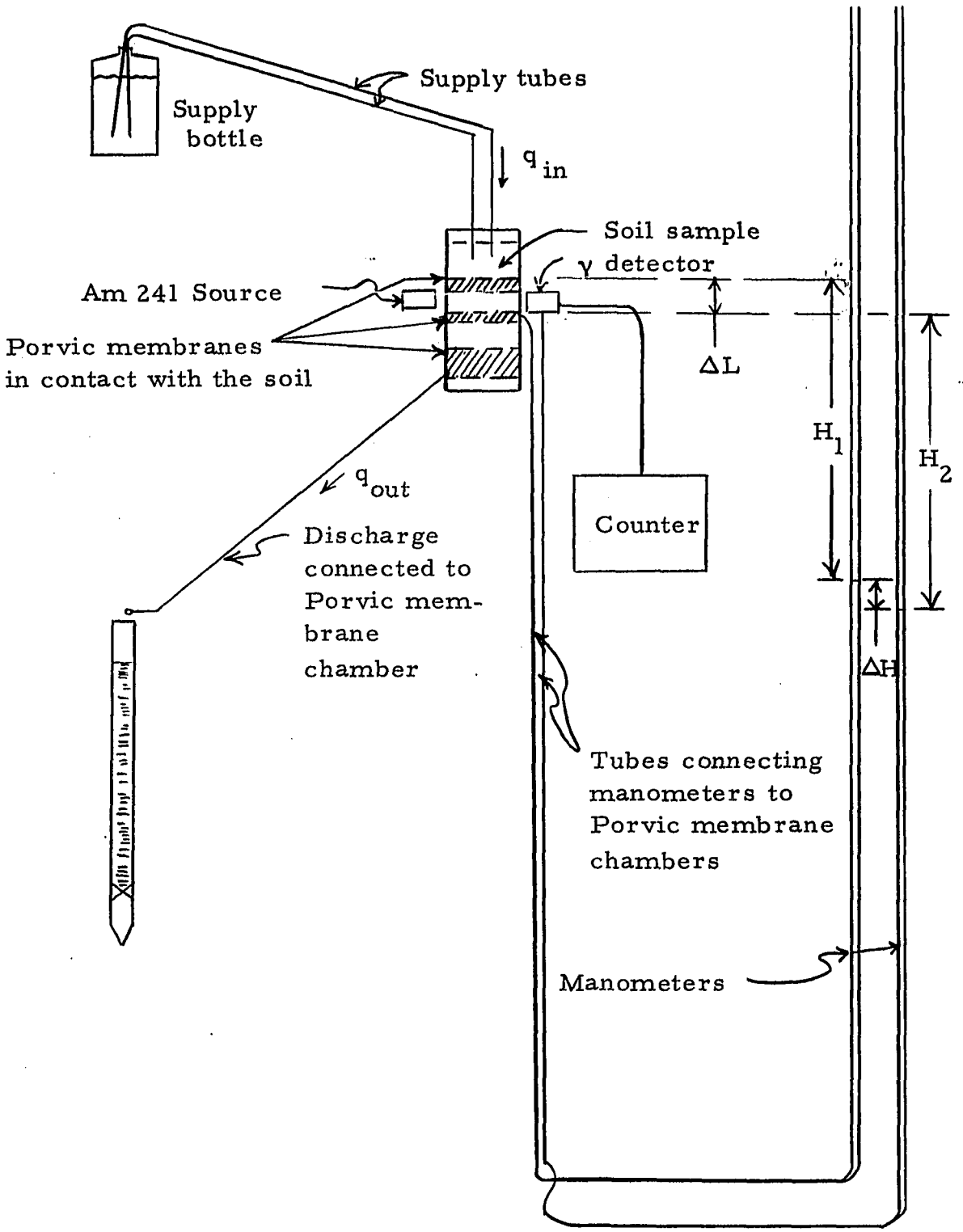

Figure 4.6 Equipment used to obtain ψ-k_r-S relationships for numerical model

make ψ nearly constant throughout the sample. Calculations required to find ψ, k, or S values are:

$$\psi = \frac{H_1+H_2}{2} - P_{c_{tube}} / \gamma \qquad (4.13)$$

$$K = \frac{q_{out}}{A} \frac{\Delta L}{\Delta H} \quad \text{for a saturated condition}$$

$$K k_r = \frac{q_{out}}{A} \frac{\Delta L}{\Delta H} \quad \text{for unsaturated conditions}$$

$$S = 1.0 - \frac{C - C_{100}}{C_{100} - C_0}$$

in which

$P_{c_{tube}}$ = capillary pressure rise in manometer tubes,

A = cross sectional area of the soil sample,

C = counter reading ratio = $\frac{\text{count (sample)}}{\text{count (standard)}}$,

C_{100} = counter reading at S = 1.0, and

C_0 = counter reading at S = 0.0 .

The saturation, S, and counter reading ratio, C, are determined for an air dry sample. A straight line is drawn through C_{100} and $C_{air\ dry}$ on a C vs. S graph. The value of C at S = 0.0 is C_0.

Three k vs. ψ curves (Figure 4.7) were obtained for the sandy clay loam, two using Soltrol and one using water. Two k vs.

ψ curves (Figure 4.8) were obtained for the loam, one using Soltrol and one using water.

Soltrol is often used as the infiltrating fluid in this type of test to overcome several problems encountered with water. Water reacts with the soil causing shrinkage or swelling, thereby resulting in considerable data scatter (Figure 4.7). Soil shrinkage and water evaporation at the Porvic barrier causes loss of contact between the soil sample and the Porvic barrier. When loss of contact occurs, the soil sample must be discarded and a new sample prepared.

The saturated permeability values obtained for water and Soltrol are considerably different. This indicates permeability may not be a unique property of the soil for the sandy clay loam and loam tested.

A straight line reasonably fits a plot of log k vs. log ψ at higher values of ψ (Figures 4.7 and 4.8). This straight line fit, on logarithmic coordinates, between capillary pressure and permeability, is discussed by Brooks and Corey (5) and presented as an equation:

$$k_r = \left(\frac{P_b}{P_c}\right)^m \quad \text{for} \quad P_c > P_b \qquad (4.14)$$

in which

k_r = relative permeability

P_b = bubbling pressure - approximately the minimum P_c on the drainage cycle at which a continuous non-wetting phase (e.g. air) exists in a porous medium

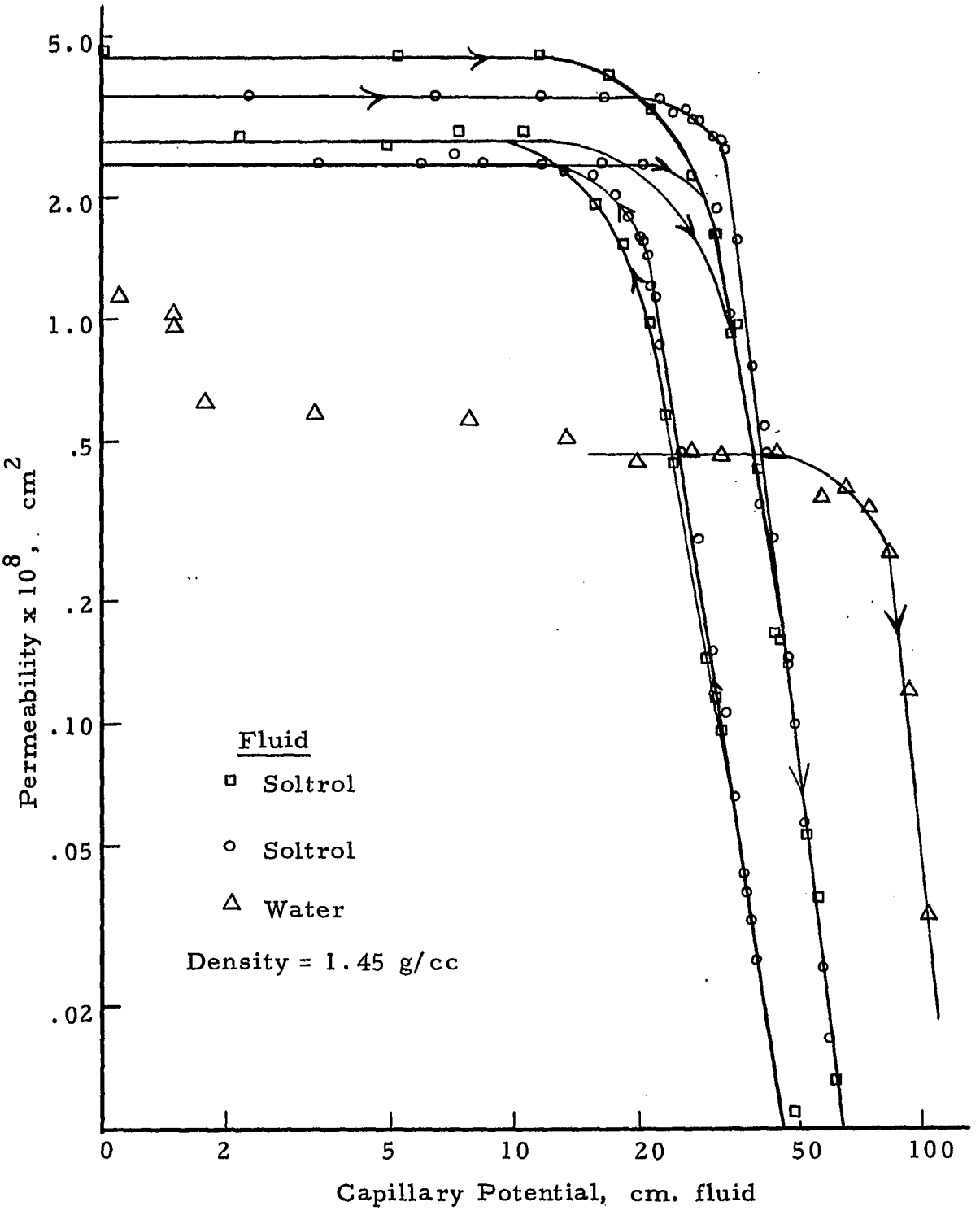

Figure 4.7 Permeability-capillary pressure relationships for sandy clay loam

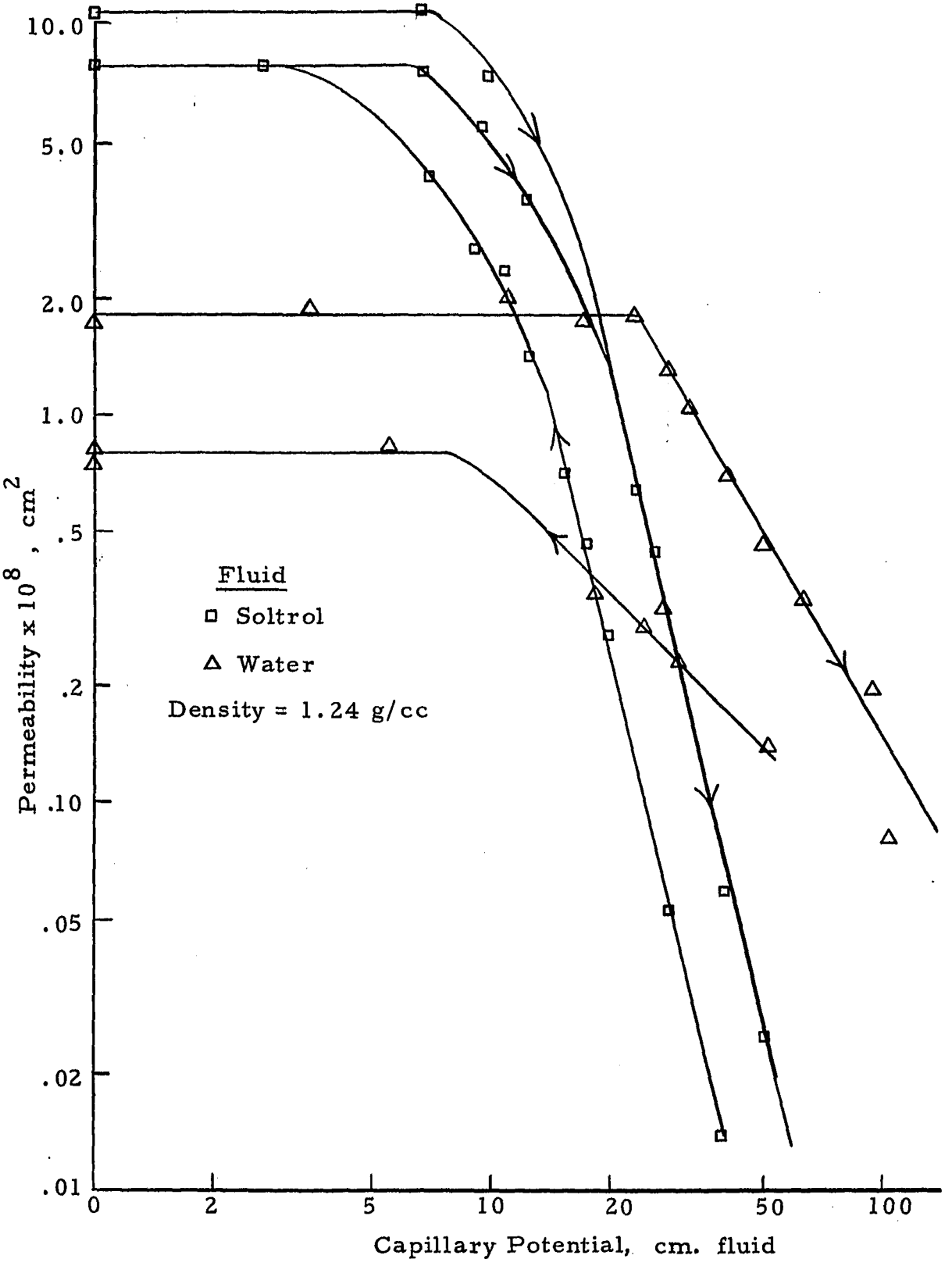

Figure 4.8 Permeability-capillary pressure relationships for loam

P_c = capillary pressure

m = an exponent.

Values for permeability vs. capillary pressure for $k < 0.1 \times 10^{-8}$ cm^2 were derived using the relationship expressed in Equation 4.14.

The upper imbibition curve of Figure 4.7 (Soltrol) was used to calculate the relationship between relative permeability, k_r, and capillary potential, ψ, for the sandy clay loam. Also, the imbibition curve of Figure 4.8 (Soltrol) was used to calculate the k_r vs. ψ relationships for the loam. The Soltrol curves were used rather than the water curves because a better defined curve was obtained with Soltrol.

The relationship between the capillary pressure (expressed in cm. of fluid) for water and Soltrol was experimentally found to be

$$\left(\frac{P_c}{\gamma}\right)_w = 2.23 \left(\frac{P_c}{\gamma}\right)_{So} \qquad (4.15)$$

where the subscripts w and So designate water and Soltrol, respectively.

The moisture-tension curves for the two soils are shown in Figure 4.9. The loam has a more gradual desaturation curve than the sandy clay loam indicating a more gradual change in pore sizes for the loam than for the sandy clay loam.

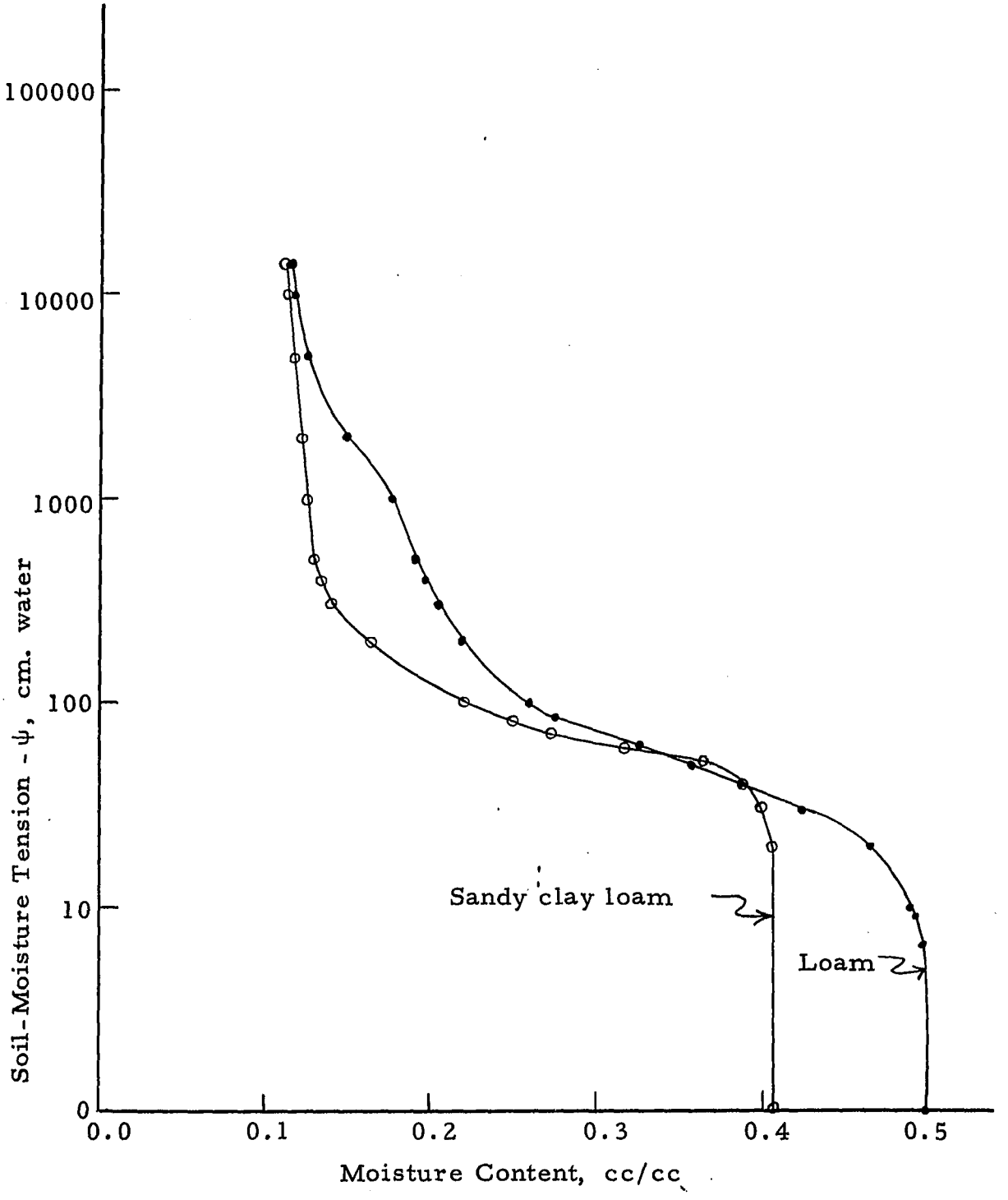

Figure 4.9 Moisture-tension relationships of experimental soils

Iteration

The values of $k_{r_i}^j$, $(STOR)_i^j$, and $(SL)_i^j$ are dependent on the values of ψ_i^j, thereby making Equation 2.28 non-linear. These variables are evaluated by a trial and error solution, where the value of one of the variables is estimated, then knowing the hydraulic properties of the soil the other variables can be calculated. Then, the estimated variable can be calculated and the process repeated until the estimated and calculated value become nearly identical.

The iterative procedure followed in Smith's program is as follows:

1. An initial estimate is made of ψ_i^j, i=1, N, from which values of $k_{r_i}^j$, $(STOR)_i^j$, and $(SL)_i^j$ are found knowing the soil hydraulic relations.
2. The coefficients a, b, and c are computed and Equation 4.12 is solved.
3. The estimated values of ψ_i^j of step (1) are compared with the computed values of ψ_i^j in step (2). If the estimated and computed values agree within a prescribed limit of the error criteria, Equation 4.12 is considered solved. If the estimated and computed values do not agree within the prescribed limit of the error criteria, and if this was the first or second iteration, the ψ_i^j values obtained in step (2) are used as estimated values of ψ_i^j's.

4. If after three iterations, Equation 4.12 does not meet the error criteria, the ψ_i^j values obtained in step (2) are "damped" by a weighted average with the last ψ_i^j.

Selection of Depth and Time Increments

The solution of a non-linear finite difference scheme involves a selection of efficient grid sizes. Selecting very small grid sizes results in excessive computer time. Selecting grid sizes too large causes the solution to diverge or to be very inaccurate.

Depth increments, for this model, are chosen very small at the surface and increase in size downward.

Time increments are changed throughout an event. The criteria for the time increment size are the change in $\Delta S/\Delta\psi$ over the previous time step and the local change in curvature $(\Delta^2 S/\Delta\psi^2)_i^j$ of the soil moisture-tension relation.

Infiltration Calculation

Infiltration can be calculated at the surface when n=1 by use of Equation 4.11. For $t <$ time of ponding

$$Q = \frac{1}{t} \sum_{i=1}^{N} \Delta Z_i \, \phi_i^j \left[S^j - S^{j-1} \right]_i \qquad (4.16)$$

serves as a continuity test on the performance of the numerical scheme.

Solution Sensitivity

The accuracy of a numerical model, simulating soil moisture flow, depends on the size of the depth increments, time increments and error criteria. The model was tested for sensitivity to change in size of depth increments, time increments and error criteria.

Depth Increment

Changing the depth increment size near the surface had considerable effect on the time that runoff began and on the infiltration curve for the loam (Figure 4. 10). A certain depth increment size required a limited time increment size to allow the model to operate. The time increment size limit is analogous to a wave or impulse problem in which the speed of the wave or impulse must be less than the distance increment divided by the time increment.

The depth increments are made smaller near the surface both to accurately define the time runoff begins and to properly define the steeply varying pressures encountered in the upper zone as the moisture begins to disperse into the soil.

The model which was finally used divided the upper three inches into 0. 1-inch increments and the lower 25 inches into 0. 5-inch increments. Dividing the upper part of the column into smaller increments than 0. 1 inches increased the computation time considerably, but caused only minor changes in the infiltration curves resulting from the model. Dividing the lower part of the soil

Saturated Conductivities

Depth, inches	Saturated conducitivites, inches per hour
0.0 to 0.2	0.024
0.2 to 25	0.070

Initial Conditions

Depth, inches	Saturation
0.0	0.264
1.5	0.384
3.0	0.406
6.0	0.408

	Depth, inches	Depth increment, inches
———	0.0 to 0.06	0.03
	0.06 to 0.16	0.05
	0.16 to 3.16	0.10
	3.16 to 25.0	0.50
— — —	0.0 to 3.0	0.3
	3.0 to 25	0.5
— - —	0.0 to 3.0	0.2
	3.0 to 25	0.5
- - - - -	0.0 to 3.0	0.1
	3.0 to 25	0.5

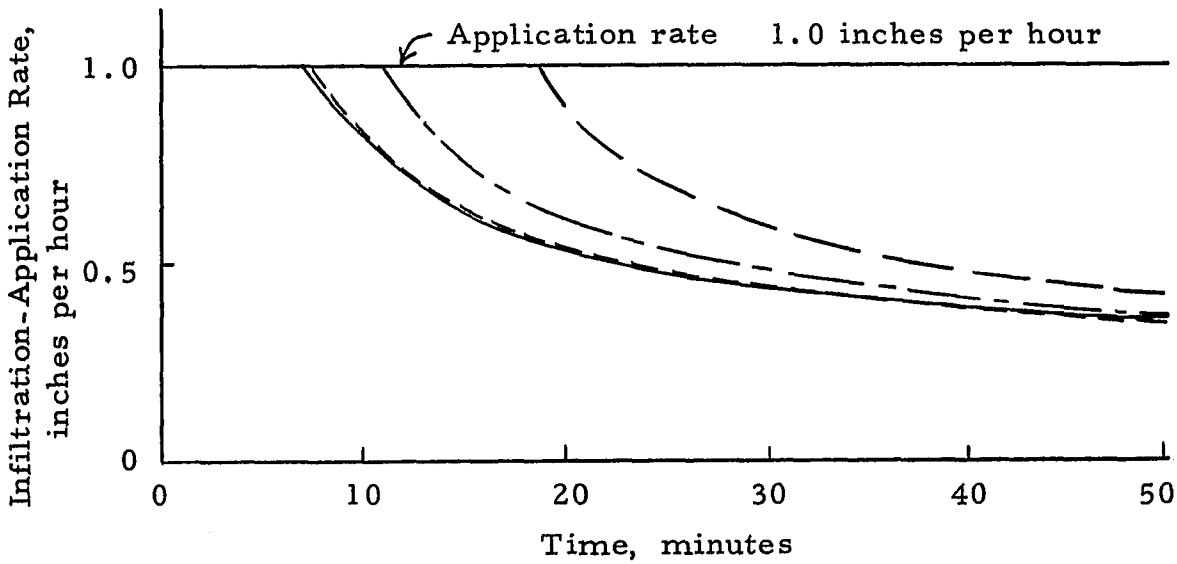

Figure 4.10 Example of the effect of depth increment size on model's infiltration rate curve - loam

column into smaller increments than 0.5 inches only increased computation time.

Time Increment

The computer solution did not prove to be very sensitive to changes in time increment, unless the time increment was too large for the depth increment used, which would cause the model not to run.

No difference occurred with the infiltration curves as t_{max} was reduced from 0.5 to 0.25 minutes and t_{min} was reduced from 0.05 to 0.025 minutes. Therefore, the model used a t_{max} of 0.5 minutes and a t_{min} of 0.05 minutes.

Error Criteria

The allowable error, ϵ, is defined as the maximum difference allowable between the estimated capillary potential, ψ, and the computed capillary potential (step 2 of Iteration). Changing the allowable error, ϵ, from 0.02 to 0.04 inches caused no change in the infiltration curve for the loam. The allowable error was made small enough to nearly eliminate variation in the model infiltration curve. The maximum ϵ value used in the model was 0.05 cm.

CHAPTER V

RESULTS AND DISCUSSION

Constant and Two Step Application Rate Patterns

Constant and two-step application rate pattern tests were run in the laboratory to determine relationships between infiltration rate with time and infiltration rate with depth of intake for the two soils and to calibrate the model.

Initial moisture contents of the tests are shown in Table 5.1. The soil bulk density for the sandy clay loam was 1.45 g./cc, except near the surface. The soil bulk density for the loam was 1.24 g./cc except near the surface.

Table 5.1 Initial moisture contents

	Percent Moisture by Volume	
Depth, inches	Sandy Clay Loam	Loam
0	13.6	13.2
1	20.3	15.3
2	22.1	19.4
6	23.4	20.4

Infiltration curves are shown in Figures 5.1, 5.2, and 5.3 for nine tests of each soil using three patterns: 8-5, 2-5 and 5. The application rates associated with the patterns are:

8-5 12 minutes of 1.6 iph (inches per hour) followed by 32 minutes of 1.0 iph,

2-5 12 minutes of 0.4 iph followed by 40 minutes of 1.0 iph, and

5 48 minutes of 1.0 iph.

Each plotted point represents the average infiltration rate of six soil compartments over a two- or four-minute time interval.

The nine sandy clay loam tests were run in the following order: 5, 8-5, 2-5, 2-5, 8-5, 5, 2-5, 5, and 8-5. The nine loam tests were run in the following order: 5, 2-5, 8-5, 8-5, 2-5, 5, 8-5, 5, 2-5.

Data from only six of the eight soil compartments is used because compartments 1 and 8 gave quite variable results. Large cracks developed because heated air flowed on one side of each of these two compartments.

The laboratory infiltration data points of Figures 5.1, 5.2, and 5.3 are averaged and the resulting smoothed curves are drawn on Figures 5.4 and 5.5. The infiltration curves of patterns 8-5 and 5 nearly coincide, but the infiltration curve of pattern 2-5 is completely separated from the other two curves. Therefore, representing infiltration rate only as a function of time is questionable for different types of application rate patterns.

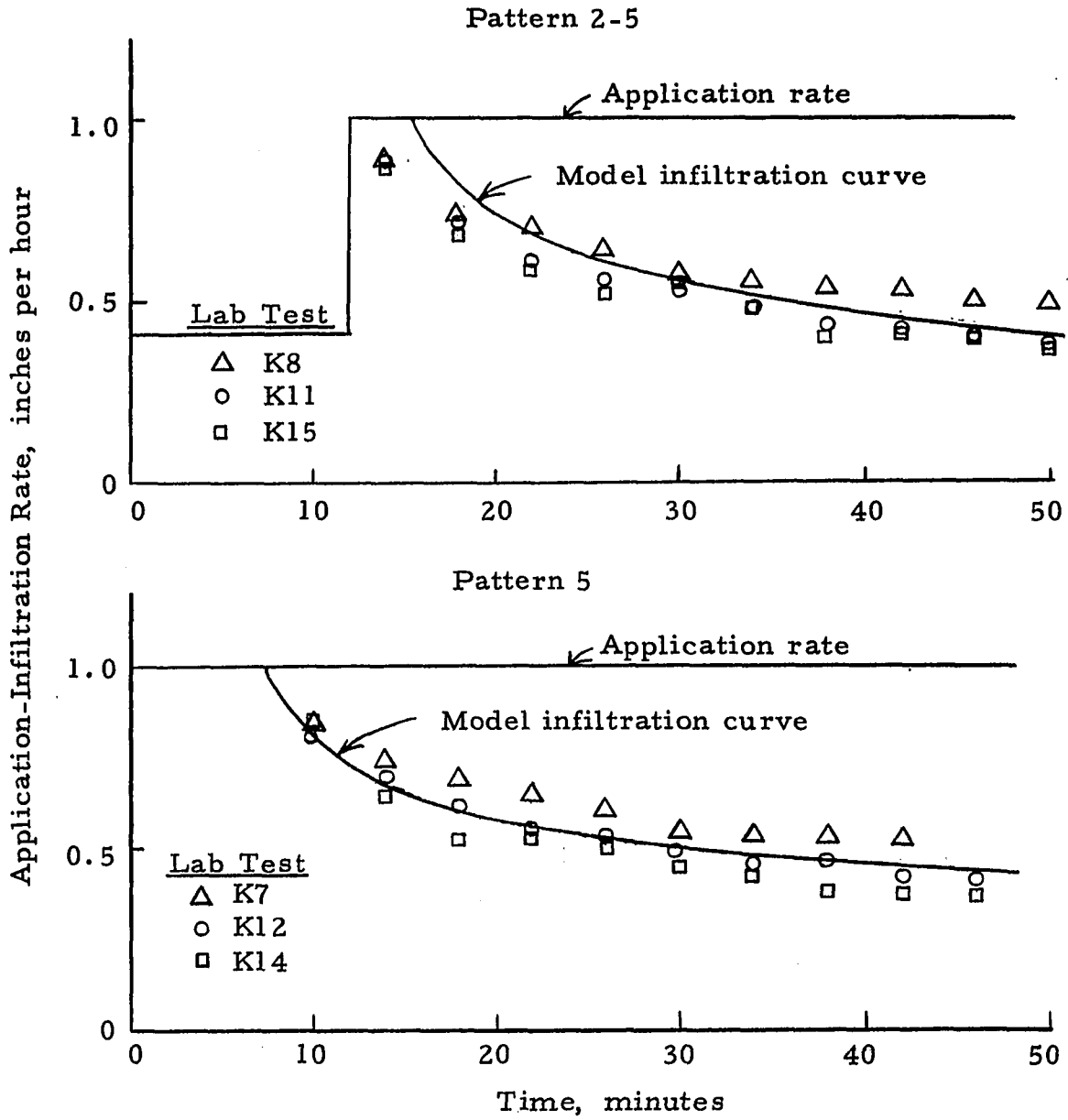

Figure 5.1 Infiltration rate curves for constant and two-step application rate patterns - loam

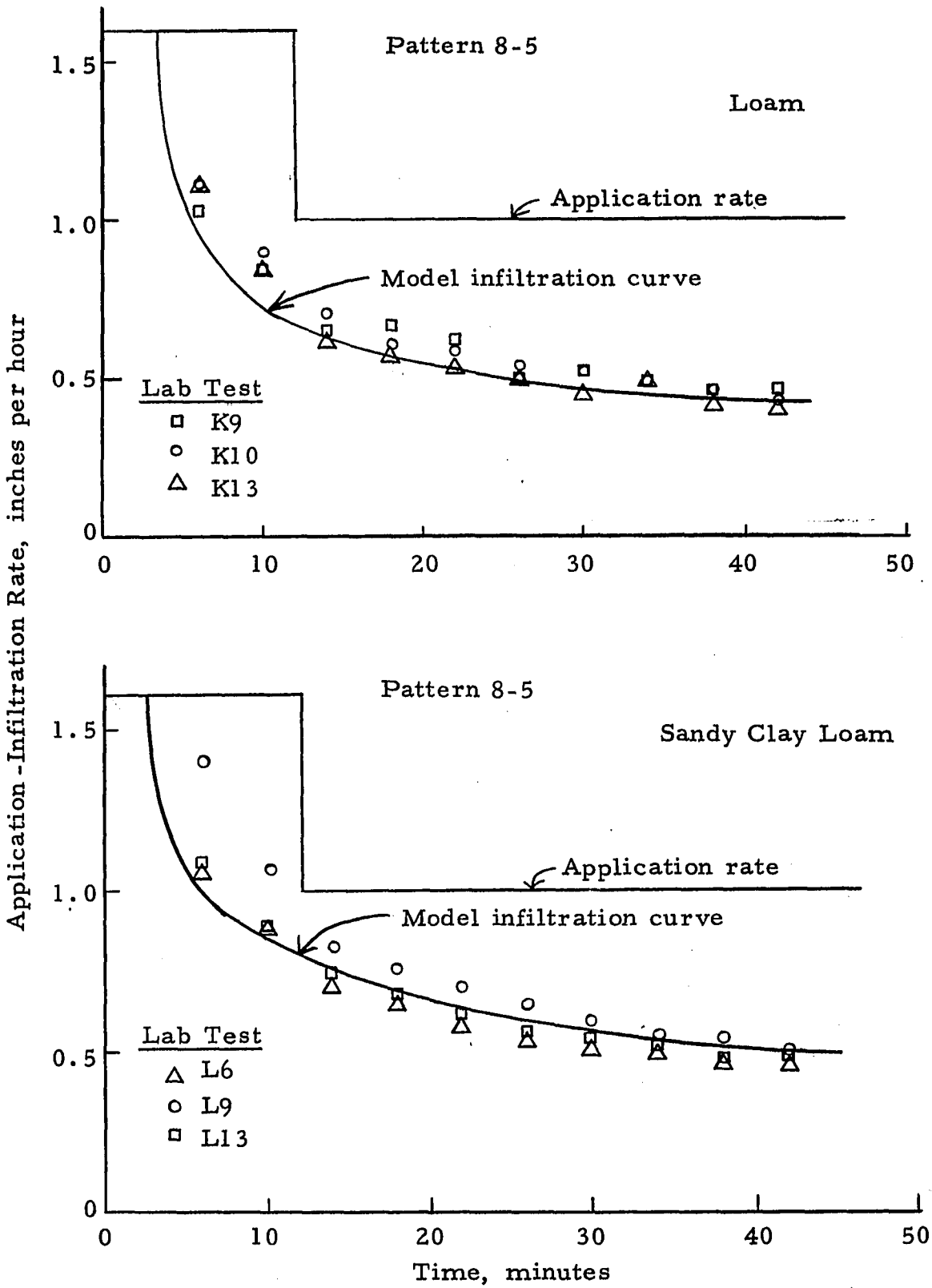

Figure 5.2 Infiltration rate curves for two-step application rate patterns

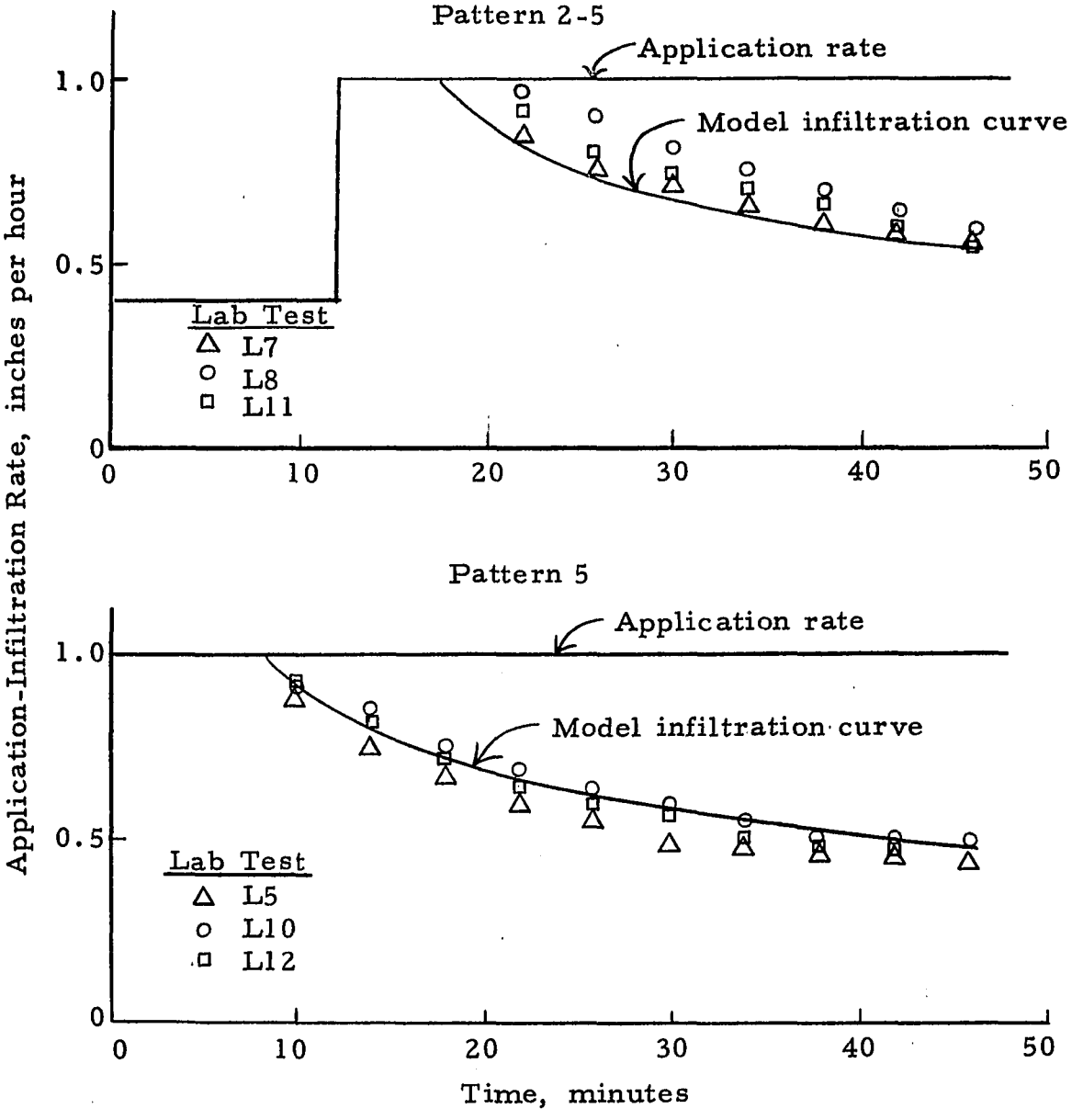

Figure 5.3 Infiltration rate curves for constant and two-step application rate patterns - sandy clay loam

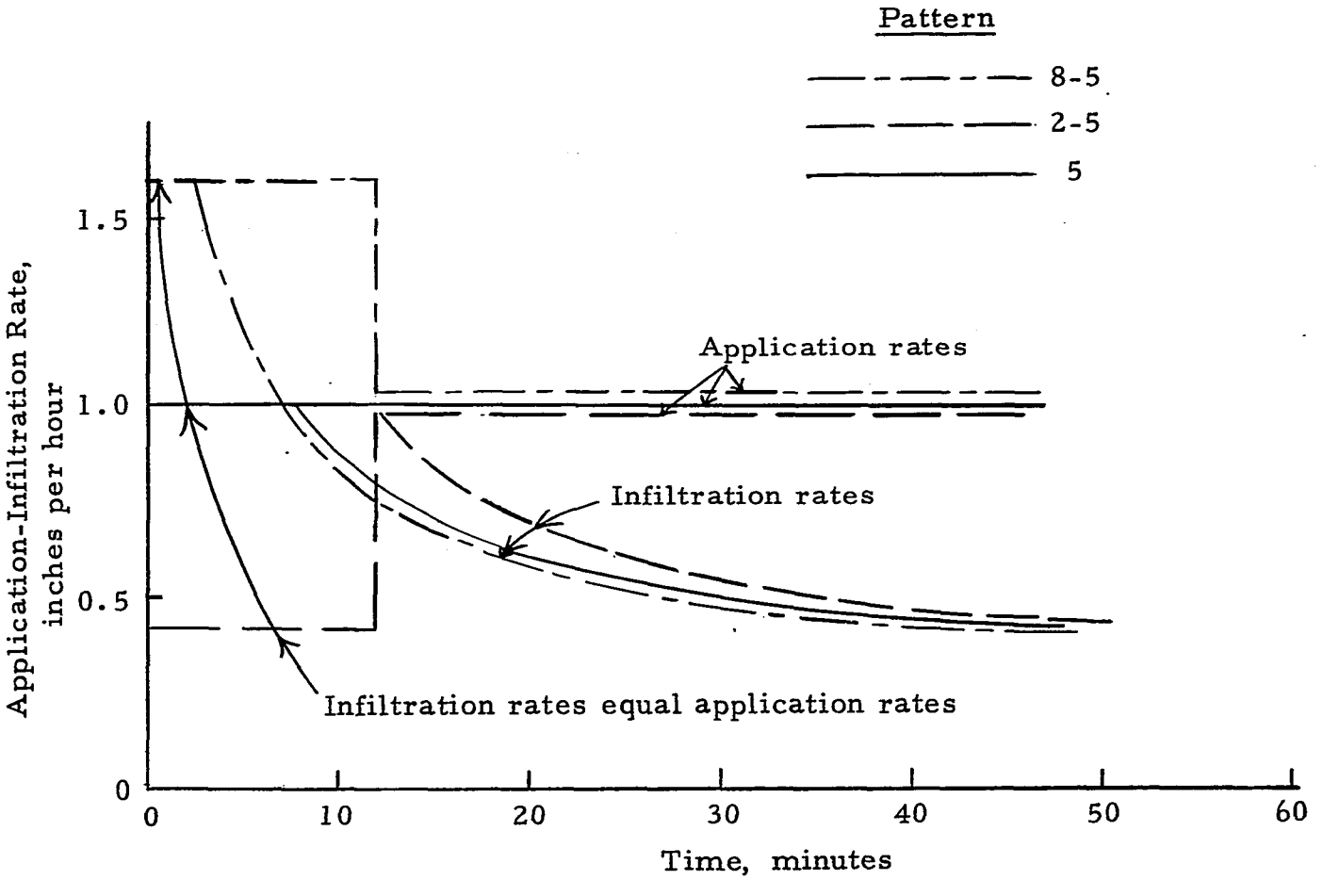

Figure 5.4 Average infiltration rate and time for a loam from laboratory tests

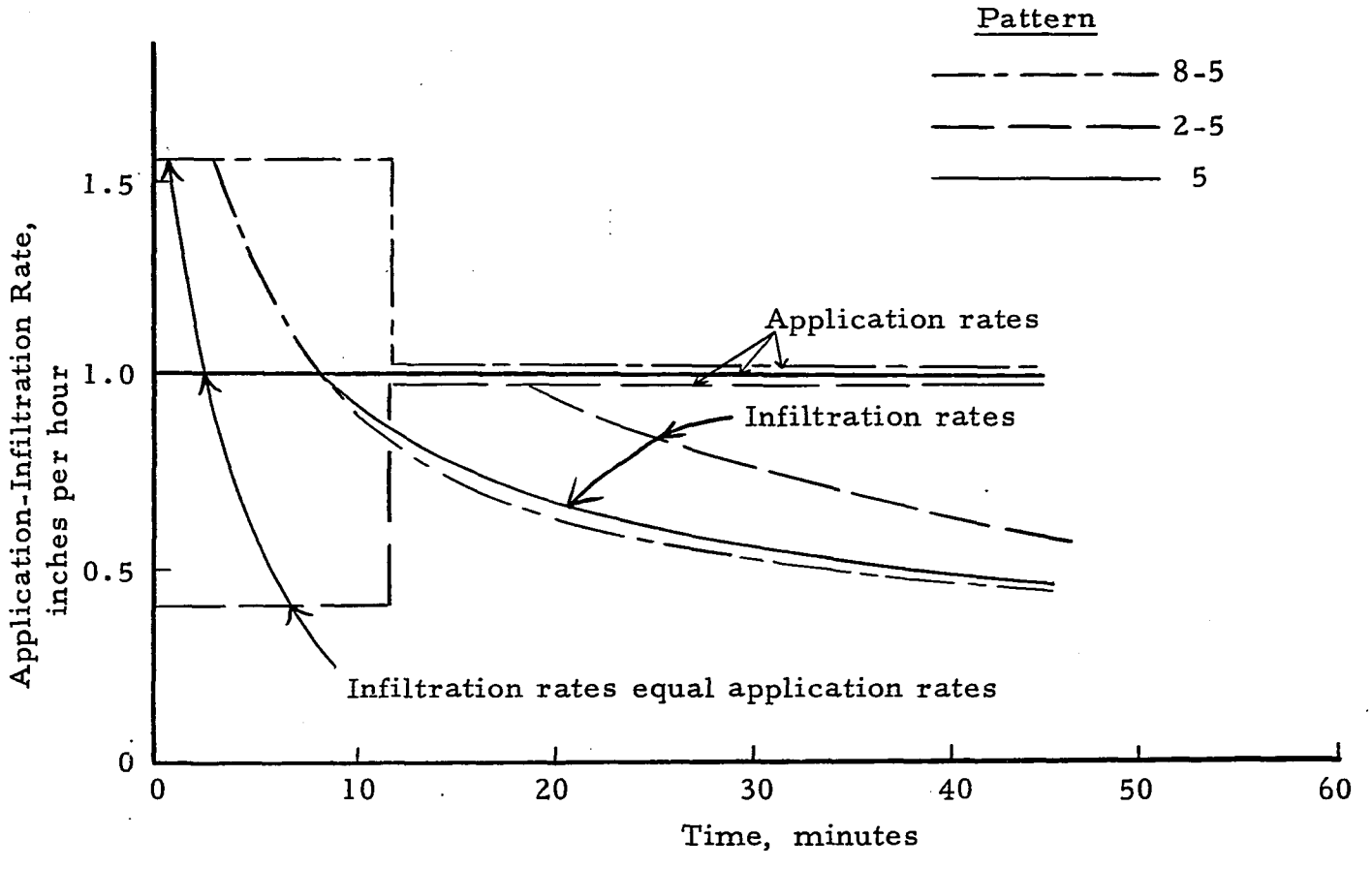

Figure 5.5 Average infiltration rate and time for a sandy clay loam from laboratory tests

Next, the relationship between infiltration rate and depth of intake was determined. The laboratory data of Figures 5.1, 5.2, and 5.3 were averaged to establish relationships between infiltration rate and depth of intake (Figures 5.6 and 5.7). For the loam (Figure 5.6), the infiltration curves for patterns 5 and 2-5 are nearly identical, but the infiltration curve for pattern 8-5 is substantially different. However, for the sandy clay loam (Figure 5.7), the infiltration curves for patterns nearly coincide. Therefore, representing infiltration rate only as a function of intake depth may be valid for one soil but questionable for another, since the type of application rate pattern affects this relationship.

Calibration of Model to Fit Laboratory Tests

The model was calibrated to achieve a reasonable simulation of the laboratory data. Three possibilities were considered for ensuring that the model would simulate the laboratory tests. The possibilities tested consisted of using a homogeneous soil, using a stratified soil, and choosing saturated conductivity, K, values other than those obtained in the permeability tests for the homogeneous and stratified soil. Before discussing the three possibilities, some important aspects of the model will be discussed that pertain to verifying the simulation.

The model utilizes a numerical solution to two basic moisture flow equations -- Darcy's law and continuity. Moisture-tension-

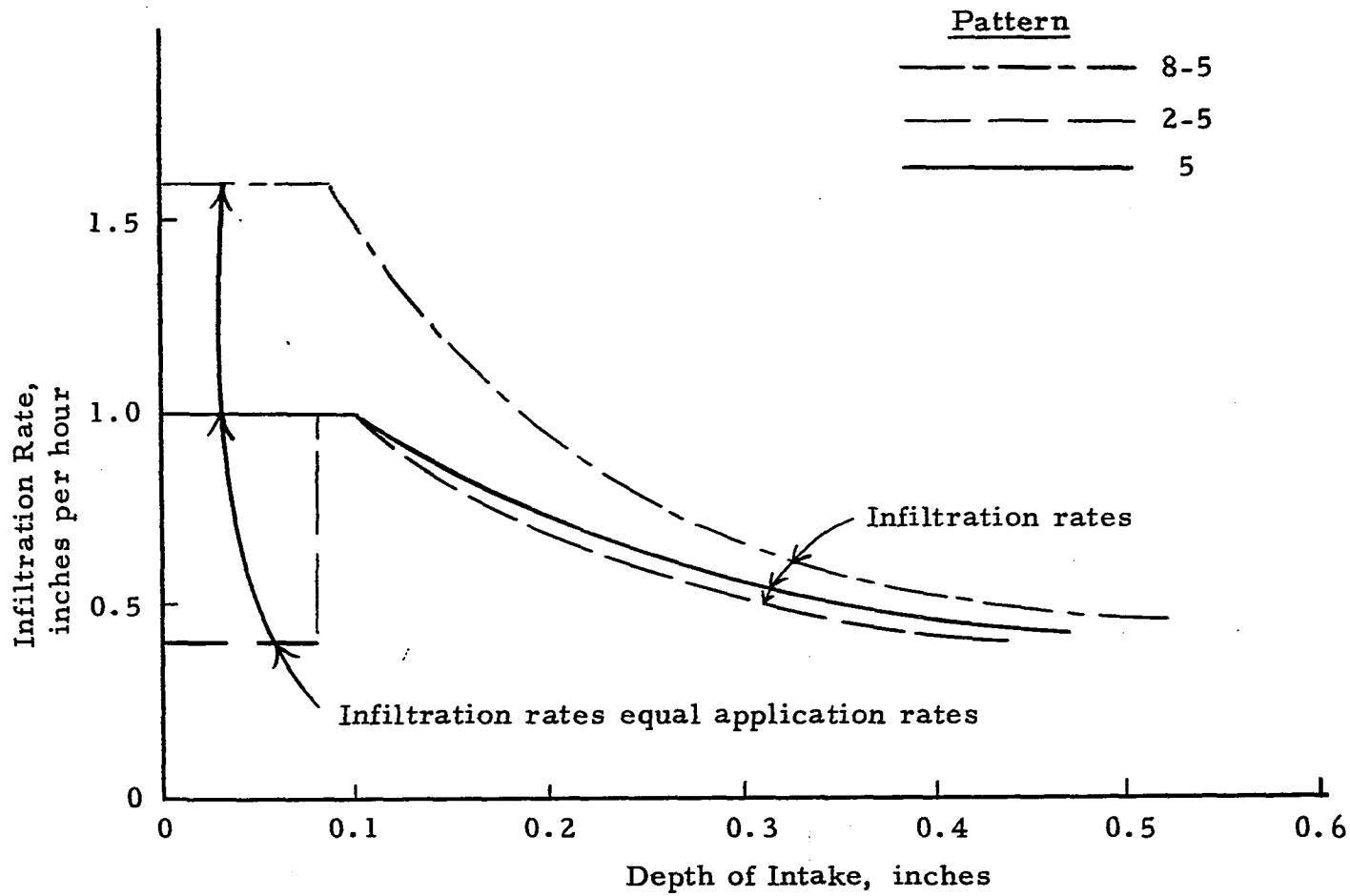

Figure 5.6 Average infiltration rate and depth of intake for a loam from laboratory tests

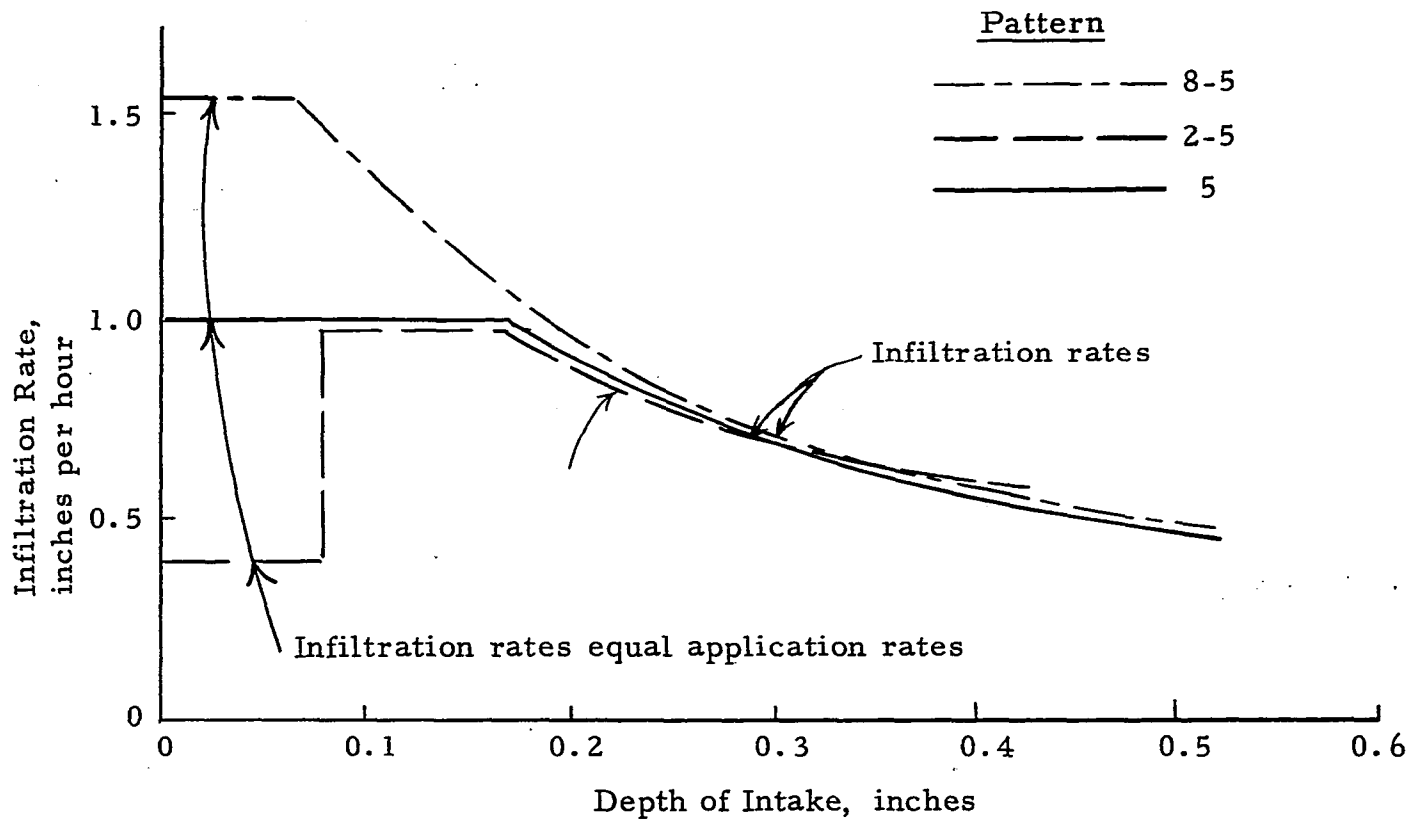

Figure 5.7 Average infiltration rate and depth of intake for a sandy clay loam from laboratory tests

permeability relationships for a particular soil were employed as model inputs. Initial moisture contents (Table 5.1) were used as the initial conditions for the model.

A semi-infinite column (25 inches) was assumed for the lower boundary condition of the model by prescribing a constant potential at 25 inches. Static equilibrium is assumed below the lowest depth specified (six inches) for the initial moisture contents (Table 5.1).

The upper boundary conditions are the application rate, until runoff begins, and a saturated upper boundary - zero potential - after runoff begins.

Homogeneous Soil Model

Several saturated conductivity, K, values and a homogeneous soil were input to the model to simulate the laboratory infiltration tests of patterns 8-5, 5, and 2-5. The fitting of the model to the infiltration curve of pattern 5 for the sandy clay loam is described here.

The model indicated no runoff using a K value of 0.415 inches per hour estimated from the water permeability test (Figure 4.7). The model did not produce a good fit using other K values for a homogeneous soil. A K value of 0.04 inches per hour produced the closest approximate average fit (Figure 5.8); however, the infiltration curve was too steep and was not well fitted to the data. A K value lower than 0.04 inches per hour would be required to make the computed curve fit the

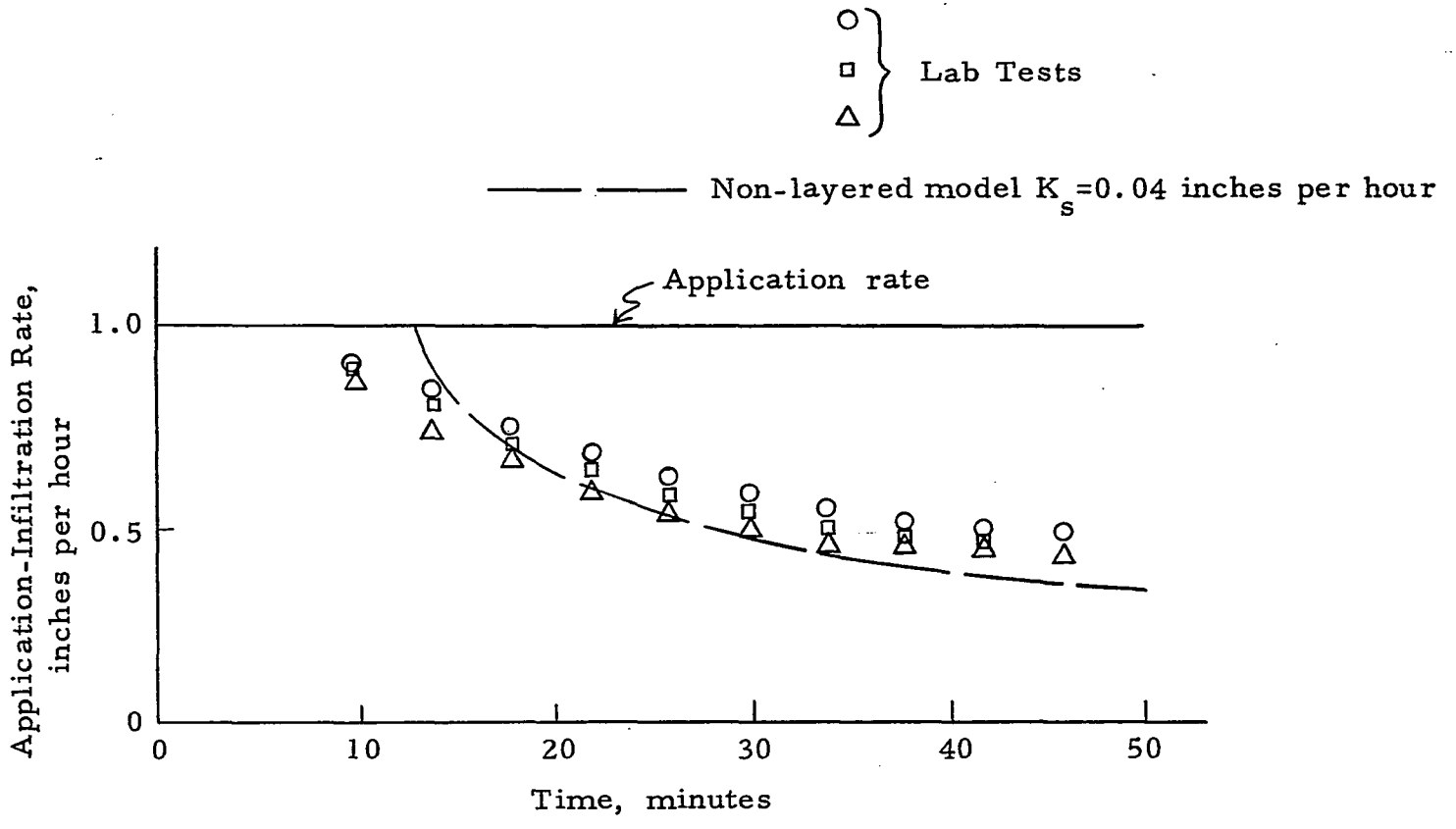

Figure 5.8 Infiltration rate comparison between a non-layered model and laboratory test data - sandy clay loam

data in the initial runoff stage. A K value higher than 0.04 inches per hour would be required to make the computed curve fit the data in the final part of the tests. Therefore, no single value of saturated conductivity would yield a curve whose shape was reasonably matched by the laboratory data.

Stratified Soil Model

The soil surface appeared to be puddled in the laboratory tests; therefore, simulating a stratified soil should give a better approximation to laboratory conditions (and very likely field conditions) than simulating a homogeneous soil.

Several combinations of K values and layer thicknesses were tested. First, a low K value was used for the upper 0.2 inches and the K value of 0.415 inches per hour estimated from the water permeability test (Figure 4.7) was used for the lower layer. An example of using a low K value (0.007 inches per hour) at the surface is shown in Figure 5.9. Using 0.415 inches per hour for the K value in the sublayer required a low K value for the surface layer to approximate the final laboratory infiltration rate. The low K value for the surface layer caused runoff to begin too soon and resulted in an infiltration curve which was too steep at the start of runoff.

Secondly, increasing the K value at the surface to 0.017 inches per hour and increasing the surface layer thickness to 0.5 inches, while the K value for the lower layer remained 0.415 inches per hour, caused an infiltration curve which was also too steep at the time of

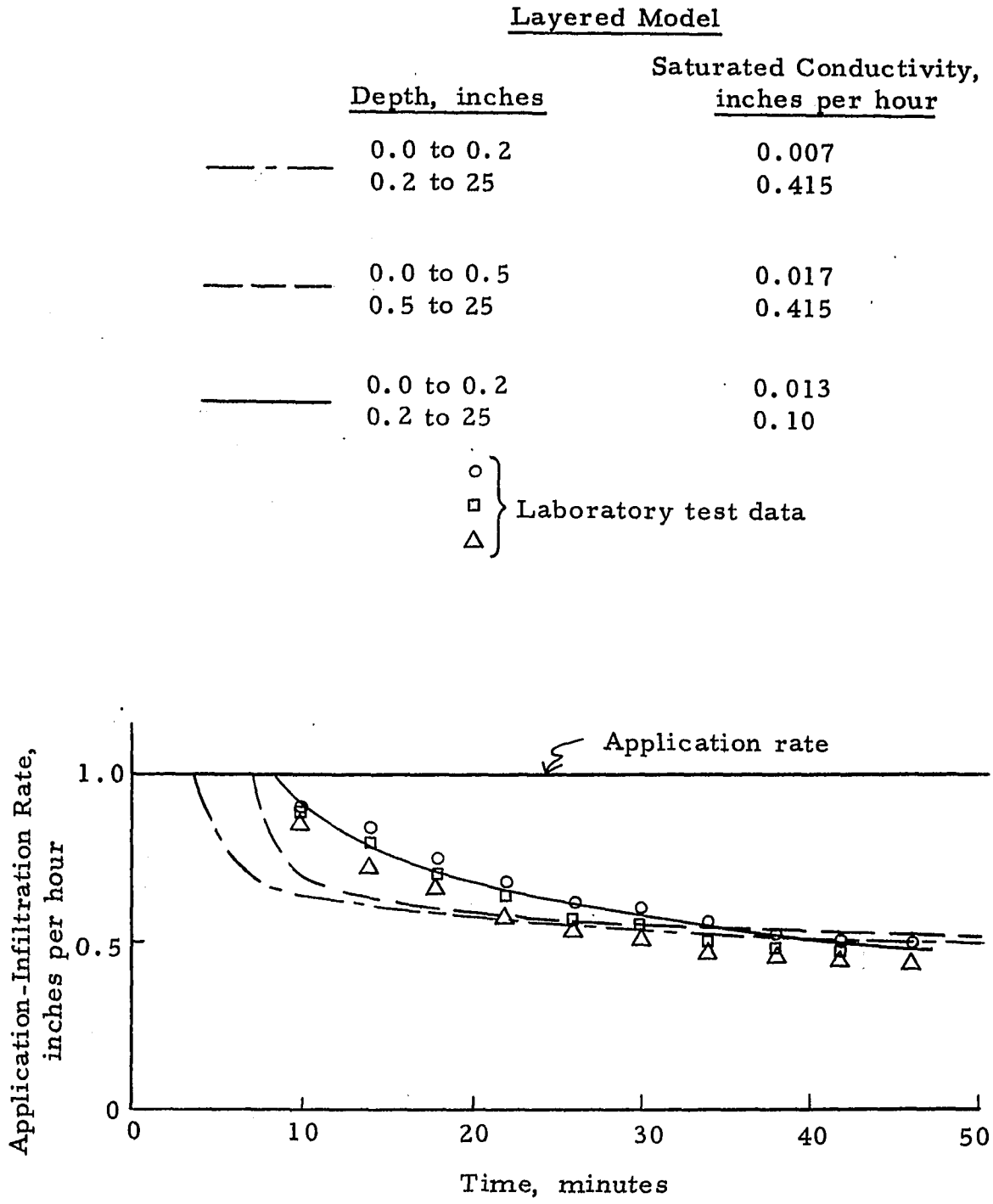

Figure 5.9 Infiltration rate comparison between a layered model with a high K value in the lower layer and laboratory test data - sandy clay loam

runoff. After reasoning that the puddled layer should not be over 0.5 inches thick, the conclusion was that the K value in the lower layer had to be reduced below 0.415 inches per hour.

Third, K values and layer thicknesses were chosen to obtain a reasonable fit of the model simulation to the laboratory infiltration curves. After numerous trials, a K value of 0.013 inches per hour was chosen for a surface layer thickness of 0.2 inches, while a K value of 0.10 inches per hour was chosen for the lower layer (Figure 5.9) for the sandy clay loam.

Three combinations of K values and surface layer thickness described for the sandy clay loam were also used for the loam. The K values which produced the best model-experiment agreement for the two soils are listed in Table 5.2.

Table 5.2 Saturated conductivity values chosen for the model

Soil	Saturated Conductivity, inches per hour	
	0.2 Inches of Surface Soil	Soil Below 0.2 Inches
Sandy Clay Loam	0.013	0.10
Loam	0.020	0.10

The K values could have been higher in the permeability tests than in the laboratory infiltration tests for several reasons, such as small errors in density measurement and differences in microbiological activity. A small increase in density can decrease conductivity

considerably as described in the literature review (Equations 2.1 and 2.2). An increase in microbiological activity can result in slime coating the pores and decreasing conductivity.

At this point, the following data are required for the model:

1. Relationships between moisture content or saturation and capillary pressure (Figure 4.9);
2. Relationships between relative permeability and capillary pressure (e.g., the upper Soltrol imbibition curve shown in Figure 5.2 and the Soltrol imbibition curve shown in Figure 5.3 are used to calculate the k_r-ψ relationships for the sandy clay loam and loam, respectively);
3. Initial moisture contents of laboratory infiltration tests (Table 5.1); and
4. Saturated conductivity values (Table 5.2), which were chosen to attain good agreement between laboratory tests and an assumed stratified soil model.

Model Verification

Computed infiltration curves, using the model, are presented in Figures 5.1, 5.2 and 5.3, along with the laboratory data. A reasonable fit was obtained between laboratory and model tests for the constant and two-step application rate patterns.

Simulated Center-Pivot Application Rate Patterns

The next steps were to use center-pivot application rate patterns in laboratory infiltration tests, simulate the laboratory tests with the model using the same center-pivot patterns, and check the fit of the model infiltration curves with the laboratory infiltration curves.

One symmetrical and two non-symmetrical application rate patterns were selected for study (Figures 5.10 to 5.14). The symmetrical pattern is similar to a pattern existing near the outer end of many center-pivot systems in the field. The non-symmetrical patterns, humped toward the front, are possibilities for proposed patterns.

Because of laboratory equipment limitations, laboratory patterns are stair-stepped rather than smooth curves as encountered with field center-pivot patterns.

Peak application rates, time lengths and applied depths considered practical in the field were chosen for the patterns; however, the peak rates, time lengths and applied depth can vary considerably in the field. Each pattern applied the same total depth of water.

Infiltration rates for the tests simulating center-pivot patterns are shown in Figures 5.10 to 5.14. Each plotted point represents the average infiltration rate of six soil compartments over a two- or four-minute time interval.

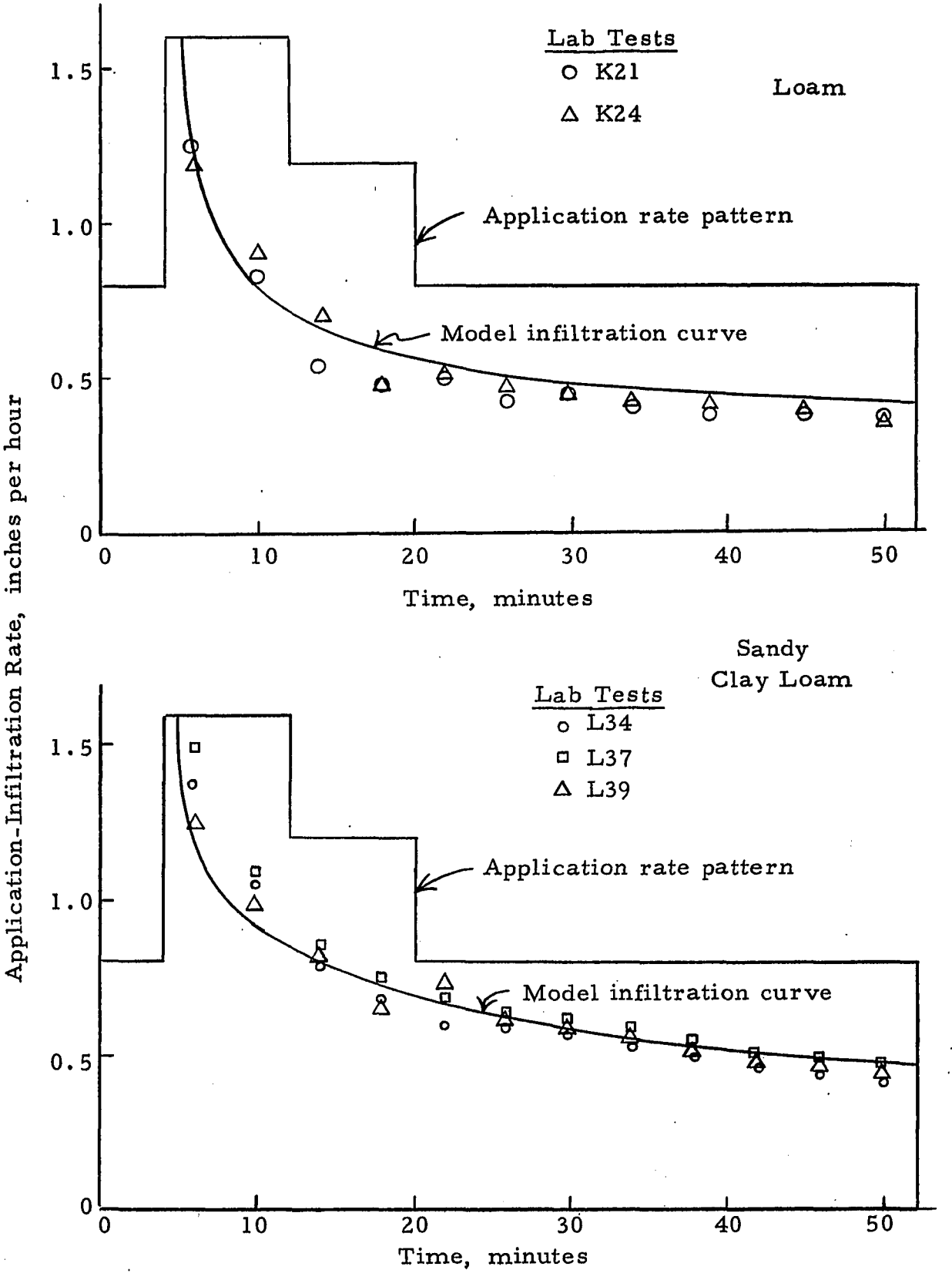

Figure 5.10 Application and infiltration rates for center-pivot pattern B

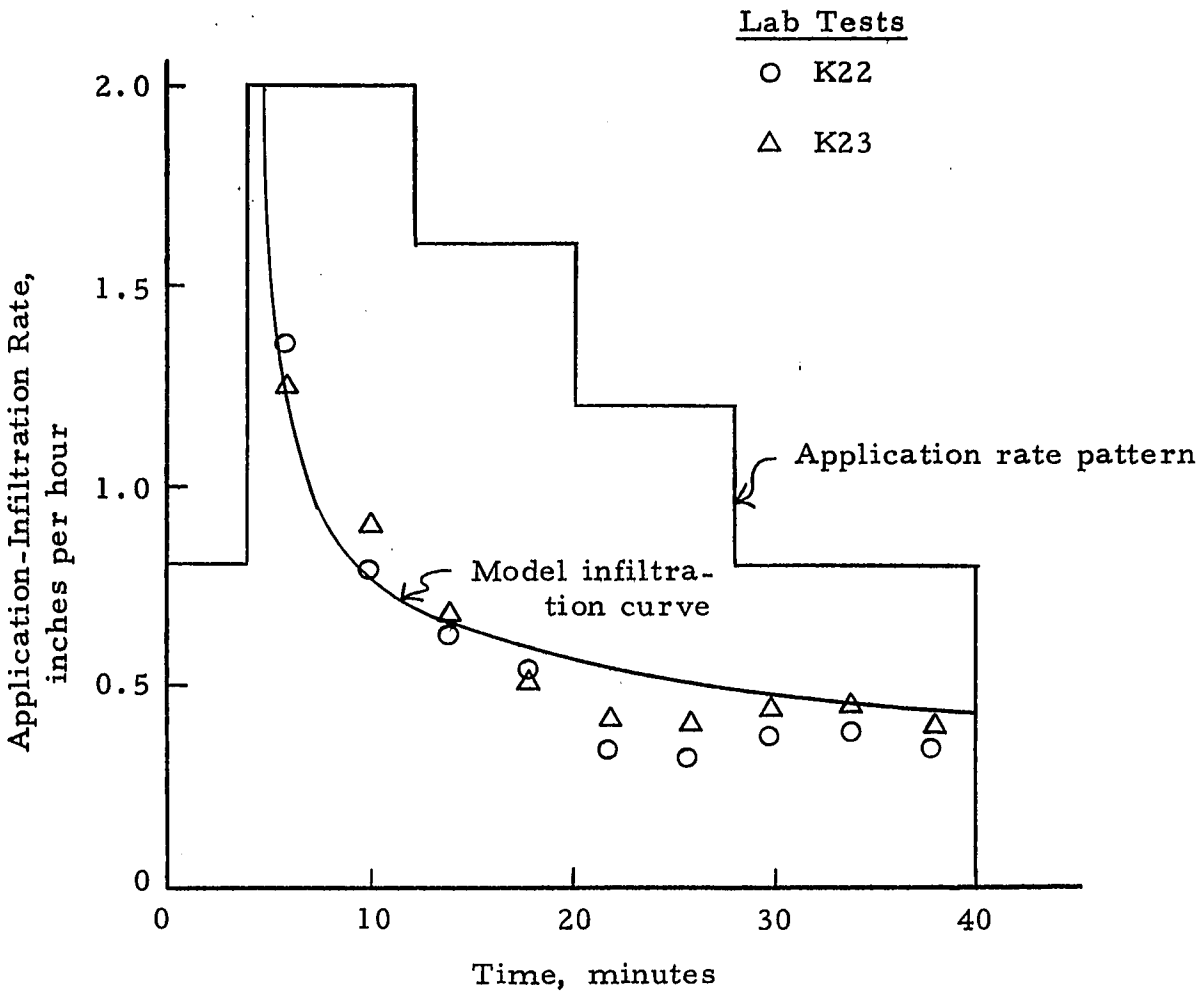

Figure 5.11 Application and infiltration rates for center-pivot pattern C - loam

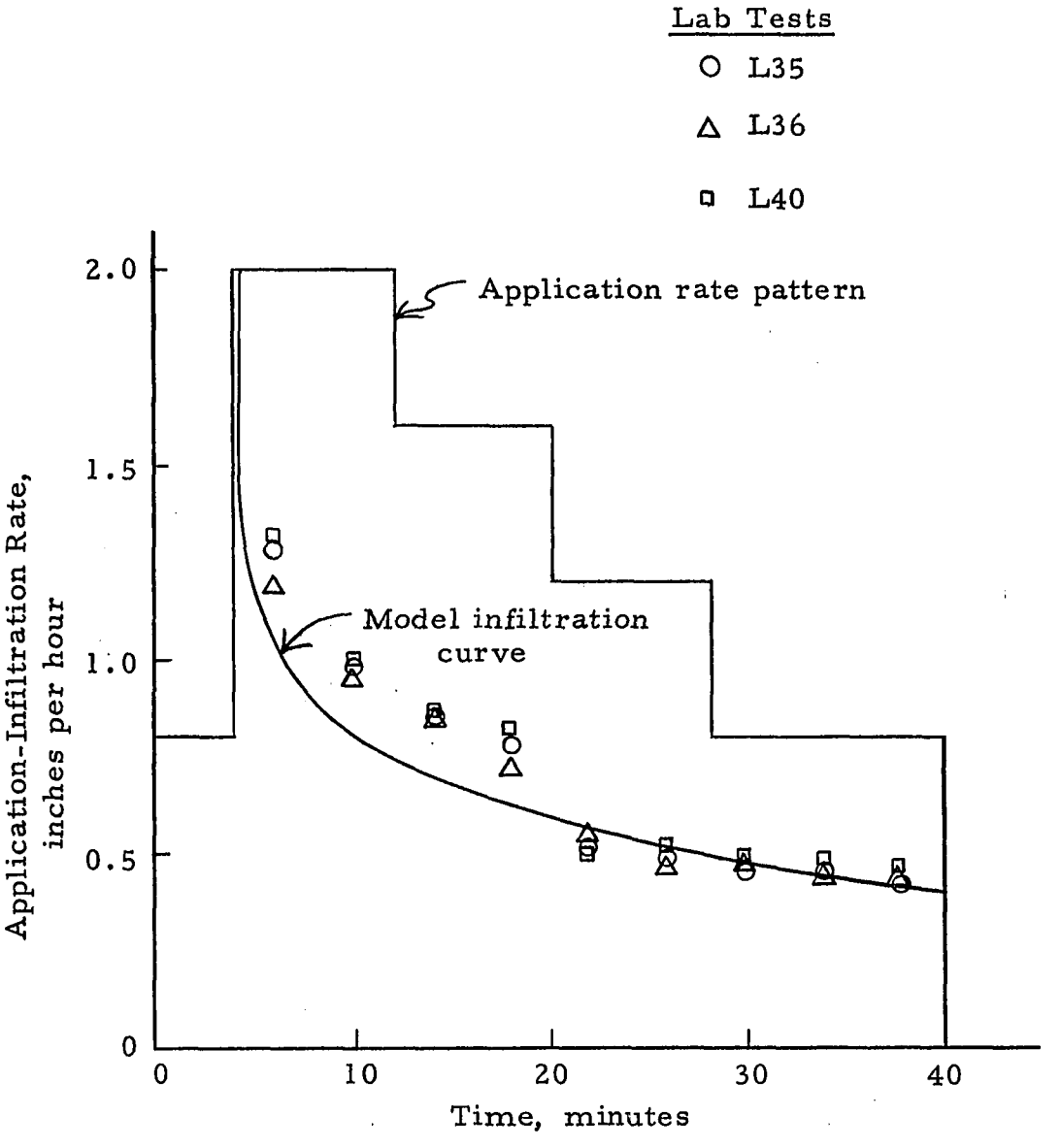

Figure 5.12 Application and infiltration rates for center-pivot pattern C - sandy clay loam

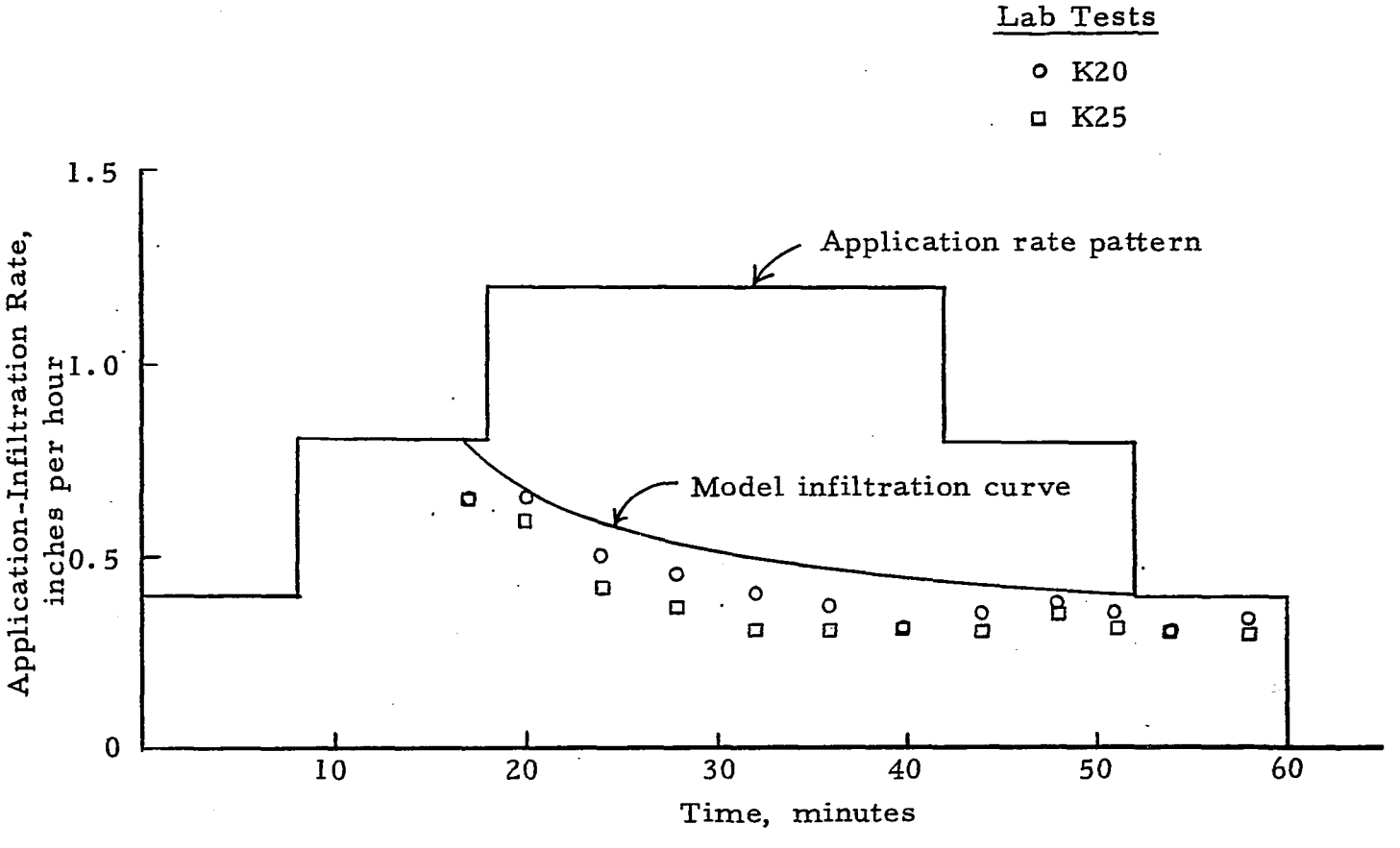

Figure 5.13 Application and infiltration rates for center-pivot pattern A - loam

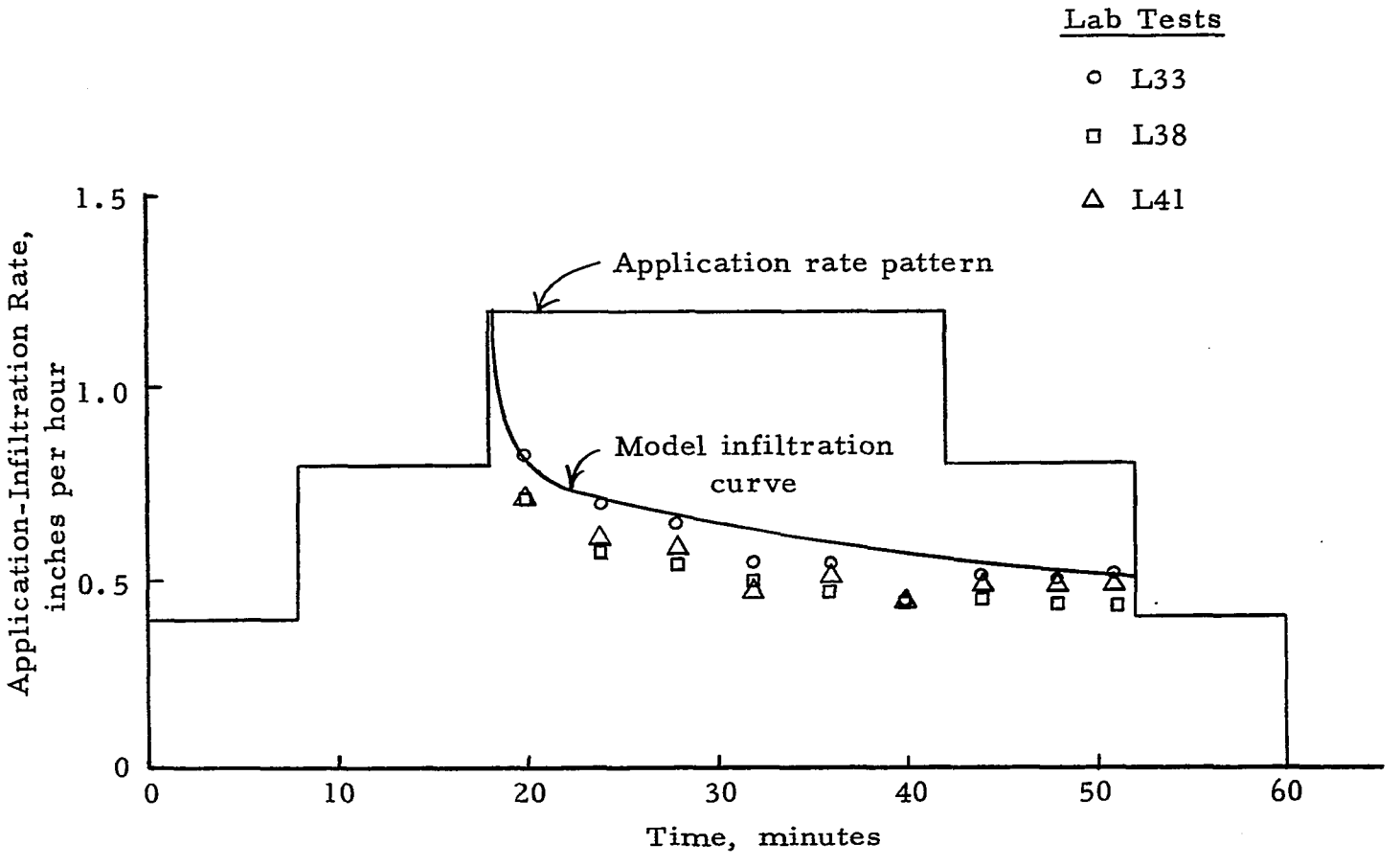

Figure 5.14 Application and infiltration rates for center-pivot pattern A - sandy clay loam

The six tests on the loam were run in the following order: A, B, C, C, B, and A. The nine tests on the sandy clay loam were run in the following order: A, B, C, C, B, A, B, C, and A.

Average intake depth for each pattern for the sandy clay loam is presented in Table 5.3. For the laboratory results, pattern B had a significantly higher intake depth than A or C at the 95% confidence level, as tested with a paired t statistic and described by Dixon and Massey (12) (Appendix A). There is no significant difference in intake depth between patterns A and C. The laboratory intake depth of pattern C is approximately the same as for pattern A; however, the pattern C's time length is two thirds the time length of A.

Table 5.3 Intake depth for center-pivot patterns on a sandy clay loam soil - applied depth of 0.85 inches

Pattern[2]	Time Length Minutes	σ_D[1]	Intake Depth, inches Laboratory	Model
A 2 4 6 4 2 	60	0.058	0.55	0.59
B 4 8 6 4 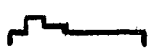	52	0.078	0.61	0.59
C 4 10 8 6 4 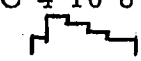	40	0.106	0.54	0.49

[1] σ_D is the standard deviation of the differences from a paired t statistic, e.g. 0.058 is the standard deviation of paired differences of patterns A's and B's intake depth (Appendix A).

[2] The numbers behind the pattern letter indicate number of nozzles operating. Each nozzle applied 0.2 inches per hour.

Average intake depth for each pattern for the loam is presented in Table 5.4. For the laboratory tests, there are significant differences, at the 95% confidence level, between the intake depths of all three patterns for the loam.

Table 5.4 Intake depths for center-pivot patterns on a loam - applied depth of 0.85 inches

Pattern	Time Length Minutes	σ_D[1]	Intake Depth, inches Laboratory	Model
A 2 4 6 4 2 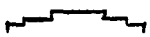	60	0.047	0.44	0.53
B 4 8 6 4 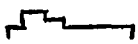	52	0.031	0.49	0.52
C 4 10 8 6 4 	40	0.051	0.41	0.44

[1] σ_D is the standard deviation of the differences from a paired t statistic e.g. 0.058 is the standard deviation of paired differences of patterns A's and B's intake depth (Appendix A).

The laboratory tests indicate a definite advantage for front-humped non-symmetrical application rate patterns. For both soils, the laboratory tests show approximately an 11 percent increase in intake depth of humped pattern B over symmetrical pattern A even though the time length was reduced approximately 13 percent (Tables 5.3 and 5.4).

The laboratory tests also indicate a disadvantage for front-humped patterns if the time length is shortened considerably. Humped pattern C had approximately two percent and seven percent less intake

depth than symmetrical pattern A for the silty clay loam and loam, respectively; however, the time length of pattern C is 33 percent less than A.

The next question was, how well does the model simulate the laboratory infiltration tests using the center-pivot patterns.

Model Simulation of Infiltration Under Center-Pivot Application Rate Patterns

The initial moisture contents of the laboratory tests using the center-pivot patterns were approximately the same as the tests with the constant and two-step patterns. Therefore, the only change in the model is the upper boundary with the center-pivot application rate patterns.

A reasonable fit of the model to the laboratory tests was achieved as illustrated in Figures 5.10 to 5.14. The main differences between the model and laboratory tests occurred in the model's overestimating the infiltration rate for symmetrical pattern A on both soils (Figures 5.13 and 5.14).

The ratios between model and laboratory intake depths for three center-pivot patterns (Table 5.5) show that the model overestimated intake depth for pattern A more than for the other two patterns.

Table 5.5 Ratios of model and laboratory intake depths taken from Tables 5.4 and 5.5

Pattern	Ratio - $\frac{\text{Model Intake Depth}}{\text{Laboratory Intake Depth}}$ Sandy Clay Loam	Loam
A 2 4 6 4 2 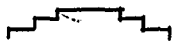	1.07	1.20
B 4 8 6 4 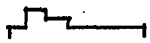	0.97	1.06
C 4 10 8 6 4 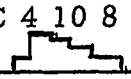	0.91	1.07

If K were allowed to decrease with time from the start of a test, a better estimate of intake depth should have resulted. A reduction of K with time should have reduced the computed intake depth for pattern A more than for patterns B and C because A's time length is longest and A's peak application rate occurs later in time than B's or C's.

A reduction of K with time can possibly be explained by swelling. As the soil dries, shrinking occurs causing cracks and increasing K. When water is added, swelling occurs which decreases K. As shown in Figure 2.2, time has considerable effect on the amount of swelling. The conclusion drawn was that noticeable errors are introduced in the model by assuming the porous media (soil) is stable.

Extension of Model to Situations Beyond Laboratory Tests

The model was next applied to situations beyond the laboratory tests. The laboratory tests were somewhat limited in range of initial moisture content values and conductivity values. Several other application rate patterns appear frequently on center-pivot systems. The time length was shortened as the peak application rate of the pattern increased. Perhaps the time length for a humped pattern could be the same as the time length for a symmetrical pattern. Also, the time step was quite large in the laboratory tests and the effect of this large time step was checked. The effect of changing initial moisture content, conductivity, application rate patterns, time length, and time step size were studied using the model.

Effect of Initial Moisture Content

The drying method used in the laboratory tests dried the surface soil but left the soil at the two-inch depth near field capacity. In the field, the moisture content might be in a dry range to a depth of one foot or more.

The model indicates that lowering the initial moisture content in the lower layers increases the intake depths as expected (Tables 5.6 and 5.7), but the increase is not large.

Table 5.6 Intake depths for two moisture levels - sandy clay loam - applied depth of 0.85 inches

Pattern	Time Length Minutes	Computed Intake Depth, inches: Initial Moisture Contents @ Table 4.1	Computed Intake Depth, inches: Initial Moisture Content 0.136 cc/cc
A 2 4 6 4 2 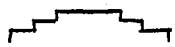	60	0.59	0.61
B 4 8 6 4 	52	0.59	0.63
C 4 10 8 6 4 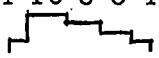	40	0.49	0.52

Table 5.7 Intake depths for two moisture levels - loam - applied depth of 0.85 inches

Pattern	Time Length Minutes	Computed Intake Depth, inches: Initial Moisture Contents @ Table 4.1	Computed Intake Depth, inches: Initial Moisture Content 0.132 cc/cc
A 2 4 6 4 2 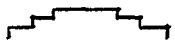	60	0.53	0.54
B 4 8 6 4 	52	0.52	0.53
C 4 10 8 6 4 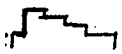	40	0.44	0.46

The humped pattern B now shows a greater intake depth than symmetrical pattern A for the lower initial moisture content on the sandy clay loam (Table 5.6).

Lowering the initial moisture content would increase shrinking and crack sizes on the sandy clay loam and loam in actual tests. An increase in shrinking should produce a greater advantage in intake depth for humped non-symmetrical patterns B and C than for symmetrical pattern A.

Effect of Conductivity

Low conductivity values for the two soils in the model have been used to approximate the laboratory infiltration curves. The soils were sieved in the laboratory tests, thereby reducing the conductivity. Very likely the soils would have had higher conductivity values in the field because the soils would have had more structure if they were not sieved.

Increasing the conductivity values used in the model by 30 percent increased the intake depths 12 percent to 18 percent for the sandy clay loam (Table 5.8) and 10 percent to 14 percent for the loam (Table 5.9). After increasing the conductivity values, the model shows greater intake depths for both soils for the humped pattern B than for the symmetrical pattern A.

Table 5.8 Intake depth for two conductivity levels - sandy clay loam - applied depth of 0.85 inches

Pattern	Time Length Minutes	Computed Intake Depth, inches K = 0.013 iph K = 0.100 iph	Computed Intake Depth, inches K = 0.0169 iph K = 0.130 iph
A 2 4 6 4 2 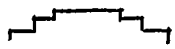	60	0.59	0.67
B 4 8 6 4 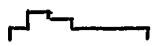	52	0.59	0.70
C 4 10 8 6 4 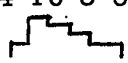	40	0.49	0.55

Table 5.9 Intake depths for two conductivity levels - loam - applied depth of 0.85 inches

Pattern	Time Length Minutes	Computed Intake Depth, inches K = 0.020 iph K = 0.100 iph	Computed Intake Depth, inches K = 0.026 iph K = 0.130 iph
A 2 4 6 4 2 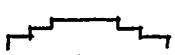	60	0.53	0.59
B 4 8 6 4 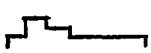	52	0.52	0.60
C 4 10 8 6 4 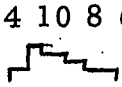	40	0.44	0.51

If shrinking and swelling were considered in the tests shown in Tables 5.8 and 5.9, pattern B should have an 11 percent or greater intake depth than A. The 11 percent is the percentage difference of the intake depths between patterns B and A given in the laboratory tests (Tables 5.3 and 5.4).

Effect of Distance From Pivot and Sprinkler Spacing

The application rate pattern varies at different points along a center-pivot system. At the pivot, the peak application rate is lower and the time length is longer than near the outer end of the system. Pattern A (Figure 5.13) would occur (as a smooth curve without the steps) near the outer end of many center-pivots. Pattern D (Figure 5.15) would be approximated near the center of many center-pivots. The computed intake depths of pattern D are considerably greater than the computed intake depths of pattern A for both soils (Table 5.10).

Some systems use smaller sprinklers spaced closer together than a typical system with 30- to 33-foot sprinkler spacings. At the outer end, the sprinkler spacing may be only seven feet. The application rate pattern resulting from this close spacing is shown in Figure 5.15 as pattern E. Pattern E shows a considerably smaller computed intake depth for both soils than pattern A (Table 5.10).

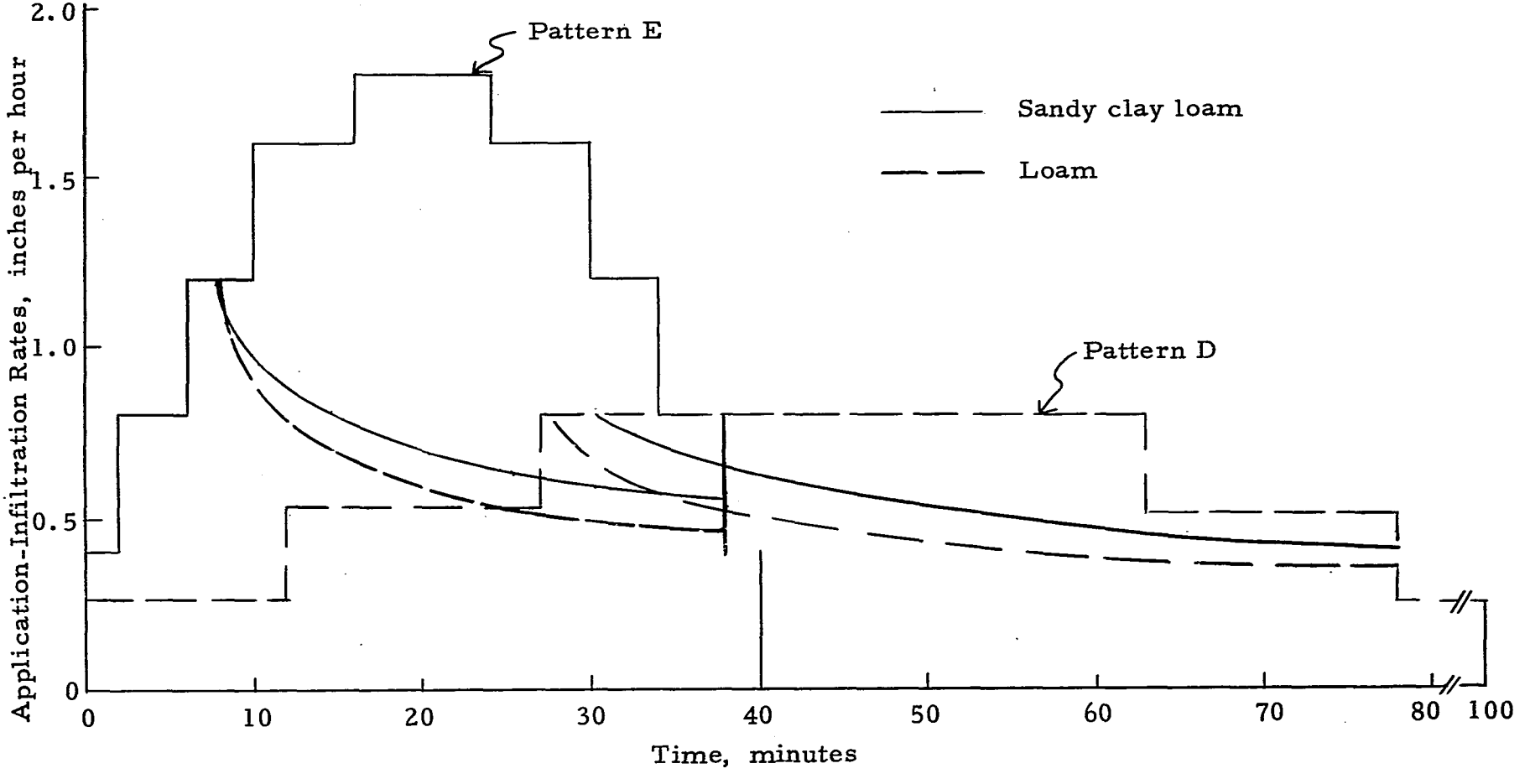

Figure 5.15 Application rates and computed infiltration curves - Patterns D and E

Table 5.10 Intake depths for three symmetrical patterns with different peak rates and different time lengths - applied depth of 0.85 inches

Pattern	Time Length Minutes	Computed Intake Depth, inches Sandy Clay Loam	Loam
E 2 4 6 8 9 8 6 4 2 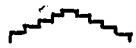	40	0.48	0.43
A 2 4 6 4 2 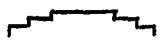	60	0.59	0.53
D 1.3 2.6 4 2.6 1.3 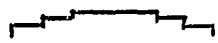	90	0.73	0.63

If shrinking and swelling were considered, the short symmetrical pattern E should have more increase in intake depth than the longer symmetrical pattern D especially for fine textured soils which were allowed to get drier between irrigations. However, the intake depth would still be lower for pattern E under the conditions of the laboratory tests.

Effect of Time Length

A humped non-symmetrical pattern would most likely require a shorter time length than a symmetrical pattern.

The ideal pattern is a humped pattern having the same time length as a symmetrical pattern, applying an equal depth. Extending pattern B to 60 minutes, with the model, increases the intake depth approximately seven to ten percent (Table 5.11). Extending pattern C

Table 5.11 Intake depths for different time lengths using patterns A, B and C - applied depth of 0.85 inches

Pattern	Time Length Minutes	Intake Depths, inches Computed / Laboratory Sandy Clay Loam	Loam
A 2 4 6 4 2 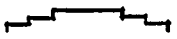	60	0.59 / 0.55	0.53 / 0.46
B 4 8 6 4 	52	0.59 / 0.61	0.52 / 0.49
B_m 4 8 6 4 2[2] 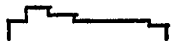	60	0.63[1] / 0.65	0.57[1] / 0.54
C 4 10 8 6 4 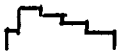	40	0.49 / 0.54	0.44 / 0.41
C_m 4 10 8 6 4 2[3] 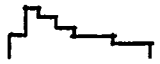	60	0.61[1] / 0.67	0.57[1] / 0.53

[1] Lower number is potential intake depth assuming laboratory tests had gone 60 minutes; e.g. for sandy clay loam - B_m -

$$\frac{\left[\left(\frac{0.63 - 0.59}{0.59}\right) 0.61 + 0.61\right] - 0.55}{0.55} = 0.65$$

[2] Pattern B_m consists of 4 minutes of .08 iph, 4 minutes of 2.0 iph, 4 minutes of 1.5 iph, 8 minutes of 1.2 iph, 20 minutes of 0.8 iph, and 20 minutes of 0.4 iph.

[3] Pattern C_m consists of 4 minutes of 0.8 iph, 6 minutes of 1.6 iph, 6 minutes of 1.2 iph, 34 minutes of 0.8 iph, and 10 minutes of 0.4 iph.

to 60 minutes increases the intake depth approximately 25 to 30 percent (Table 5.11). The model now shows a greater intake depth for humped patterns B_m and C_m than for symmetrical pattern A.

Extending the time length of the humped patterns with the laboratory tests to 60 minutes would also increase the humped patterns' intake depths. Assuming the same percentage increase in intake depth would occur in the laboratory tests, as occurred with the model simulation, because of extending the tests to 60 minutes (Table 5.11), the potential results would be as follows:

loam - 60-minute humped pattern B_m would have a 23 percent greater intake depth than symmetrical pattern A;

- 60-minute humped pattern C_m would have a 20 percent greater intake depth than symmetrical pattern A;

sandy clay loam - 60-minute humped pattern B_m would have an 18 percent greater intake depth than symmetrical pattern A;

- 60-minute humped pattern C_m would have a 22 percent greater intake depth than symmetrical pattern A.

Effect of Time Step Size

The effect of size of time increment was described under solution sensitivity. In this section, the effect of size of the time step used in the application rate pattern will be examined.

A center-pivot system produces a smooth application rate pattern and no steps such as are used in this study. A model comparison using sandy clay loam soil was made between pattern A and a smoother pattern, but with the same general shape as A. The results (Figure 5.16) show the same intake depth for both patterns.

The upper pattern of Figure 5.16 is slightly steeper than the lower pattern which may have had a small effect on intake depth; however, the conclusion is reached that the size of time step has little effect on intake depth as long as the general shape of the pattern is maintained.

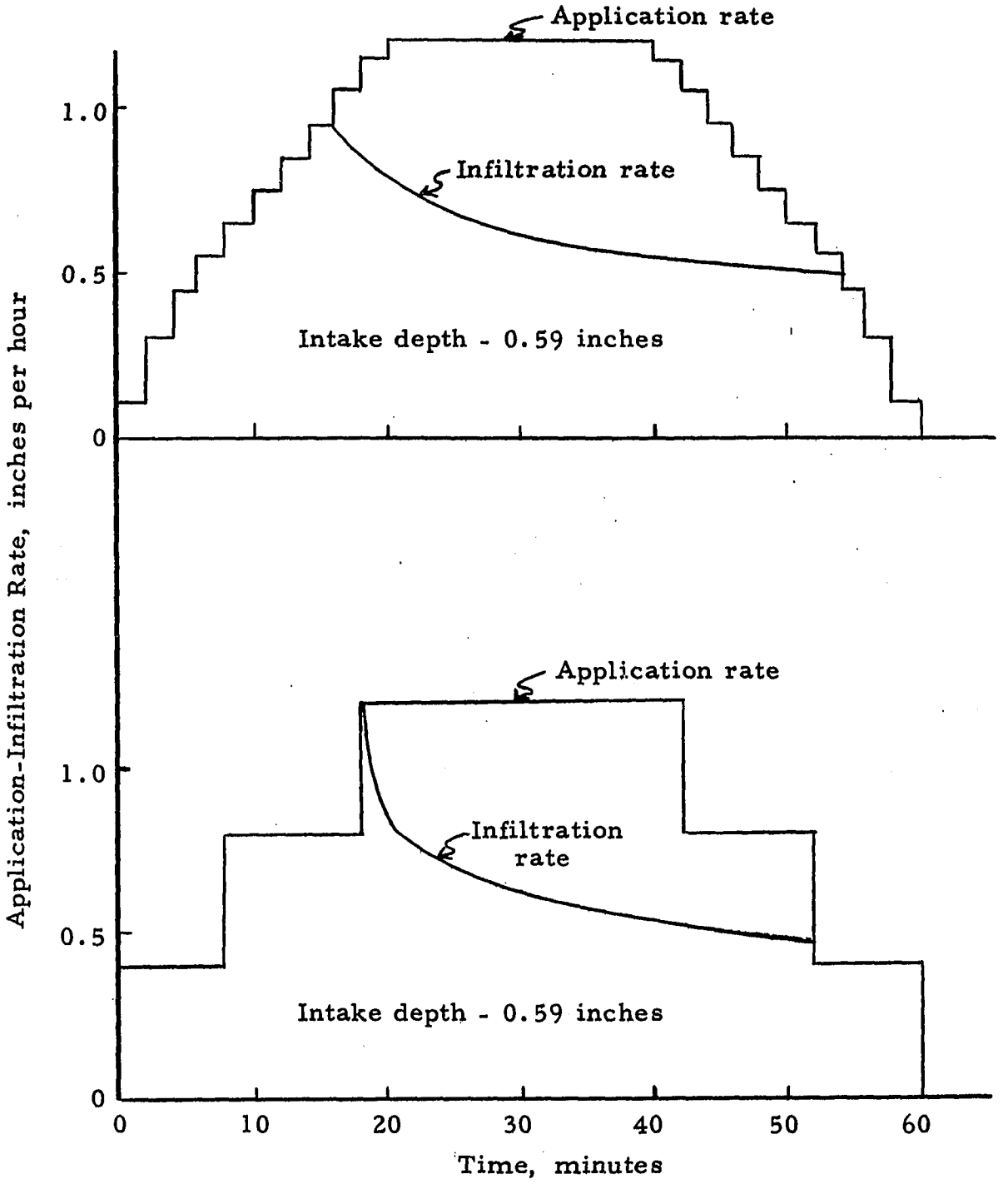

Figure 5.16 Infiltration curves for two patterns with different time-step sizes using the model - sandy clay loam - applied depth of 0.85 inches

Chapter VI

DESIGN CONSIDERATIONS

The items discussed in this chapter are a proposal for handling shrinking and swelling in the model, employing a modified infiltration rate theory proposed by Kincaid, et al., (28), and general design considerations.

Changing Model to Fit Swelling Soil

The numerical model, as used in this study, must be modified to include the effects of shrinking and swelling. Little advantage was observed for humped patterns if the effect of shrinking and swelling on conductivity was not included in the model (Tables 5.4 and 5.5). When shrinking and swelling were included (laboratory tests, Tables 5.4 and 5.5) humped pattern B indicated approximately an 11 percent increase in intake depth over symmetrical pattern A.

The model should be modified prior to further research or design of center-pivot patterns by making saturated conductivity a function of swelling. An equation, proposed to relate conductivity to the main swelling variables, is:

$$K_m = K[\, f(\theta_{0.25}) + f(\theta_{1.5}) + f(\rho) + f(t) + f(ID)] \qquad (6.1)$$

in which

K_m = modified saturated conductivity

K = saturated conductivity

f = indicates functional relationship

$\theta_{0.25}$ = initial moisture content at the 0.25-inch depth

$\theta_{1.5}$ = initial moisture content at the 1.5-inch depth

ρ = soil density

t = time

ID = intake depth.

Testing Theory of Kincaid

The first method proposed for calculating runoff under center-pivots is a modified infiltration rate theory of Kincaid, et al., (28). A comparison was made between intake depths using the model and the modified infiltration rate theory. The center-pivot application rate patterns A, B, and C (applying a depth of 0.85 inches) were used in the comparison.

Three equations (Equations 2.7, 2.15, and 2.20) are required for the modified infiltration rate theory of Kincaid, et. al., (28). The modified infiltration rate before runoff begins is

$$I_m = I D_p / D_a \qquad (2.15)$$

in which

$$I = I_o t^n. \qquad (2.7)$$

The infiltration rate after runoff begins is

$$I = I_o (t - \Delta t)^n. \qquad (2.20$$

The layered, non-uniform initial moisture content, non-swelling model was used to obtain ponded infiltration rate curves for the sandy clay loam and loam (Figure 6.1). Equation 2.7 was fitted to the ponded infiltration curve data and values for I_o and n obtained.

The results of using the modified infiltration equations indicate a good fit to the model for the sandy clay loam and loam (Tables 6.1 and 6.2). The modified infiltration rate theory results would not need to match the laboratory results because the infiltration curves used for the theory came from the model and not the laboratory experiments. Therefore, the question remains as to how Kincaid's theory would fit a soil which is allowed to shrink and swell. The question will be examined by looking at the effect of time and intake depth on ponded infiltration curves (which are the basis of Kincaid's theory) and looking at ponded infiltration curves which do not fit Equation 2.7.

Ponded Infiltration Curves

The modified infiltration theory of Kincaid, et al., (28) may give a good estimate of runoff to be expected under a center-pivot if the ponded infiltration curve is representative of soil conditions under the center-point at time of irrigation. These soil conditions include

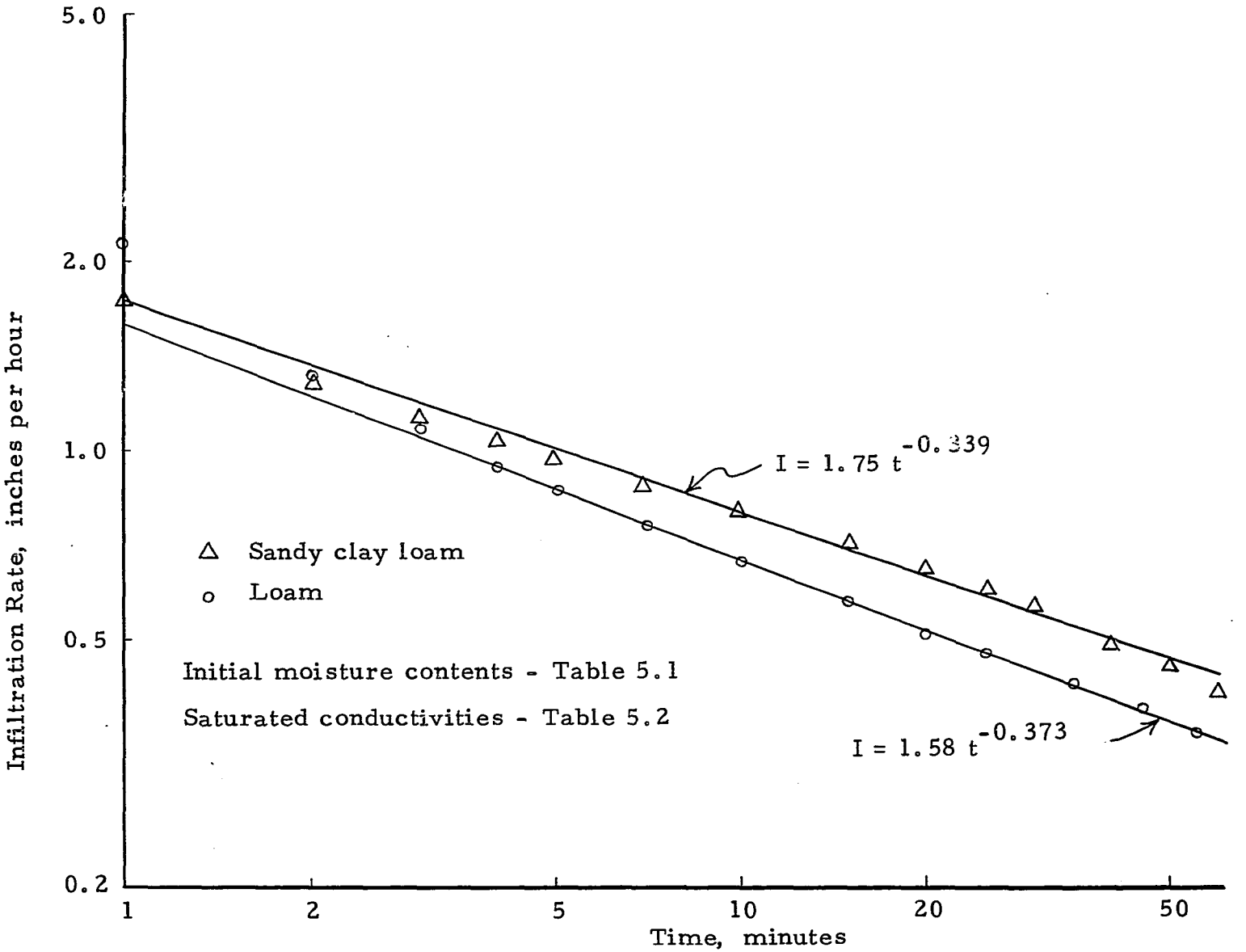

Figure 6.1 Ponded infiltration rate curves using model

Table 6.1 Comparison of intake depths between model and modified intake rate theory of Kincaid, et al., (28)--applied depth of 0.85 inches--center-pivot patterns--sandy clay loam

Pattern	Time Length	Intake Depth, inches		
	Minutes	Laboratory	Model	Kincaid
A 2 4 6 4 2 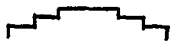	60	0.55	0.59	0.61
B 4 8 6 4 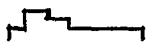	52	0.61	0.59	0.59
C 4 10 8 6 4 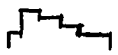	40	0.54	0.49	0.48

Table 6.2 Comparison of intake depths between model and modified intake rate theory of Kincaid, et al., (28)--applied depth of 0.85 inches--center-pivot patterns--loam

Pattern	Time Length	Intake Depth, inches		
	Minutes	Laboratory	Model	Kincaid
A 2 4 6 4 2 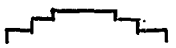	60	0.44	0.53	0.53
B 4 8 6 4 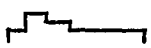	52	0.49	0.52	0.50
C 4 10 8 6 4 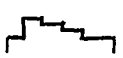	40	0.41	0.44	0.42

initial moisture content, density, stratification, and relationships between S, Ψ and k. However, the use of the modified infiltration theory may not result in a good estimate of the difference in intake depth between a front-humped and a symmetrical application rate pattern.

As an example, two hypothetical soils -- A1 and A2 -- have approximately the same ponded infiltration curves, but the curves could have resulted from different variables for each soil. Infiltration into soil A1 could be mainly influenced by swelling. Infiltration into soil A2 could be mainly influenced by the conductivity values of a stratified, non-swelling condition or by intake depth. A front-humped pattern would have a greater intake depth in soil A1 than A2 assuming swelling is mainly a function of time (Figure 2.2).

Categories of Ponded Infiltration Curves

Using only Equation 2.6 to represent infiltration characteristics of a soil for center-pivot infiltration studies can lead to important variables not being considered. Ponded infiltration rate curves on some soils do not fit Equation 2.6, particularly shrinking and swelling soils, which are important in the study of infiltration under non-symmetrical application rate patterns.

Three categories of ponded infiltration curves from 400 infiltrometer runs are presented by Fletcher and El-Shafei (19) as shown in Figure 6.2:

> First, those completely linearized by the log-log plot; second, those which produced more than one linear portion and third, those which were linear only after the first 5 or 10 minutes of a run being convex upward during the first portion of a run.

Fletcher and El-Shafei (19) attribute each break in a curve to either a new stratum in the soil, in the case of abrupt breaks, or a gradual change in the organic matter content to reflect a change in the wettability. Other reasons for the breaks in the curves (Figure 6.2) would be a change in moisture content or swelling.

Swelling could cause a logarithmic decrease in conductivity and not cause a break in the curve. However, swelling could occur at the start of infiltration and then essentially stop because of the soil structure resisting any further decrease in macro- or micro-pore space. A type 3 infiltration curve (Figure 6.2) could result if swelling initially occurred and then stopped.

Fitting of Equation 2.7 to a ponded infiltration curve is not required to apply the theory of Kincaid, et al., (28). If a type 2 or 3 ponded infiltration curve (Figure 6.2) is encountered, the actual infiltration curve could be used in place of Equation 2.7. The infiltration rate after runoff begins would be the actual infiltration curve moved over a distance Δt (Δt of Equation 2.20).

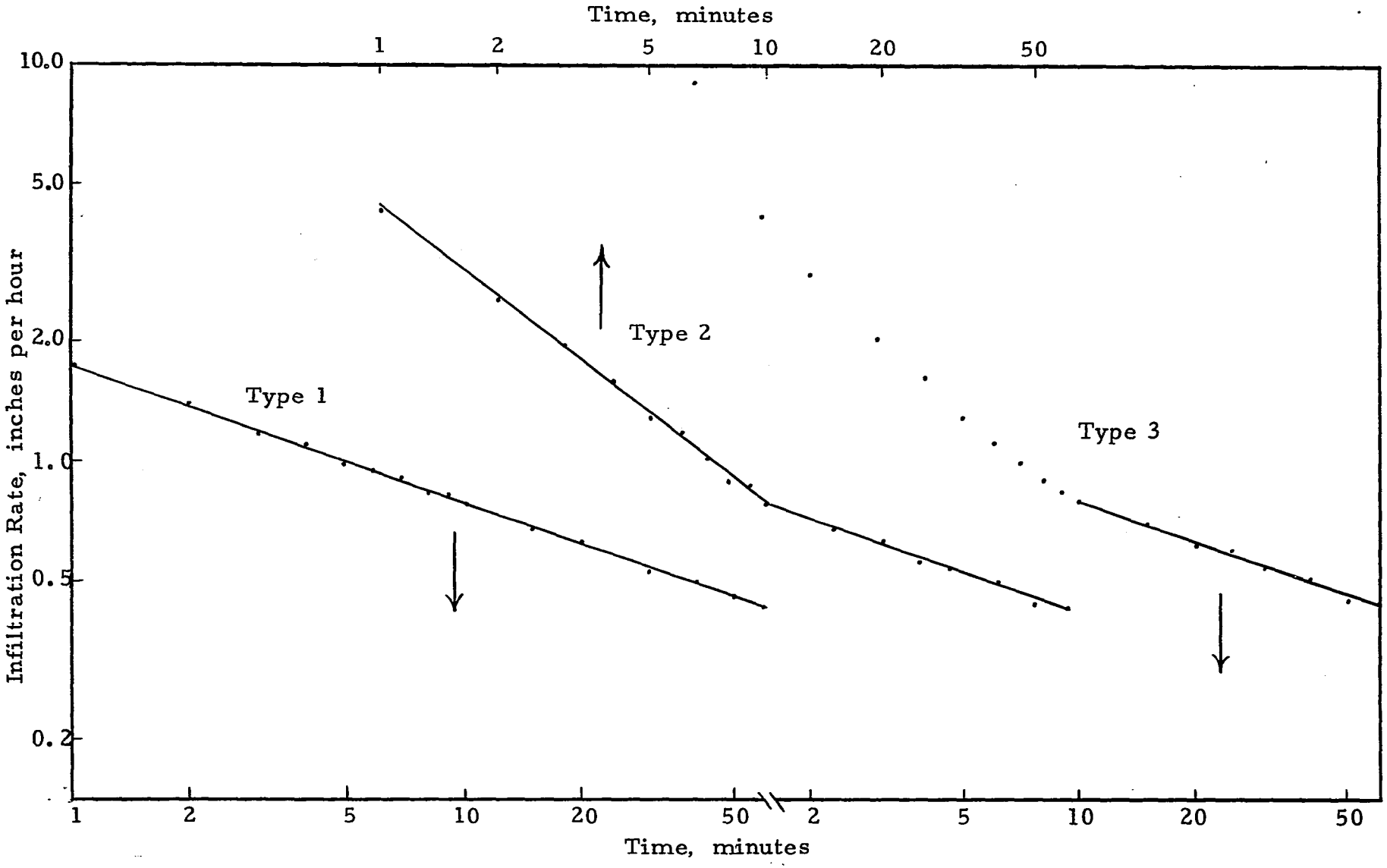

Figure 6.2 Types of ponded infiltration curves presented by Fletcher and El Shafei

General Design Considerations

Some adjustments in saturated conductivity and layering had to be made with the numerical model after comparing model tests with laboratory tests. Also, much time is required to obtain the relationships between ψ - S - k_r. Therefore, even though the model could be changed to handle shrinking and swelling soils, use of the model would very likely be feasible only for research work.

Ponded infiltration time curves obtained by sprinkling or flooding provide some information regarding the infiltration characteristics of a soil. The problem is the difficulty in relating a ponded infiltration time curve to infiltration under center-pivot application rate patterns. However, some guidelines can be postulated from ponded infiltration time curves, general infiltration knowledge, and the laboratory tests and model study reported herein.

In general, a soil having a steeper ponded infiltration rate curve will benefit more from a front-humped application rate pattern. Also, a type 2 or 3 ponded infiltration curve (Figure 6.2) would indicate an advantage for a front-humped pattern over a symmetrical pattern.

The peak of a front-humped pattern can be too high and cause considerable runoff. For the loam and the sandy clay loam, a peak application rate over approximately 1.2 inches per hour mostly

produced runoff for patterns B and C at the moisture conditions of the tests (Figures 5.10, 5.11, and 5.12).

The application rate for the latter part of a pattern can be too high and cause considerable runoff. Water applied in excess of 0.5 inches per hour for the last 20 minutes of patterns A and B (Figures 5.10, 5.11, and 5.12) was mainly runoff on the loam and sandy clay loam soils.

A graph is an ideal summary of general design considerations. An example of a possible design graph is shown in Figure 6.3. This example design graph was prepared using a design intake depth of 0.60 inches. A 60-minute ponded infiltration time curve of the soil must first be obtained. The soil must be at the density and moisture content condition which would exist when the center-pivot is to apply a sufficient depth to result in an intake depth of 0.60 inches.

Graphs for design intake depths other than 0.60 inches would be required to cover the wide variety of conditions that would be encountered under field conditions. A choice of design intake depth must be made. A few years ago the trend appeared to be headed in the direction of applied depths of 0.3 to 0.5 inches and one to two days per revolution for center-pivots. Today, the trend appears to be in the direction of greater applied depths (one inch or more) and longer time periods per revolution.

Area major part of curve falls in from 4 to 7 minutes	Area major part of curve falls in from 40 to 60 minutes	Application rate pattern recommended
A_1	A_2	A or B
B_1	B_2	B
C_1	A_2	A, B, or C
C_1	B_2	B or C
C_1	C_2	C

If curve falls below A_1 or C_2, or in areas A_1B_2, A_1C_2, or B_1C_2 center-pivot is not recommended for a 0.60 inch design intake depth.

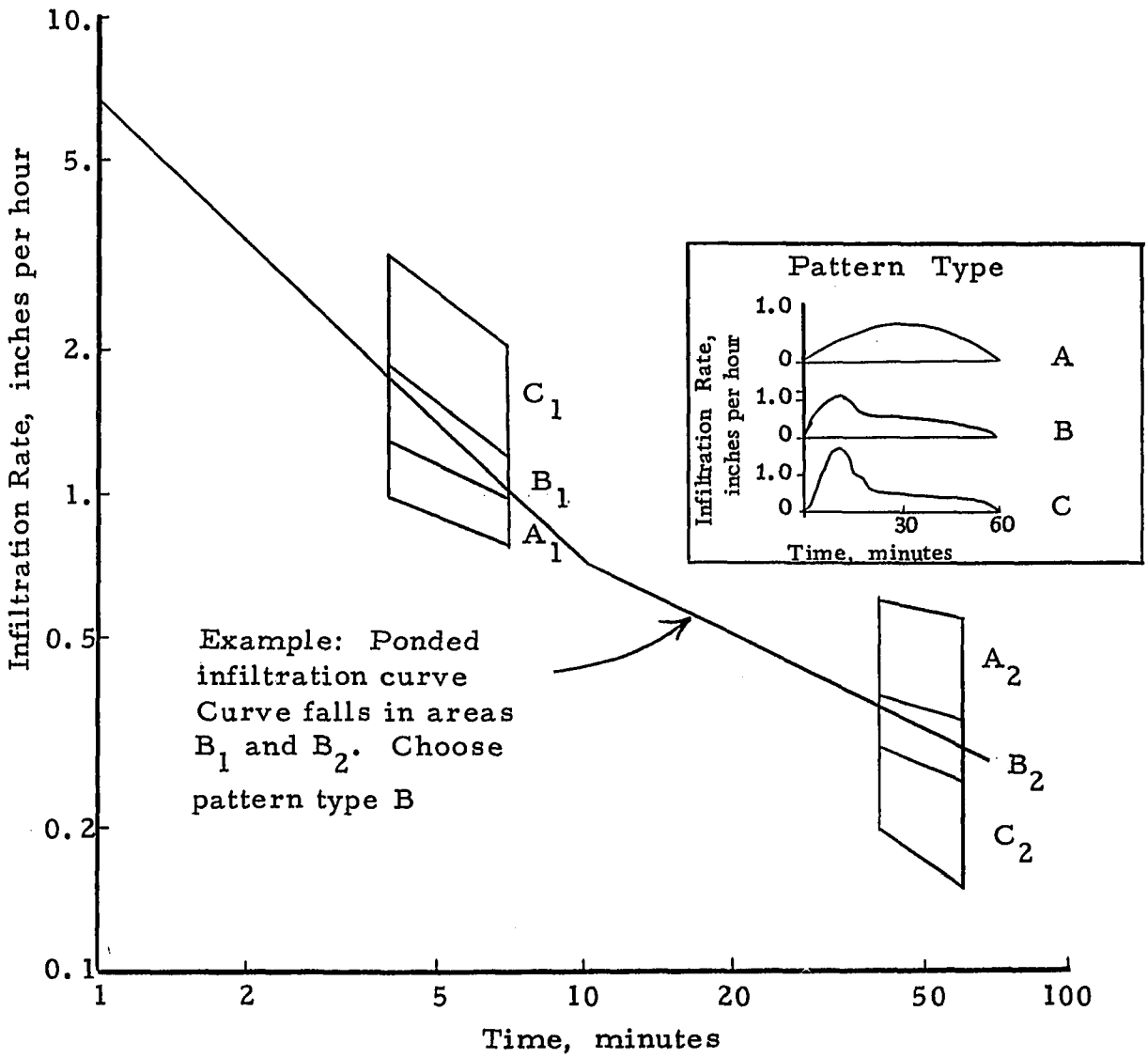

Figure 6.3 Example of a possible design graph for center-pivots--0.60 inch design intake depth--60 minute maximum time length

Obtaining a ponded infiltration curve, which is truly representative of the soil prior to a pass by the center-pivot sprinkler system, is a problem. Runoff problems usually occur on a crusted soil which has not been cultivated since the previous irrigation. Dry, disturbed samples of most soils will indicate adequate infiltration rates so that no runoff would occur under center-pivot sprinkler irrigation, which is misleading. The sample should be undisturbed and crusted and should have densities and initial moisture conditions that would be encountered in the field prior to a pass of the center-pivot.

To produce the type of humped application rate patterns proposed in this study would require a new type of sprinkler or, possibly, special settings of existing part-circle, vane type sprinklers. Either sprinkler type would very likely result in more mechanical problems than a normal full-circle impact sprinkler.

The proposed front-humped patterns sharply increase the application rate at the leading edge of the pattern and decrease rapidly in application rate after the peak is reached. Therefore, these front-humped patterns may be difficult to attain. Wind could change the shape of the pattern considerably. Also, the pattern would have to be reversed if a machine were reversed.

Chapter VII

CONCLUSIONS AND RECOMMENDATION

Conclusions

The main conclusions drawn from the study are that a numerical moisture-flow model can be a helpful research tool and that non-symmetrical application rate patterns have potential for reducing runoff under center-pivot sprinkler systems.

The Model as a Research Tool

Some adjustments of saturated conductivity and layering had to be made in the calibration of the model. After these adjustments were made, a reasonable fit to laboratory infiltration tests was obtained.

Noticeable errors occurred because of ignoring shrinking or swelling in the model. The model would be more useful if shrinking and swelling were included; therefore, an equation, allowing for swelling effects on conductivity, was proposed. However, the model used can be considered a helpful research tool.

Advantage of Non-Symmetrical Patterns

Non-symmetrical center-pivot application rate patterns have potential for reducing runoff. Laboratory tests using loam and sandy clay loam indicate approximately an 11 percent increase in intake depth for a 52-minute front-humped pattern over a 60-minute symmetrical pattern.

Front-humped patterns would indicate a greater advantage (more than 11 percent) over symmetrical patterns if the time length was equal for both types of patterns. Comparing intake depths for 60-minute patterns, front-humped patterns indicate a potential increase in intake depth over a symmetrical pattern of 18 to 23 percent (Table 5.11).

Recommendations

Recommendations for future study are as follows:

1. Soil shrinking and swelling should be studied as these relate to the problem of water infiltration under center-pivot sprinkler systems.
2. The effect of pressure on drop size, using 10 to 30 gpm sprinklers, should be studied.
3. The effects of drop sizes and instantaneous application rates on infiltration, resulting from different sprinkler spacings on center-pivots, should be studied.

4. Actual sprinkler infiltration tests with various application rate patterns should be run on soils using low initial moisture contents because a greater advantage may occur for front-humped patterns due to increased shrinking and swelling.
5. Additional studies should be made on various soils to produce a series of design graphs similar to Figure 6.3 with different design intake depths. These graphs should be verified in the field.

BIBLIOGRAPHY

1 Baver, L. D. and H. F. Winterkorn, Sorption of Liquids by Soil Colloids, II. Surface Behavior in the Hydration of Clays. Soil Science, Vol.40, p. 403, 1935.

2 Bisal, F., Infiltration Rate as Related to Rainfall Energy. Canadian Journal of Soil Science, Vol. 47, pp. 33-37, 1967.

3 Bityukov, K. K., Preservation of Soil Structure During Overhead Irrigation. Trans. Jour. Agr. Engr. Res., Vol. 2, No. 4, pp. 313-320, 1951.

4 Borst, H. L. and R. Woodburn, The Effect of Mulching and Methods of Cultivation on Runoff and Erosion from Muskingums Silt Loam. Agr. Engr., Vol. 23, pp. 19-22, 1942.

5 Brooks, R. H. and A. T. Corey, Hydraulic Properties of Porous Media. Hydrology Paper No. 3, Colorado State University, March, 1964.

6 Carmen, P. C., Fluid Flow through Granular Beds. Transactions, Institute of Chemical Engineering (London). Vol. 15, 1937.

7 Childs, E. C. and N. Collis-George, Soil Geometry and Soil-Water Equilibria. Discussion Faraday Society, Vol. 3, pp. 78-85, 1948.

8 Childs, E. C. and N. Collis-George, The Permeability of Porous Materials. Proc. Royal Society, Vol. 201A, pp. 394-405, London, 1950.

9 Corey, A. T., Flow in Porous Media. A. E. 728 and 730 Class Notes, Colorado State University, Agricultural Engr. Dept., Fort Collins, Colorado, 1969.

10 Darcy, H., Les Fontaines Publiques de la Ville de Dijon. Victor Dalmont, Paris, 1856. as quoted in Hubbert, L. J., Darcy's Law and the Field Equations of the Flow of Underground Fluids. Jour. of Petr. Tech., October, pp. 24-59, 1956.

11 Day, P. R. and G. G. Holmgren, Microscopic Changes in Soil Structure During Compression. Soil Science Soc. of Amer. Pro., Vol. 16, pp. 73-77, 1952.

12 Dixon, W. J. and F. J. Massey, Introduction to Statistical Analysis. McGraw Hill Book Co., Inc., New York, 1957.

13 Dubose, L. A., Discussion of Engineering Properties of Expansive Clays. Trans. ASCE, Vol.121, pp. 674-676, 1956.

14 Duley, F. I., Surface Factors Affecting the Rate of Intake of Water by Soils. Soil Science Soc. Amer. Proc., Vol. 4, pp. 60-64, 1940.

15 Edwards, W. M. and W. E. Larson, Infiltration of Water Into Soils as Influenced by Surface Seal Development. ASAE Paper 68-212, 1968.

16 El-Shafei, Y. Z., A Study of Flooded and Rain Infiltration Relations with Surface Ponding. PhD Thesis, Utah State University, Logan, Utah, 1970.

17 Ellison, W. D. and C. S. Slater, Factors That Affect Surface Sealing and Infiltration of Exposed Soil Surfaces. Agr. Engr., Vol.26, pp. 156-157, 1945.

18 Fair, G. M. and L. P. Hatch, Factors Governing the Streamline Flow of Water Through Sand. Amer. Water Works Ass. Jour., Vol. 25, pp. 1551-1563, 1933.

19 Fletcher, J. E. and Y. Z. El-Shafei, A Theoretical Study of Infiltration into Range and Forest Soils. PRWG60-1, Utah Water Research Laboratory, Utah State University, Logan, Utah, July, 1970.

20 Freeze, R. A., The Mechanism of Natural Ground-water Recharge 1. One-dimensional, Vertical, Unsteady, Unsaturated Flow above a Recharging or Discharging Ground-water Flow System. Water Resources Res., Vol. 5, No. 1, pp. 153-179, 1969.

21 Frost, K. R. and H. C. Schwalen, Sprinkler Evaporation Losses. Agr. Engr., Vol. 36, pp. 328-328, 1955.

22 Green, W. H. and G. A. Ampt, Studies on Soil Physics, Part 1, The Flow of Air and Water Through Soils. Jour. of Agr. Science, Vol. 4, Part 1, pp. 1-24, 1911.

23 Hanks, R. J. and S. A. Bowers, Numerical Solution of the Moisture Flow Equation for Infiltration Into Layered Soils. Soil Science Soc. Amer. Proc., Vol. 26, pp. 530-534, 1962.

24 Holtan, H. N., A concept for Infiltration Estimates in Watershed Engineering. Agr. Res. Service 41-51 1961.

25 Holtan, H. N., C. B. England and V. O. Slanholtz, Concepts in Hydrologic Soil Grouping. Trans. ASAE, Vol. 10, pp. 407-409, 1967.

26 Horton, R. E., An Approach Toward a Physical Interpretation of Infiltration Capacity. Soil Science Soc. Amer. Proc., Vol. 5, pp. 399-417, 1940.

27 Keller, J., The Effect of Application Rate on Moisture Content and Settlement of a Loam Soil During Watering. PhD Thesis, Utah State University, 1967.

28 Kincaid, D. C., D. F. Heermann and E. G. Kruse, Application Rates and Runoff in Center-Pivot Sprinkler Irrigation. Trans. ASAE, Vol. 12, No. 6, pp. 790-794, 1969.

29 Klute, A., A. Numerical Method for Solving the Flow Equation for Water in Unsaturated Materials. Soil Science, Vol. 73, No. 2, pp. 105-116, 1952.

30 Kostiakov, A. N., On the Dynamics of the Coefficient of Water Percolation in Soils and on the Necessity for Studying it From a Dynamic Point of View for Purposes of Amelioration. Trans. 6th Comm. Intern Soil Science, (Russian), Part A, pp. 17-21, 1932. quoted from Childs, E. C., The Physical Basis of Soil Water Phenomena, John Wiley and Sons, Ltd., 1969.

31 Laws, J. O., Recent Studies in Raindrops and Erosion. Agr. Engr., Vol. 21, No. 11, pp. 431-433, 1940.

32 Levine, G., Effects of Irrigation Droplet Size on Infiltration and Aggregate Breakdown. Agr. Engr., Vol. 33, pp. 559-560, 1952.

33 Mannering, J. V., The Relationships of Some Physical and Chemical Properties of Soils to Surface Sealing. PhD Thesis, Purdue Univ., 1967.

34 Mantell, A. and D. Goldberg, The Effect of Water Application Rate on Soil Structure. Jour. of Agr. Engr. Res., Vol. 11, No. 2, pp. 76-79, 1966.

35 McIntyre, D. S., Soil Splash and the Formation of Surface Crusts by Raindrop Impact. Soil Science, Vol. 85, pp. 261-266, 1958.

36 Moldenhauer, W. C. and D. C. Long, Influence of Rainfall Energy on Soil Loss and Infiltration Rates, I. Effects Over a Range of Texture. Soil Science Soc. Amer. Proc., Vol. 28, pp. 813-814, 1964.

37 National Technical Advisory Committee, FWPCA, Water Quality Criteria. U. S. Gov. Printing Office, Wash., D. C., 1968.

38 Palmer, R. L., Waterdrop Impact Forces. Trans. ASAE, Vol. 8, pp. 69-70, 1965.

39 Peele, T. C. and O. W. Beale, Laboratory Determination of Infiltration Rates of Disturbed Soil Samples. Soil Science Society Amer. Proc., Vol. 19, p. 429-432, 1955.

40 Philip, J. R., The Theory of Infiltration: 1. The Infiltration Equation and its Solution. Soil Science, Vol. 83, No. 5, pp. 345-357, 1957.

41 Philip, J. R., The Theory of Infiltration: 4. Sorptivity and Algebraic Infiltration Equations. Soil Science, Vol. 84, No. 3, pp. 257-264, 1957.

42 Philip, J. R., Hydrostatics and Hydrodynamics of Swelling Soils, Water Resources Research, Vol. 5, No. 5, October, 1969, pp. 1070-1077.

43 Richards, L. A., Capillary Conduction of Liquids Through Porous Mediums. Physics, Vol. 1, p. 318-333, 1931.

44 Rubin, J., Theory of Rainfall Uptake by Soils Initially Drier than Their Field capacities and its Application. Water Resources Res., Vol. 2, No. 4, pp. 739-749, 1966.

45 Sor, K. and A. R. Bertrand, Effects of Rainfall Energy on the Permeability of Soils. Soil Science Soc. Amer. Proc., Vol. 26, pp. 293-297, 1962.

46 Smith, R. E., Mathematical Simulation of Infiltrating Watersheds. PhD Thesis, Colorado State University, 1970.

47 Smith, R. E. and D. A. Woolhiser, Overland Flow on an Infiltrating Surface. Water Resources Res., Vol. 7, No. 4, pp. 899-913, 1971.

48 Swartzendruber, D., R. W. Skaggs and D. Wiersma, Characterization of the Rate of Water Infiltration into Soil. Purdue Univ., Water Resources Research Center, Lafayette, Indiana, Technical Report 5, December, 1968.

49 Tressler, R. E., and W. O. Williamson, Particle Arrangements and Differential Imbibitional Swelling in Deformed on Deposited Kaolinite-Illite Clay, Clays and Clay Minerals: Proc. of 13th Nat. Conf., pp. 399-410, 1964.

50 U. S. D. I., FWPCA, Southeast Water Laboratory, Role of Soils and Sediment in Water Pollution Control, Part 1, 1968.

51 Varga, R. S., Matrix Iterative Analysis. Prentice-Hall, Englewood Cliffs, N. Y., 1962.

52 Whisler, F. D. and A. Klute, The Numerical Analysis of Infiltration, Considering Hysteresis, into a Vertical Soil Column at Equilibrium under Gravity. Soil Science Soc. Amer. Proc., Vol. 29, No. 5, pp. 489-494, 1965.

53 Winterkorn, H. F. and L. D. Baver, Sorption of Liquids by Soil Colloids, I. Liquid Intake and Swelling by Soil Colloidal Materials. Soil Science, Vol. 39, pp. 291-298, 1934.

APPENDICES

Appendix A

Testing of Significant Differences Between Intake Depths of Patterns A, B, and C With a Paired t Statistic

To remove the differences between plots (soil compartments) and to remove trend differences (gradual decrease in intake depths in a test series), paired observations were used as described in Dixon and Massey (12), pages 124-127.

An example of the pairing used is shown in Table A. 1. This same method of pairing was used to test for significant differences between patterns B and C, and, C and A.

A t statistic is used

$$t = \frac{\bar{d} - 0}{\sigma_D / \sqrt{N}}$$

in which

$$\bar{d} = \frac{\Sigma d_i}{N}$$

N = number of pairs

σ_D^2 = variance of the differences, d_i

$$\sigma_D^2 = \frac{\Sigma d_i^2 - (\Sigma d_i)^2 / N}{N - 1}$$

Table A. 1 Example of pairing used to test for significant difference between intake depths of patterns A and B--chronological order of patterns--A, B, C, C, B, A

	Intake Depths[1]		Difference of[2] Intake Depths d_i
	A2	B2	A2 - B2
	A3	B3	A3 - B3
A, B	.	.	. .
part of series	.	.	. .
	.	.	. .
	A7	B7	A7 - B7
	A2	B2	A2 - B2
	A3	B3	A3 - B3
B, A	.	.	. .
part of series	.	.	. .
	.	.	. .
	A7	B7	A7 - B7
			Σd_i

[1] Letters A and B refer to patterns and figures 2 to 7 refer to soil compartments; e. g. A2 is the intake depth of box 2 using application rate pattern A.

[2] An example of difference in intake depths is A2 - B2 is the difference in intake depth of box 2 using pattern A and box 2 using pattern B.

Appendix B

Data Intake Rates (inches per hour x 100)

Time (minutes)	Box 2	3	4	5	6	7
K7						
0	94	94	94	94	94	94
4	93	93	93	91	91	93
8	93	93	91	88	83	89
12	91	94	86	79	70	79
16	82	93	76	68	60	66
20	74	89	68	60	53	62
24	70	82	62	56	48	60
28	63	77	57	50	45	54
32	60	77	54	50	37	48
36	54	76	51	46	42	53
40	59	77	51	45	36	46
44	54	74	46	42	40	46
48	56	73	48	39	34	45
K8						
0	40	40	40	40	40	40
12	98	98	98	98	98	98
16	98	98	90	81	73	85
20	98	98	71	62	56	56
24	87	94	67	56	45	64
28	82	91	62	51	42	53
32	74	87	55	45	38	45
36	71	84	56	45	39	45
40	68	84	50	41	30	42
44	67	82	48	36	31	39
48	64	82	47	35	28	36
52	65	81	48	36	27	38

Time (minutes)	Box 2	3	4	5	6	7
K9						
0	154	154	154	154	154	154
4	153	153	136	133	133	136
8	134	139	87	79	81	88
12	98	113	71	71	70	76
16	76	87	59	55	51	61
20	74	87	58	58	55	58
24	67	79	51	51	44	51
28	62	76	44	41	38	45
32	58	74	42	42	39	45
36	58	74	44	41	38	42
40	56	73	41	38	31	44
44	55	73	41	31	33	41
K10						
0	159	159	159	159	159	159
4	157	157	142	137	137	146
8	152	159	83	83	88	92
12	105	142	68	65	69	74
16	76	91	61	61	58	65
20	71	85	53	53	51	54
24	65	79	48	50	50	56
28	61	79	44	47	39	48
32	53	71	42	42	44	50
36	59	70	41	41	39	47
40	54	68	33	38	35	42
44	50	68	31	31	30	36
K11						
0	40	40	40	40	40	40
12	98	98	98	98	98	98
16	94	98	96	73	74	90
20	87	94	64	61	58	62
24	78	84	56	53	50	55
28	71	74	48	45	45	47
32	62	68	42	41	41	44
36	62	65	41	41	38	42
40	55	61	35	31	30	33
44	50	56	33	33	28	36
48	51	55	30	30	28	33
52	50	58	28	27	27	33

Time (minutes)	Box 2	3	4	5	6	7
K12						
0	100	100	100	100	100	100
4	100	100	100	100	100	100
8	95	100	89	83	83	89
12	87	97	69	69	72	73
16	77	84	60	63	61	63
20	69	77	52	52	52	52
24	64	70	44	47	47	44
28	58	67	44	46	44	57
32	52	61	38	40	40	43
36	52	60	35	37	33	41
40	52	61	37	40	38	41
44	46	57	32	32	29	37
48	46	60	30	33	32	37
K13						
0	163	163	163	163	163	163
4	158	163	161	141	141	149
8	104	156	140	81	90	96
12	87	101	72	72	78	84
16	67	78	54	54	58	61
20	67	70	48	51	54	56
24	62	68	48	48	51	54
28	58	61	44	42	44	51
32	51	59	42	42	42	45
36	47	58	36	38	36	45
40	47	56	34	36	36	42
44	47	54	38	36	38	45
K14						
0	100	100	100	100	100	100
4	100	100	100	100	100	100
8	94	100	82	79	88	94
12	80	91	65	66	71	72
16	69	77	54	56	60	63
20	63	69	28	48	51	52
24	56	62	57	45	45	49
28	56	59	42	40	45	49
32	46	52	36	36	37	45
36	48	52	32	36	37	39

Time (minutes)	Box 2	3	4	5	6	7
K14 Continued						
40	43	49	29	28	29	37
44	42	49	28	29	31	37
48	42	48	28	31	31	36
K15						
0	40	40	40	40	40	40
12	99	99	99	99	99	99
16	92	95	76	78	82	89
20	76	82	58	58	65	65
24	69	73	53	52	53	55
28	62	65	44	44	45	49
32	55	62	44	45	47	45
36	56	56	38	41	45	44
40	49	52	35	35	38	39
44	47	50	32	33	36	36
48	44	50	30	33	29	35
52	41	47	29	29	30	35
L5						
0	102	102	102	102	102	102
4	102	102	102	102	102	102
8	100	98	98	98	98	98
12	94	82	91	83	86	85
16	86	69	80	71	69	71
20	83	65	69	60	63	62
24	68	57	63	57	55	57
28	57	51	60	52	51	52
32	55	51	57	46	45	48
36	49	48	54	45	42	46
40	49	46	54	46	42	46
44	51	43	49	43	40	43
48	48	43	46	42	35	42

Time (minutes)	Box 2	3	4	5	6	7
L6						
0	144	144	144	144	144	144
4	141	138	138	140	140	140
8	120	103	114	104	106	109
12	98	84	95	83	83	87
16	80	71	78	71	69	72
20	77	69	75	64	61	68
24	68	60	64	54	54	58
28	61	58	57	54	49	54
32	58	55	61	51	48	54
36	55	54	57	46	44	48
40	51	46	54	46	41	46
44	46	52	54	44	41	48
L7						
0	40	40	40	40	40	40
12	101	101	101	101	101	101
16	99	98	96	98	96	96
20	96	86	93	92	96	98
24	84	73	84	82	86	95
28	73	66	75	72	75	90
32	67	63	70	70	72	84
36	63	56	64	61	66	79
40	55	53	59	58	59	76
44	55	50	58	53	58	73
48	50	49	55	53	55	70
L8						
0	40	40	40	40	40	40
12	102	102	102	102	102	102
16	102	102	102	102	102	102
20	102	99	101	101	101	99
24	99	90	98	96	98	99
28	96	78	90	89	89	98
32	87	70	81	79	78	92
36	79	66	75	73	73	84
40	76	61	69	66	64	76
44	72	56	67	62	59	73
48	66	53	59	55	56	67

Time (minutes)	Box 2	3	4	5	6	7
L9						
0	157	157	157	157	157	157
4	155	155	155	155	153	153
8	144	132	138	132	137	143
12	110	103	113	98	109	110
16	84	82	82	79	81	84
20	79	78	73	72	75	78
24	70	70	65	65	72	68
28	65	67	61	61	64	65
32	58	58	55	55	61	61
36	55	62	53	52	56	55
40	55	56	50	49	59	53
44	52	55	47	45	50	50
L10						
0	96	96	96	96	96	96
8	95	95	95	95	95	95
12	94	91	93	94	89	91
16	88	82	86	85	82	88
20	76	74	76	76	74	74
24	71	68	69	68	71	66
28	63	63	66	60	65	62
32	59	59	60	57	62	56
36	56	57	59	51	59	53
40	56	53	53	48	57	48
44	40	53	51	46	53	48
48	50	53	54	45	46	45
L11						
0	42	42	42	42	42	42
12	105	105	105	105	105	105
16	105	103	105	105	105	103
20	103	94	100	100	95	102
24	97	85	92	89	89	97
28	89	74	83	80	75	86
32	80	71	78	68	66	78
36	77	63	74	65	63	74
40	72	63	72	60	57	71
44	68	58	66	52	52	65
48	60	54	60	48	46	57

Time (minutes)	Box 2	3	4	5	6	7
L12						
0	103	103	103	103	103	103
4	103	103	103	103	103	103
8	98	95	101	101	103	101
12	84	86	94	100	95	105
16.5	73	73	80	84	81	92
20	64	68	73	75	71	83
24	58	61	66	64	63	70
28	54	55	60	55	55	64
32	50	55	58	54	54	63
36	46	52	52	46	46	57
40	44	50	50	49	46	52
44	44	50	50	49	46	52
L13						
0	157	157	157	157	157	157
6	113	118	104	149	146	151
8	90	96	90	117	114	127
12	76	84	77	96	94	107
16	60	68	60	75	74	80
20	58	62	57	65	65	71
24	52	60	54	60	60	63
28	49	57	48	54	54	62
32	46	52	49	49	51	57
36	45	52	46	48	46	54
40	42	49	42	45	45	49
44	39	48	42	43	42	49
K20						
0	41	41	41	41	41	41
8	83	83	83	83	83	83
12	81	81	77	80	83	83
15	67	77	67	67	79	81
18	60	73	56	56	73	69
22	62	79	50	59	73	60
26	50	62	36	42	57	51
30	47	57	34	37	51	45
34	40	48	33	31	45	39
38	36	45	27	33	43	36
42	31	37	23	25	39	34

Time (minutes)	Box 2	3	4	5	6	7
K20 Continued						
46	33	45	28	32	38	35
50	36	47	30	33	39	38
52	36	42	30	30	39	39
56	29	37	27	27	30	35
60	33	40	30	29	33	35
K21						
0	81	81	81	81	81	81
4	162	162	162	162	162	162
8	115	134	105	112	134	159
12	79	99	72	79	100	68
16	52	65	44	47	61	58
20	48	56	44	38	53	58
24	47	56	44	44	52	55
28	41	53	33	33	44	50
32	42	52	41	39	45	53
36	39	48	38	38	39	36
40	38	47	35	33	36	42
44	35	44	30	29	36	39
48	35	45	33	33	35	39
52	35	45	33	32	33	36
K22						
0	80	80	80	80	80	80
4	201	201	201	201	201	201
8	144	120	133	104	124	133
12	127	83	58	73	90	88
16	59	70	54	53	71	71
20	53	56	44	47	59	65
24	39	40	28	26	37	39
28	32	39	25	25	31	39
32	40	37	31	31	39	42
36	39	46	32	34	40	45
40	34	39	29	31	37	39

Time (minutes)	Box 2	3	4	5	6	7
K23						
0	80	80	80	80	80	80
4	201	201	201	201	201	201
8	104	125	93	138	144	148
12	73	82	71	79	105	115
16	57	67	59	60	80	85
20	48	50	42	42	64	68
24	40	42	32	34	49	57
28	40	39	34	34	48	59
32	39	45	39	40	54	57
36	42	46	35	40	46	54
40	39	43	34	39	48	54
K24						
0	80	80	80	80	80	80
4	159	159	159	159	159	159
8	101	109	108	121	144	147
12	72	95	75	82	108	119
17	47	53	48	51	69	81
20	40	48	42	40	56	68
24	44	51	46	51	58	66
28	40	47	41	43	54	66
32	35	43	40	41	51	58
36	34	43	37	38	49	55
42	34	41	35	35	43	53
48	28	36	28	36	42	50
52	29	40	31	34	43	49
K25						
0	41	41	41	41	41	41
8	82	82	82	82	82	82
12	76	81	79	81	81	81
16	59	66	64	73	81	82
18	55	58	55	64	76	79
22	52	58	47	52	66	73
26	39	41	33	36	46	58
30	32	39	32	30	39	49
34	32	32	26	24	32	41
38	33	33	26	26	32	42
42	35	30	26	27	32	42
46	27	32	27	29	30	42

Time (minutes)	Box 2	3	4	5	6	7
K25 Continued						
50	35	38	29	30	33	41
52	27	33	24	30	33	42
56	29	31	29	29	31	34
60	28	32	28	31	32	37
L33						
0	41	41	41	41	41	41
8	82	82	82	82	82	82
18	123	123	123	123	123	123
22	83	80	68	86	90	93
26	66	68	57	76	77	88
30	56	62	50	70	68	86
34	46	51	39	54	59	79
38	48	53	45	59	59	60
42	39	46	37	51	53	57
46	45	50	44	53	53	60
50	45	48	44	53	50	59
52	42	48	42	54	54	64
56	36	36	38	41	38	39
60	38	38	39	39	38	41
L34						
0	84	84	84	84	84	84
4	168	168	168	168	168	168
8	145	140	117	149	140	132
12	111	108	94	120	117	111
16	79	79	68	82	85	82
20	66	69	57	71	74	74
24	56	59	52	64	62	66
28	56	58	52	59	61	64
36	49	52	45	53	53	58
40	47	49	42	52	52	55
44	46	46	39	47	47	52
48	41	44	36	44	42	49
52	42	41	35	44	44	49

Time (minutes)	Box 2	3	4	5	6	7
L35						
0	84	84	84	84	84	84
4	210	210	210	210	210	210
8	159	162	116	134	136	133
12	113	131	87	102	110	110
16	92	105	80	95	100	95
20	86	97	77	89	95	91
24	65	71	52	63	68	65
28	59	65	48	60	65	65
32	56	58	47	58	61	61
36	61	56	52	56	58	61
40	50	55	46	53	56	58
L36						
0	84	84	84	84	84	84
4	212	212	212	212	212	212
8	160	138	118	149	151	143
12	120	108	94	112	120	111
16	98	95	86	98	104	98
20	93	92	84	95	101	95
24	69	63	64	69	74	67
28	64	63	52	63	67	64
32	62	57	53	62	67	63
36	63	59	56	62	63	62
40	59	54	53	56	60	59
L37						
0	85	85	85	85	85	85
4	170	170	170	170	170	170
8	161	147	152	150	150	142
12	130	119	119	119	119	113
16	95	86	83	86	86	83
20	80	74	69	77	77	75
24	71	65	67	73	71	70
28	68	64	62	62	64	65
34	64	58	58	61	58	60
40	59	54	53	57	54	55
44	56	50	50	50	48	53
48	53	48	50	51	48	50
52	54	45	44	45	42	45

Time (minutes)	Box 2	3	4	5	6	7
L38						
0	42	42	42	42	42	42
8	84	84	84	84	84	84
12	84	84	84	84	83	83
16	84	84	83	83	78	78
18	81	78	78	78	72	66
22	90	74	65	71	65	66
26	70	60	54	62	56	45
30	63	56	48	57	54	53
34	57	51	45	54	50	45
38	53	48	39	50	45	45
42	46	45	40	50	46	46
46	47	43	43	49	46	46
50	47	41	40	46	41	41
52	44	41	38	44	38	47
56	39	33	37	39	36	37
60	42	39	39	41	36	39
L39						
0	85	85	85	85	85	85
4	170	170	170	170	170	170
8	150	128	113	122	122	114
12	119	102	91	103	103	97
16	89	78	71	75	75	74
20	74	67	58	67	67	66
28	65	61	56	63	63	60
32	62	59	53	57	56	53
36	59	57	50	56	56	54
40	54	53	46	53	51	50
44	51	48	45	48	48	50
48	50	48	43	48	46	46
52	48	46	40	46	43	45

Time (minutes)	Box 2	3	4	5	6	7
L40						
0	84	84	84	84	84	84
4	211	211	211	211	211	211
8	160	137	114	126	133	122
12	125	105	91	103	116	90
16	103	94	84	95	107	83
20	90	89	74	84	86	80
24	69	66	57	65	74	60
28	63	63	51	59	62	57
32	61	60	53	60	60	55
36	61	60	53	55	55	53
40	60	56	52	55	56	55
L41						
0	40	40	40	40	40	40
8	81	81	81	81	81	81
14	81	81	81	81	80	80
18	81	76	73	79	72	73
22	77	77	66	73	73	65
26	63	65	57	63	62	59
30	60	50	54	60	60	56
34	48	54	48	49	59	51
38	53	57	46	53	54	48
42	45	54	42	48	48	46
44	44	44	47	47	47	44
48	50	53	47	52	50	50
52	50	53	49	49	50	49
56	38	38	39	39	38	38
60	41	41	41	41	39	41